Parameterisation of 2D Hydrodynamic Models and Flood Hazard Mapping for Naga city, Philippines

This study has been conducted under the ITC research project entitled "Strengthening Local Authorities in Risk Management (SLARIM)"

K.B.M. Tennakoon
February, 2004

Parameterisation of 2D hydrodynamic models and flood hazard mapping for Naga city, Philippines

by

K.B.M. Tennakoon

Thesis submitted to the International Institute for Geo-information Science and Earth Observation in partial fulfilment of the requirements for the degree of Master of Science in Urban Planning and Land Administration.

Thesis Assessment Board

1. Prof. Dr. W.H. van den Toorn (Chairman)
2. Dr. T.W.J. van Asch (External examiner)
3. Ir. Mark G.J. Brussel M.Sc.
4. Ir. Gabriel N. Parodi M.Sc.
5. Drs. Dinand Alkema M.Sc.

INTERNATIONAL INSTITUTE FOR GEO-INFORMATION SCIENCE AND EARTH OBSERVATION
ENSCHEDE, THE NETHERLANDS

I certify that although I may have conferred with others in preparing for this assignment, and drawn upon a range of sources cited in this work, the content of this thesis report is my original work.
Signed ……..

Disclaimer

This document describes work undertaken as part of a programme of study at the International Institute for Geo-information Science and Earth Observation. All views and opinions expressed therein remain the sole responsibility of the author, and do not necessarily represent those of the institute.

Abstract

Urban areas are vulnerable to floods due to a high density of population and infrastructure. Often manmade structures in urban areas are located close to each other. Thus, in a flood situation this causes a complex overland flow pattern, which cannot be modelled accurately using conventional 1D models. However, recently developed 2D hydrodynamic models are capable to model complex flow patterns in built up areas. To be able to carry out such modelling, high resolution DTM is required.

This study was carried out focussing on the city of Naga in the Philippines to achieve two key objectives: (i.) Evaluate the effect of pixel resolution of the input DTM on model results and (ii.) development of a multi-parameter flood hazard map by incorporating multiple hazard parameters.

High resolution DTMs were generated from detailed topographic maps collected from various utility organizations. Delft FLS (2D) and SOBEK (1D & 2D) hydrodynamic models were used for simulations. Model results were evaluated for three different scenarios varying the spatial resolution between 5, 7.5 and 10m, while maintaining the same boundary and initial conditions. Finally, a multiple-parameter flood hazard map was created by combining three parameters: kinetic energy, depth of inundation and duration of inundation.

In relation to urban feature representation in the DTM, it was observed that continuous overland flow along roads cannot be represented in the model if the road width is less than $\sqrt{2}(Pixel\ resolution)$. Also effective flow paths between buildings disappear with the increase of pixel size. With respect to the effects of pixel resolution on model results, it was found that there is increase in velocity with the decrease of pixel resolution within the flood plain**.** Also relatively higher velocity and water depth were observed in built-up areas as compared to none built up areas. Two reasons were explored to justify the above variation. (i) Reduction of slope of the DTM with the decrease of spatial resolution. (ii) Loss of flow paths between buildings with the increase of pixel size. The slope reduction results due to the undulation of the terrain and significant reduction does not occur along a longitudinal section of the entire terrain. Finally, the multiple-parameter hazard map was compared with a conventional single-parameter (water depth) hazard map. The multiple-parameter map gave a 16% increase in high hazard zones and a 14% and 2% decrease in low and medium hazard zones, respectively.

Based on the study the following conclusions were drawn: to represent overland flow, roads should be modelled in the DTM with a smaller pixel size if their elevation differs from that of the natural terrain. A high resolution (better than 7.5m) DTM is required for studies related to exploration of flow conditions around individual structures. A DTM having 10m-pixel size is sufficient for generating realistic urban flood hazard maps. More reliable and meaningful flood hazard delineation can be reached with multiple hazard parameters rather than using inundation depth.

Acknowledgements

To begin with I would like to acknowledge here the enormous strength and courage bestowed on me by my beloved **parents** and my wife **Niranthi** to make this study a success.

I would also like to express my sincere gratitude to the Management of, **Sri Lanka Land Reclamation and Development Corporation (SLLRDC)** and Netherlands fellowship Program (NFP) for offering me this opportunity to study in Netherlands. I believe that the eighteen months I spent at the **International institute for geo-Information Science and Earth Observation (ITC)**, helped a lot to build my carrier.

I deeply appreciate my three supervisors for their kind advices and huge support extended to me right through this study specially for orienting me in the correct direction. It was none other than **Mr.Mark Brussel** who diverted me out from vague proposals to a useful research topic showed the correct pathway. Continuous support and guidance imparted given by Mr Mark all the way from the concept proposal stage to the final abstract preparation made this study a success.

I have my special regards for **Mr. Gabriel Parodi** who enlightened me on principles of hydrology and hydraulics, which made the backbone of this study. His enormous support and encouragements not only eased my pressure but also contributed a lot to improve the quality of the work. Also the amendments and valuable comments given by Mr Parodi guided me towards a structured and comprehensive report.

This study would have been a daydream if not for **Mr. Dinand Alkema** who took a lot of pain in initialising the necessary software requirements and putting the foundation for the study. I appreciate with gratitude the support of Mr Dinand who allowed me to work with his personal Delft-FLS program for initial simulations and efforts he made to purchase and install the SOBEK in ITC enabling me to widen the scope of this study.

My sincere thanks go to **Mrs. Nanette Kigma** for her kind cooperation and support extended during the field work also to **Mr Frans Bosch** for allocating me several computers for parallel simulations and all the UPLA staff members who supported in completing this study.

I should also acknowledge **Mr. Arnesto Elcamel** of Naga municipality and former ITC student **Ms Arlene Dayao** for their kind assistance given during the fieldwork.

I wish to thank my colleague **Kabir** for allowing me to use his computer for overnight simulations and entire **UPLA 2002** group for their numerous supports during the entire period.

I would like to thank all my country mates especially to Lal, Vajira, Senani and Kithsiri for their continuous encouragement and support given during my stay in Netherlands.

Finally to all those who shared this premises, a big thank you for the support, patience and more than all the friendship extended to me during past one and half years

K.B.M. Tennakoon
Enschede, February 2004.

Table of contents

List of Figures

List of Tables

Abbreviations

ASCII	Raster file format
Delft FLS	Delft flooding system (a software program)
DEM	Digital elevation model
DHI	Danish hydraulic institute
D_{ij}	Depth of inundation at (i, i)th pixel
DTM	Digital terrain model
EIA	Environmental impact assessment
FEMA	Federal Emergency Management Agency
HHZ	High Hazard Zone
GIS	Geographical information system
GPS	Global positioning system
GUI	Graphical user interface
$Ke_{i,j}$	Kinetic energy at (i, i)th pixel
LHZ	Low Hazard Zone
LS	Longitudinal section
LIDAR	Light detecting and ranging (Air borne laser, elevation data source)
.m	Mass of water colums
MHZ	Medium Hazard Zone
MSL	Mean sea level
NEDA	National Economic and Development Authority
RS	Remote sensing
SLARIM	Strengthening local authorities in risk management
SAR	Synthetic aperture radar (remotely sensed image)
T	Total duration of a flood event
$T_{i,j}$	Duration of inundation at (i, i)th pixel

TIN	Triangulated irregular network
V	Velocity
ρ_w	Density of water
1D	One-dimensional
2D	Two-dimensional

1. Introduction

1.1. General

All over the world floods poise a major threat to settlements and human life. This can strike with little forewarning. “The impact of floods to human civilization is a topic as recorded history, as evidence by Egyptian stage measurements” (Eltahir, 1999). Impervious surfaces and hydrologically improved man made drains contribute for flash floods in urban areas even during a rainfall of moderate intensity. Therefore, vulnerability due to a flood event in an urban area is severe and it results in great economic losses too. It is observed that the frequency of flooding and the consequential economic losses have significantly increased over the recent decades. Main reasons for this increase can be attributed to increasing population in the urban centres and close proximities as well as the vast development of urban infrastructure without paying due consideration to drainage aspects.

Conventionally flood damage assessments have been developed from fully dynamic one-dimensional (1D) models. These models are capable of calculating flood levels and discharges quite accurately in applications where the flow path is mainly a “linear” feature. However, results of 1D model are questionable in urban areas where the flow paths are complex and take many directions due to the presence of man made structures, such as buildings, roads, bridges and embankments. Particularly, difficulties arise when it is required to analyse flows around individual structures. Hence, 1D-modelling applications are limited in their capability to accurately represent the resulting complex flow paths in urban applications. Also with an “increased public awareness of flooding and flood-related issues, many municipalities and regulatory authorities require a higher degree of accuracy in modelling” (Granger, 1999).

This situation has demanded a shift from 1D modelling to two-dimensional (2D) flow models especially in urban applications. In general, 2D simulation generates time series of inundation depths at user specified time intervals. 1D models are limited to river reaches and capable of generating the inundation depths within the river reaches. 2D approach provides pixel level inundation within the entire flood plain since 2D modelling is based on raster grids or triangular grids. Thus 2D modelling provides adequate information to generate flood hazard maps and finally to prepare risk maps by incorporating land use and economic return of the flood plain. The model can be applied to anything between a regional level watershed to a small urban flood plain or even to a single street where detailed analysis of the flow conditions is required.

However, 2D modelling applications particularly for an urban area require a considerable cost and time for data collection. Although this is similar to any other hydraulic or hydrological modelling, 2D modelling requires not only accurate topographic data but also building footprints in the study area. Therefore in this case accurate inundation depth in the flood plain could be obtained only if the input data are representative of actual terrain. Therefore the accuracy of inundation depth in the flood plain heavily depends on how well the actual terrain is represented in the input data.

Most of the medium scale local authorities, which face frequent flood threats, do not have proper flood hazard maps or flood risk maps that are essentially required for urban planning activities. The major obstacle for them to apply 2D modelling is non-availability of proper elevation data sets and other hydrological parameters.

Therefore it is important to identify low cost data sources for 2D modelling as well as methods to represent urban characteristics within the model with required accuracy.

1.2. The problem statement

Though 2D modelling provides better options and flexibility in understanding the urban area flooding process, it requires good representation of topography as an accurate Digital terrain model (DTM). Presently, most of the modelling efforts have been made using latest laser and radar elevation data sources. However medium scale local authorities in developing countries are incapable of acquiring such data due to lack of financial support and skills involved in pre-processing. Therefore it is important to identify alternative elevation data sets for generating a DTM as an input for 2D hydrodynamic modelling in a data scarce situation. Also limitations as well as accuracy of model results obtained from such data sources are decisive. However, this attempt does not justify the rejection of high-resolution airborne elevation data for DTM construction.

Furthermore in a detailed urban flood modelling exercise it is vital to incorporate urban features such as buildings and road network in the DTM. Buildings in the DTM obstruct the flow while road network conveys the overland flow. Since in the past most of the 2D modelling work has been focused at regional level, optimum pixel resolution for representing urban features in a detailed urban modelling has not been sufficiently discussed in the literature. Therefore the effect on model results at different spatial resolutions of the input data is matter of research.

Reliable and meaningful flood hazard maps are a requirement for good urban planning practice. In the past flood hazard maps were generated based only on inundation depths. However flood hazard depends on the duration of inundation, the amount of energy that is contained in the overland flow and the available warning time to evacuate the population. Therefore it is important to identify techniques to generate multiple-parameter flood hazard maps by incorporating all possible hazardous elements of a flood event.

In general, any 2D hydrodynamic model takes considerable computation time varying from several hours to several days. The number of pixels in the input DTM is directly prepositional to the computation time. However, in detailed urban modelling applications, smaller pixel sizes are chosen for better representing the urban structures in the DTM. As a result simulation takes long computation time. Also in the past literature little discussion has made on the model results variation with pixel resolution. Therefore it is important to explore model results variation with pixel resolution since it will directly help to save several hours of computation.

1.3. Research objectives

1.3.1. Main Objective

- Development of GIS based methods for establishing 2D hydrodynamic modelling parameters and construction of an urban 2D flood model.

1.3.2. Sub objectives

- Identification of alternative elevation data sets for generation of detailed DTM in urban area under a data scarce situation.
- Identification of optimum raster resolution to incorporate roads, building and other physical structures inside the DTM looking at accuracy and hydrodynamic modeling requirements.
- Development of a GIS model of the urban built up area to serve as input for the 2D Hydrodynamic model.
- Developing a flood hazard map by incorporating kinetic energy, depth and duration of inundation.
- Investigate the effect of model results with the change of spatial resolution in the 2D model.

1.4. Research questions

- What are the alternative data sources that can be used to generate an urban DTM under a data scarce situation? What are their limitations?
- What is the optimum raster resolution for representing urban features in 2D hydrodynamic modelling and what is the effect of the model result by changing the DTM resolution?
- What is the better representation of buildings in the model? A high roughness coefficient at building footprints or buildings as a solid blocks in the DTM.
- How to generate meaningful flood hazard maps by incorporating multiple hazard parameters?

1.5. Research design

This study has three key elements; Identification of alternative data for parameterisation of 2D hydrodynamic models, Identification of model results variation on spatial resolution and generation of a multiple-parameter flood hazard map. The key elements are shown in the Figure 1-1 below.

The fieldwork primarily concentrated for searching detailed elevation data and filling the data gaps using a simple and fast spot height collection technique explained in chapter 2. Then separate elevation models were generated for natural terrain, road surface and buildings to create a terrain model of the area. The resulting DTM with hydrological initial and boundary conditions were entered into the Delft FLS 2D hydrodynamic model. At the last stage of the research it was feasible to model the River network and flood plain separately using SOBEK which is a combined 1D and 2D flow simulation model.

Model result variation with pixel resolution was investigated using three separate DTMs having spatial resolution 5m, 7.5m and 10m. They were input to the model with same initial and boundary conditions. The results were compared to identify changes in depth of inundation and velocity of floodwater at each simulation step.

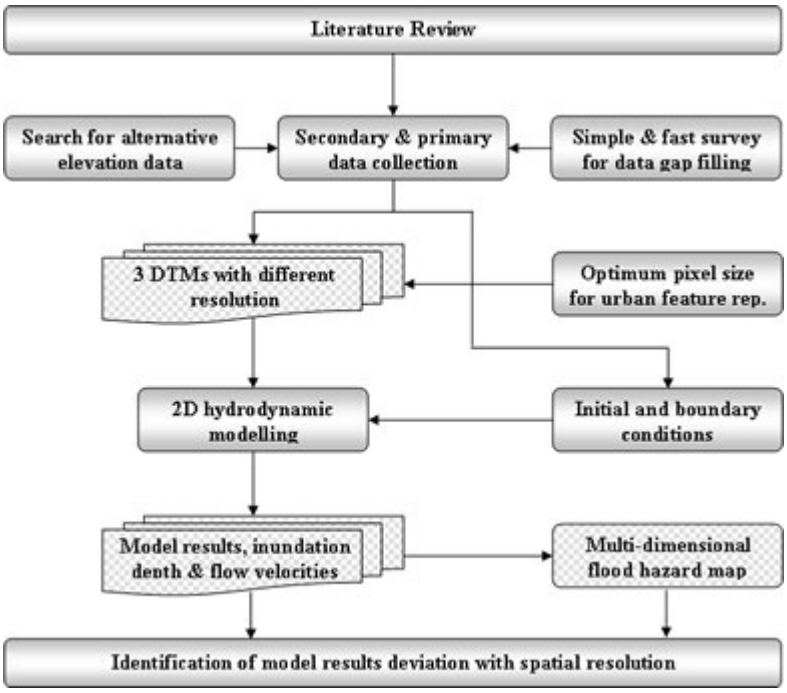

Figure 1-1:Basic steps of the study

Finally, it was attempted to incorporate additional parameters to develop a multiple-parameter flood hazard map by incorporating several hazard parameters instead of the conventional hazard map representing depth of inundation alone. Two additional parameters were combined with depth of inundation to generate a hazard map with multiple-parameters. The final combined hazard map is a representation of Depth of inundation, Duration of inundation and kinetic energy of floodwater.

1.6. Outline of the thesis

This thesis consists of nine chapters.

Chapter two contains the literature review on development of hydrological and hydrodynamic models with GIS, Comparison of 1D and 2D Hydrodynamic modelling, advantages and limitations. Potential application of 2D modelling and special features of Delft FLS and SOBEK models were also discussed. Finally a discussion was made on data sources for DTM generation and optimum spatial resolution for urban elevation models

Chapter three introduces characteristics and selection criteria of the case study city. An outline of the methods and tools used for data collection is also presented.

Chapter four explains in detail the DTM generation methodology by combining three elevation models developed for natural terrain, road surface and buildings. It discusses the optimum pixel resolution for urban feature representation and accuracy aspects of the DTM.

Chapter five describes the 2D hydrodynamic modelling procedure in steps for both the Delft FLS and SOBEK models. It compares the capabilities of SOBEK vs. Delft FLS in terms of model outputs. Some aspects of the model calibration procedure are also presented.

Chapter six illustrates the model application for development scenarios. It analyses effects of proposed Naga city master plan (year 2000 –2010) against the year 2000 land use for changes in flood conditions in the area.

Chapter seven introduces new parameters for flood hazard mapping and methods used to combine the parameters to generate a multiple-parameter flood hazard map. Comparison of multiple-parameter hazard map with the conventional inundation depth based flood hazard map also presented in this chapter.

Chapter eight is devoted to discussion of results. First, it discusses from where the alternative elevation data are available and their advantages and limitations for 2D modelling. Then it compares model results for different DTM spatial resolution. Finally it discusses on issues related to multiple-parameter flood hazard mapping.

The final chapter outlines findings, recommendations and limitations of the study. It provides suggestions for future applied studies and describes additional data to be recorded by Naga municipality for filling data gaps and model calibration.

1.7. Problems and limitation of this research

The study was conducted in a data scarce environment of Naga city as part of a broader effort to support developments in risk management for local authorities under the ITC internal research project of Strengthening Local Authorities for Risk Management (SLARIM). Data scarcity was embedded in the research and as such it suffered all the consequences of this essential lack of information.

Several previous hydrological studies conducted by consultants under foreign funded projects failed to provide the required boundary conditions for reliable 1D/2D modelling. Difficulties arisen due to none availability of proper boundary conditions has been discussed in sections 5.2.3 and 5.7.1 of chapter five.

Rating curves are described at discharge stations, which are located far away from Naga city or in sub catchments in the upper Bicol River, not related at all with this study. Therefore approximate rating curve was developed and input to the model. It has been discussed in section 5.2.3.1 and 5.7.1 of chapter five.

As part of the conclusion an identification of those essential parameters required to use the model for real applications such as EIA studies.

High computational time is the other main obstacle that hindered the fine calibration even with the available limited data. It took about a five-day computation period for simulating a four-day rainfall

event with one-hour simulation steps. Therefore proper calibration could not be realized within the specified time frame by running several iterative simulations.

The results of this thesis must be taken very cautiously. However the techniques and procedures are perfectly valid and applicable in similar studies.

2. Literature Review

In the past GIS have been practised mostly by large institutions such as country wide or regional level organizations mainly for mapping and management of spatial data. “Because of the non maturity of the use of GIS for hydrological and hydraulic modelling, the practicing engineering professionals have had only limited exposure to such field” (Maidment, 1993). This was confirmed by a survey that was developed as part of Smith's master project in 1995 (Olivera, 1997). A questionnaire was sent out to the fifty state highway agencies in the US to assess the current use and expected use of GIS for hydraulics-related highway design work. From the thirty-two responses that were received back to the researchers, it has revealed that only one-highway agency has implemented GIS for hydrologic analysis. In addition there were nine organizations using GIS mainly for mapping and data management. The rest of the organization had not used GIS at all for any purpose. Even though this situation has not changed entirely at present, application of GIS for hydrological and hydraulic modelling has become popular among the modelling community. This is mainly due to the growing awareness in the potential application of GIS in engineering design and analysis.

However major research effort towards interaction of GIS with hydrological modelling had not taken place until late 1990’s (Maidment, 1993). Current trends of GIS in hydrological and hydraulic modelling pointed out by (Suia., 1999) as “Nowadays various hydrological modelling techniques have enabled GIS users to go beyond the data inventory and visualization stage to conduct sophisticated modelling and simulation”. Today GIS tools are increasingly being used in modelling applications, where geographic data can be readily accessed, processed and displayed.

2.1.1. Loosely Coupled Models with GIS

One of the major limitations of the integration of GIS and hydrologic or hydrodynamic models is that “current GIS technology cannot represent the continuous temporal element of modelling”(McDonnell, 1996). It can only represent time as a series of ‘snapshots’. One of the most popular ways to use GIS in hydrologic modelling is a loosely coupled system where the model and GIS maintain two separate databases and interact through some form of a file exchange or conversion process. With this approach it is possible to obtain better flexibility from the model as well as the more GIS functionality for analysis and visualization of model results.

“The current HEC-GeoRAS version 3.0 is an example for a loosely coupled system, developed jointly by HEC ESRI, and distributed by HEC” (McAlister, 1997). The extension allows users with limited GIS experience to create a HEC-RAS import file. It contains river geometry and model parameters from an existing digital elevation model and shapefiles that define the stream network, cross section locations and other hydrologic characteristics of the river system. After hydraulic analysis completed in HEC-RAS, HEC-GeoRAS can develop and display themes of inundation area, water depth and water velocities from the result of the analysis.

However, there are several tightly coupled models available today. The major limitation of this type of systems is that modelling capabilities are lesser compared to standalone model. As yet available GIS functionality too will be reduced in coupled system (Drayton, 1992).

2.2. 1D hydrodynamic modelling

In 1D modelling "fluid is modelled on the base of cross sectional calculations, the cross sections are divided by vertical lines, or into cells"(Borsányi, 1998), and in these units each hydrological parameter is assumed to be uniform. In many applications, rivers, streams or canals are modelled as one-dimensional full hydrodynamic systems since in a river or stream flow direction can be well defined to a liner network. Among the several 1D hydrodynamic models available today widely used models are HECRAS developed by United States Army Crops of Engineers and MIKE 11 from Danish Hydraulics Institute (DHI). HECRAS is public domain software and it is being used all over the world. However MIKE 11 is proprietary software and it is required to purchase a registration key before using it.

The major limitation in the 1D modelling approach is that the flow is restricted to a predefined path. Although this limitation has a lesser impact on modelling a river or a canal as long as the flow is confined to the bank full discharge, it badly affects in computing inundation extent and/or depth due to overflow of rivers in a flat urban terrain. Due to the existence of heaps of man-made structures and elevated roads the flow path during a flood event cannot be predefined. However a coupled 1D model with full 2D features will provide better modelling flexibility and accuracy in computing water surface profiles as well as inundation extent. (Delft_Hydraulics, 2003) The best example for this kind of 1D and 2D coupled system is SOBEK developed by Delft Hydraulics, the Netherlands.

2.3. 2D hydrodynamic modelling

2D models are capable of providing information not only regarding the inundation depth and its spatial distribution but also the variation of flood extent and flow velocities over a user-defined time frame. Thus, 2D models are becoming more and more popular among the modelling community nowadays.

In "2D modelling fluid is divided into fluid columns, and in these cells each variable is assumed to be constant (depth-averaged values)" (Borsányi, 1998). Cells in this approach are represented as 2D finite elements (i.e. Mike 21, LISFLOOD-FP, TELEMAC-2D, SMS, Delft FLS and SOBEK). All the input and output hydrological and hydraulic parameters are assumed to be uniform within a cell.

In 2D models there are two approaches to model the flood plain. It could be as a rectangular grids format or a triangular mesh structure. Figure 2.1a and 2.1b shows a triangular mesh and raster based terrain representation.

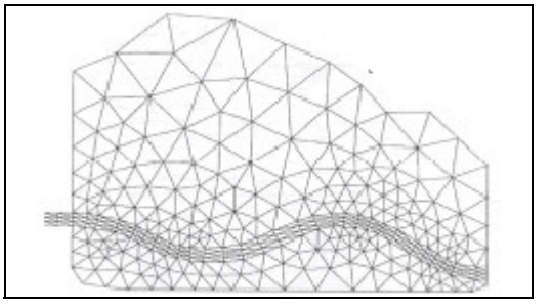

Figure 2.1a: Triangular mesh structure
(Source: (Rath, 2003))

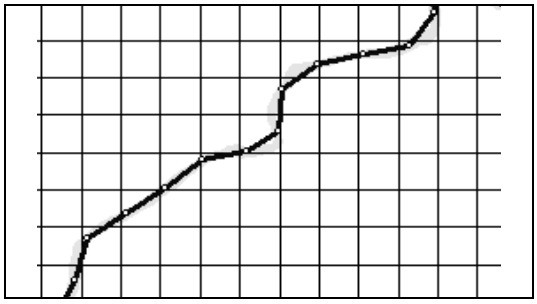

Figure 2.1b: Raster grid structure

2.3.1. Triangular mesh approach

In the triangular mesh each cell is built out of triangles having different sizes. Therefore in this approach the higher the concentration of triangles, the more accurate the resulting representation.

More concentrated mesh representation always guarantees better accuracy of the modelling effort. Also accurate representation of features like rivers, estuaries, bays, wetland areas or coastal regions is feasible using 2D finite-element meshes rather than the rectangular mesh.

For example Surface Water Modelling systems (WMS) model offers two methods to generate the mesh structure. That is direct approach or conceptual approach. In the direct approach it allows to build the mesh structure first and model parameters can incorporate later with the mesh.

In the second approach a conceptual model is created first using GIS objects including points, arcs and polygons. The conceptual model is constructed independently of the mesh. In this level description of the site including geometric features such as channels and banks, the boundary of the study area, flow rates and water surface elevations of boundary conditions and roughness coefficients such as Manning's n value. Once the conceptual model is complete, a mesh network is automatically constructed to fit the conceptual model. At this level model data are converted from the conceptual model to the elements and nodes of the mesh network (WMS, 2003).

After mesh generation filters are available to remove dense triangles from the plane regions. The main advantage of this approach is 1D features could be accurately modelled in the 2D model itself using a dense triangular mesh structure.

2.3.2. Raster grid approach

In raster based approach cells are identical all over the model. Data input to a raster-based model is fairly simple if the input data are manipulated through a raster based GIS system. Also it has the advantage of utilizing the recent high-resolution remotely sensed topographic data and the capability of exporting model results in to various GIS systems for presentation purposes. As a result the raster based 2D modelling systems are quite popular nowadays in risk assessment, planning, environmental impact assessment and studies related to dike breach or dam failure. Some of the distinctive advantages in 2D hydrodynamic modelling over the conventional 1D modelling are outlined below.

- Most of the terrain features within the study area can be incorporated in the model using a DTM.
- Actual flow paths will be determined by the model as a function of terrain, as specified in grid pixel values, and given boundary conditions.
- Surface roughness of the study area can easily be derived from a land use map and can be used as a direct input to the model as a raster layer having surface roughness value for each pixel.
- Model results (i.e. extent and depth of inundation, flow velocities) are available for each and every pixel in the study area hence can be directly used in risk assessment.
- Since output results can easily be fed in to a GIS system, further analysis of results and visual enhancement are possible.

The main disadvantage of this approach is river geometry or linear features like roads have to be represented using raster cells. If the cell size is larger it is not possible to model urban features with adequate accuracy. However, SOBEK the latest software of Delft hydraulics has the capability to represent linear features (i.e. rives and canal) using cross sections while the floodplain can be represented using raster cells. (Delft_Hydraulics, 2003)

Advantages and limitations of triangular mesh and raster-based 2D modelling techniques are given in table 2.1 below.

	Triangular mesh	**Raster**
Easy mesh structure		Yes.
Faster calculation time	Yes.	
Allows very accurate results at critical points	Yes.	
Easy integration with RS data		Yes.

Table 2-1: Comparison of triangular and raster based 2D models

2.3.3. History and advancement of 2D modelling

"2D modelling has been in existence since the late 1970's" (Beven, 2000). Most of the "initial 2D model efforts have been intended at modelling estuaries, lakes, bays and coastal areas" (McCowan, 2003). Although the concept of applying 2D models to rivers and floodplain has been considered from time to time, according to (DHI, 2003), it has only been turned out to be successful during the last five years. Today it has been successfully applied from large-scale floodplains to small urban areas on a regular basis. This has only been possible due to the enormous advancement in computational power of microcomputers, development of high-tech 2D hydrodynamic models like MIKE 21, WMS, Delft FLS, SOBEK, LISFLOOD-FP, TELEMAC-2D and recent advancement of GIS and RS technology (Horritt, 2002).

2.3.4. Applications of 2D modelling

2D modelling has a wide range of simulation possibilities. It is popular for risk and damage assessment due to its high versatility in unsteady analysis needed for overflow of river or dam break. Also it

can be used for water quality modelling studies. It is possible to apply in any terrain like lowlands, estuaries or mountain areas. In the recent past several efforts had been made to illustrate the capabilities of 2D approach in various application domains (Alkema, 2001,b, 2001,a; Alkema, 2003; Horritt, 2002; McCowan, 2003; Stelling, 1998). It has been extensively used in simulating dike/dam breaks scenarios in Europe, particularly in the Netherlands. Therefore it is a decision support tool for evacuation planning and risk assessment purpose in the case of a polder flooding due to dike breach or dam break (Meulen, 2003).

Risk maps and damage assessments could conveniently be produced from the 2D model results. It provides inundation depth and duration at a user specified time interval in raster format at pixel level. Visualization and presentation possibilities have become enhanced due to the capability of exporting model output files into any raster based GIS system.

Today "2D hydrodynamic modes have shown that they are capable of modelling water level changes down to 1cm or less in accuracy"(Gourbesville, 2002). Reaching to this level of accuracy would compel urban planners to apply them in urban and landscape planning activities.

2.3.4.1. Flood hazard assessment

Accurate and reliable flood risk maps are ideal tools for decision makers to reduce social and economic losses from eventual flood events. Also it is useful information for emergency organizations to calibrate and adjust warning system and prepare priority evacuation plans. It may be used to prevent urban planning authorities to carry out any development activities within the high hazard zones.

Conventionally, flood inundation maps were prepared from 1D model results or using flood level records collected during previous flood events. However with the advancement of 2D modelling parallel to the GIS and remote sensing today it is possible to obtain inundation maps at user defined time frames during a flood event. Also the most recent GIS technology allows the modeller to drape the modelled flood plain boundaries for various design rainfalls on a base map and "fly" through the inundation area for better visualization (Shamsi, 2002).

The inundation maps allows the evaluation of the damage assessment by overlaying the inundation depth layer with land use and other information representing investments and service facilities within the area. Finally "risk for the area could be generated based on the damage estimation and the combined probability of occurrence of rainfall event and other disasters such as dam or dike break or any other hazard"(Stelling, 1998).

2.3.4.2. Urban Planning

With the raising urban population and subsequent requirement for infrastructure and services, urban planners have to identify new lands for development. Selecting lands for development has to be done utmost carefully when it is proposing lands in urban flood plains. In general remaining non-developed lands in urban floodplains are low-lying and they may be acting as retention or detentions ponds to ease the flood level in the surrounding neighbourhood. As a consequence of development, water retention capacity of these lands decreases and imperviousness of the area increases. Thus excess water during flood event will reach to new areas where there was not experiencing any floods in the past.

The scenario simulation capabilities are a powerful tool to identify safe and suitable lands for future developments and prepare land use master plans.

2.3.4.3. EIA studies

At present regulations are fairly strong with respect to any new infrastructure development projects. It has to undergone environmental impact assessment (EIA). Therefore construction of any structure specially in low-lying areas or an urban flood prone region has to prove that it does not lead to harmful changes in overland flow pattern to its surrounding neighbourhood.

Under these circumstances 2D hydrodynamic models are ideal tool for identifying the variation in flow pattern due to the changes in the terrain. It has the possibility to make separate model runs to identify the inundation extent for various scenarios describing terrain changes or proposed mitigation plans. According to (Alkema, 2001,a) "2D modelling results could be used during the design phase of an infrastructure project in such a way that positive impacts are maximised, mitigation measure to reduce risk in rest of the flood plain are incorporated"

2.3.5. Data requirement for 2D modelling

2.3.5.1.DTM

Any 2D model requires a good representation of the terrain including man made structures such as roads, buildings, embankments and drainage paths within the study area. The accuracy of the model results primarily depends on how accurately the input DTM represents the real terrain. The accuracy of DTM will depend on the type and source of data and the interpolation algorithm used. Four main categories of elevation data sources are available for generation of a DTM. Each data source is described with their level of accuracy for urban modelling application.

2.3.5.1.1. Digitised contours

Contours or spot height are possibly the most common data source for generating a DTM. This is because "digital contour data have been developed from existing topographic maps which are the only source of elevation data for some parts of the world." (Hutchinson, 1999) Contours from hard copy maps can be digitised by manual digitising, semi-automated line following or automatic raster-scanning. The accuracy of the DTM derived from contours depends exclusively on the quality of the original hard copy maps from where the contours were originated.

The contour map accuracy will depend on the primary network of geometric points, secondary and eventual third level base points. The scale of the cartographic map and digitisation errors also contributes to the accuracy.

However the accuracy of this DTM will basically depend on the accuracy of digitisation and the contour maps that are used for digitising. Though it is a time consuming process, the resulting DTM would be a fairly good one. It is possible to use in urban flood modelling applications if the density of data set is fairly homogeneous within the study area and if the vertical accuracy is acceptable.

2.3.5.1.2. Ground surveying

Elevation data obtained from ground surveying is the most accurate and reliable, as the operation is designed to draw the most information from the area up to 1mm accuracy. During the survey it is possible to take into account ground surface undulations according to modelling requirements and obtain extra spot heights in those areas. Considerable time and funds would be required to carry out a conventional ground survey in a complete city. Even though regional scale modelling does not require this level of accuracy, for urban applications, a DTM obtained from ground surveying would be the perfect choice. The resulting DTM would be able to represent even a kerb line at the edge of the road surface.

2.3.5.1.3. Photogrammetric Techniques

Remote sensing methods can provided broad spatial coverage, but have a number of generic limitations such as ground cover, random errors and flow path identification particularly in areas with low relief. Aerial photographs and digital satellite imagery has been used to generate fairly accurate high-resolution topographic data using a stereo pair. These "traditional data sources can deliver elevation up to sub meter accuracy" (Hutchinson, 1999) Though a DTM generated through these methods are sufficient for regional or large scale flood modelling still the accuracy is not sufficient for detailed urban applications.

2.3.5.1.4. Active sensor data sources

At present there are quite a lot of newer data sources for DTM generation, such as Laser Altimetry and Synthetic Aperture Radar (SAR). They will provide a very accurate DTM in a fairly large area. According to (Fowler, 2002) "Laser systems are highly accurate in their ranging capabilities, providing elevation with accuracy up to a couple of centimetres over a fairly wide range of distances." Laser or SAR data could be air borne or space borne. Both the systems provide higher ground cover. Today both air borne and space borne techniques are capable to obtain elevation data up to the satisfaction of the modelling community.

LIDAR is an acronym for Light Detection and Ranging. This technology now allows large areas of precise data to be captured with relative economy. "LIDAR systems have been around for a long time, but it is only recently that these systems are usable with a high degree of accuracy from moving airborne platforms"(Fowler, 2002) Therefore, particularly well suited to flood mapping in flat terrains. It is the least expensive method of covering a large area with detailed elevation data.

Assessment of DTMs obtained from various data sources has been carried out by (Wise, 2000). According to his observations several spurious sinks or local depressions were detected in DTMs those were prepared from laser and SAR techniques. It is a significant setback with respect to hydrological or hydrodynamic modelling applications.

However to generate a DTM using these new techniques requires skilled persons and also the cost of data for a small urban application would obviously be a hurdle for a local authority in a developing country.

2.3.5.2. Boundary conditions

Hydrologic models require both boundary and initial conditions to start computations. Boundary conditions represent water states at the outer extents of the area selected for the model. These states either

feed or constrain the functioning of the model. For example, the outlet of a certain river discharges at the sea. The flowing river does not affect the water height in big storage water bodies. In this case a constant head boundary condition applies. Tidal effects can be modelled by water height harmonic waves.

In the upper catchment an "inflow" boundary condition feeds the model in time (input hydrographs). Initial conditions apply to elements inside the modelled selection. This basically indicates; what is the water state (normally height or depth) in this simulation element at time equal zero. It is obvious that the effect of the model run is different for different initial conditions.

2.3.5.3. Bottom friction

Bottom friction could be input to the model as Manning's roughness or other roughness parameter (i.e. Chezy, Strickler, etc.). Land use classes could be reclassified to hydrological roughness values from look-up-tables. Remote sensing techniques could be used to obtain a land cover classification in relatively large areas, however for urban applications land use classifications are readily available in any urban planning organization. However, there is limited information on roughness values for urban land that can be applied to this specific study case.

A raster layer containing roughness values could be conveniently input to the model as a single file a having separate value for each pixel. It is also possible to specify a single value for the entire study area if it is not possible to find a proper land use classification.

2.3.5.4. Calibration of 2D models

Any model should be calibrated with observed records and adjust its hydrological parameters so that both observed and simulated results are as close as possible. In 2D modelling, calibration could be done against extent of inundation in addition to the conventional discharge calibration at river cross sections. Even though discharge measurement at a specific cross section is feasible with manual methods, extent of inundation as a time series could not be obtained easily with manual measures. Instead, advanced Radar remote-sensing techniques, which can penetrate cloud cover, could be used to obtain inundation depth during a flood event. According to (Horritt, 2001)SAR technology has proved itself as a useful technique for mapping inundating extent with required time interval. Therefore in future 2D models, it possible to use series of SAR images for calibration and validation with superior accuracy and reliability.

The only parameter used to calibrate the 2D model for overland analysis is the roughness coefficient of the floodplain. Once having discharge data at the river cross section or other data source to prove that inundation extent at a particular time (i.e. SAR image at different time frames) by changing the roughness coefficient of the inundation area it is possible to control the overland flow or the river discharge. For example once decrease the roughness coefficient of the floodplain it will result in higher flow towards the floodplain, and lower discharge at down stream river cross sections (Alkema, 2002).

2.3.6. Delft - FLS

Delft Flooding System (Delft – FLS) is a 2D finite element raster based flood simulation package developed by WL | Delft Hydraulics. It is specially suited to simulate overland flow over initially dry

land. According to Prof. Stelling, the pioneer of the Delft – FLS program "The model is based on full 2D shallow water equations." These equations are solved following finite difference techniques on a rectangular grid and always guarantees positive water depth" Also he further assures that "The model allows a sound simulation opportunity for sub and supercritical flows and it gives accurate and stable results during flow computations on very steep slopes such as dike walls structures etc." (Stelling, 1998)

Among the raster based 2D hydrodynamic models, Delft FLS widely used in dike breach studies in Europe, especially in the Netherlands. Its robust numerical techniques are capable to simulate continuity and mass balance for rapid flows with hydraulic jumps and dam breaks. In addition it has been widely used in simulating dynamic behaviour of overland flow due to rising water level over initially dry land.

The model requires a good topographical data set as a raster DTM or other means. However the delft FLS version 2.47 allows only 500 rows and 500 columns of raster cells and expects this limitation will be removed in future developments. Initial and boundary conditions can easily input as separate text files. Surface roughness enters as a raster layer indicating Manning's n for each pixel.

There are several output files generated during the computation. Water levels and flow velocities are computed at user-defined intervals. In addition current lines and inundation depth class intervals can be created at selected time frames. These output files are in ASCII raster format and could be converted to any GIS file format for further analysis and better visualization purposes. Also "flooding can be animated immediately after computation using in house software called Delft-quickin" (Delft_Hydraulics, 2000). In addition it is possible to get the discharge though predefined cross section in order to create rating curve for a particular cross section of the river. This feature is very important when it is required to carry out engineering design for a particular section of a canal or stream.

2.3.6.1. Limitation of Delft - FLS

The model cannot represent the 1D feature with required accuracy if the pixel size of the input DTM is big. For example 25 m-river sections cannot be represented in the model with 50m-pixel when modelling a relatively large watershed. Similarly in urban applications it is difficult and sometimes impossible to represent drains and other hydrologically important urban features if the smaller dimension of the structure is less than the pixel resolution. Therefore it is important to select the optimum pixel resolution for a specific application depending on the detail expected from the model results.

The other major limitation of this software is the computation time. Computation time depends on several factors including the terrain slope and the discharge vs. water surface elevation. In general, an area represented by 497 by 497 pixels for one-hour real time simulation may take about 4 to 60 minutes of computation time in the latest Pentium IV 1300 MHz processor. Therefore simulation of a flood event of duration one day may take 90 minutes to 24 hours of computation time[1].

[1] This comment might not have any relevance in future with the advancement of PC technologies.

2.3.7. Optimum pixel size for urban modelling

In floodplain analysis most of the 2-D modelling was done with pixel sizes of 20 and higher. However modelling efforts in relatively small urban terrains are quite rare and difficult to access for the detail required for a research. Therefore it is fairly difficult to find adequate literature on the selection of optimum pixel size for representing urban features like roads and building footprints in the input DTM. In a detailed urban modelling exercise it is very important to represent the roads as close to the reality as possible since overland flow during a flood event mainly conveys along the road network. Also buildings and other structures will act as barriers to the flow direction. Moreover it is quite difficult to represent urban features satisfactorily with 10m or higher pixel size. Lesser pixel size gives better representation but in general 2D models have upper limit for number of pixels. The increase in number of pixels is directly proportional to the increase of computation time. Consequently selection of optimum pixel size is essential to preserve urban features in the DTM, maximise study area within the limited number of pixels and optimise computation time in a detailed urban 2D modelling application.

2.3.8. The model applicability under data scare situations

Most 2D modelling efforts have been made using recently developed remotely sensed topographical data sources such as ASTER, LIDAR or SAR. Elevation data sets obtained from those sources are quite dense and homogeneous. Therefore representation of terrain features from those remotely sensed data sources are quite satisfactory.

Local authorities in developing countries may not be able to obtain those new data sets due to the high cost and advanced data post processing requirements. However any urban area may have conventional elevation data sets (contours or spot heights) scattered over various government and private organizations. One of the most demanding tasks is the right compilation of this elevation information, the data quality analysis (not described in this thesis) and the data assembly. There are not many examples in the literature on the assembly of scattered elevation data for 2D hydrodynamic modelling. In this thesis a considerable amount of time was dedicated to the compilation and assembly of DTMs of different sources considering the critical importance this operation has in the final results.

3. Case study and data collection

3.1. Case study selection Naga city, Philippines

3.1.1. Location

Naga City is about 377 Km to the south of Manila, the capital of Philippines and located between 13° 36' 40'' to 13° 38' 40'' degrees North Latitude and between 123° 10' 30'' to 123° 12' 30'' degrees East Longitude. The city is centrally located in the province of Camarines Sur at the footage of Mount Isarog.

"Naga is classified as a first class city with 126,972 residents (*1995 census*) that expand to more than 180,000 in 1999" (OIDC, 1999). About 78 Km^2 of its area belongs to the Naga municipality government and it is the regional center for commercial, educational and industrial sectors. Naga is considered the heart of Bicol region.

Figure 3-1: Location of Naga city

Naga City and a large portion of its nearby municipalities known as Metro Naga are situated within the floodplains of the Bicol river basin. The Bicol River basin, being within the Philippines typhoon belt, does experience between two to five typhoons annually and extremely intense rainfall (OIDC, 1999). Considerable amount of precipitation drains through Bicol River and Naga River during typhoons and finally they join at Naga city.

As the main portion of the city is situated at low elevation within a flat topography almost levelled with the rivers, these rivers have overflowed their bank and destroyed domestic, commercial, industrial and institutional interests in the past years. The Bicol River at the progressive of Naga city is affected by inter-tidal action that can elevate the normal river water level up to 3 meters during long

term recurrence events (normally up to 1.2 m). The city is eventually affected by storm surges during typhoon events.

Recent studies have demonstrated that San Miguel Bay (Bicol outlet) has elevated the bay bed in about 2 m in the past 100 years due to sediment produced by the Bicol River during heavy rainfall in the upper catchment (Adolfo, 2003). This morphological process was not considered in the recent engineering studies of 1991 and 2003 aiming to improve Bicol River drainage and bank protection. Without much analysis we may conclude that sediment transport carried from the Mayon volcano and upper erodable areas are threatening the security of the downstream lowlands. The problem was recognized after by local experts (NEDA, Legaspi) but not emphasized in the latest feasibility consultation carried out last year. Traditionally the weight of the opinion of local experts does not match that of the internationally recognized organization.

3.1.2. Background problem

Naga city is expanding very fast and the same trend will continue in the future since Naga is the centre for commercial, educational and industrial sectors in Bicol region. The annual estimated growth rate of household population within the city limits for next ten years is over 1.6% and current estimated population is over 144 000 (Nagacity, 2003).

Naga city economic growth rate exceeds 6.5% and it is recognised as one of the fastest growing local economies in the country. At present dominant land use of Naga is agricultural covering about 42% of the total. In addition, 24% is allocated for commercial, industrial/agro-industrial and tourism purposes and 20% is for residential use (Nagacity, 2003). In order to cope with current population and economic expansion most of the agricultural lands within the city and its suburbs are converting to residential or commercial land use without a proper expansion plan.

Most of the remaining agricultural lands within the vicinity of the city are lowlands with elevation varying from 0 to 2m MSL. During flood events these lowlands may act as retention basins to ease the rising flood level of the city centre.

As mentioned above, most of these low lying agricultural lands within the city are disappearing and they are converting to residential and commercial land use with parallel to the urbanization. However proper assessment has not been taken place during the selection of lands fro future development with respect to the flood hazard. Therefore generation of detailed flood hazard maps foresees as an essential tool to help the city government in the managerial selection of new lands for future development.

3.1.3. Climate

Climate in Naga city is influenced by the northeast monsoon winds and trade winds.(Laud, 2001; OIDC, 1999) The northeast monsoon winds originate from the east of the pacific and it approaches to the Bicol region in northeast direction. It starts affecting the area in later October and reaches a maximum intensity during January to February and gradually reduces in April. The monsoon wind creates low-pressure area in the Pacific that results to a tropical cyclone that affects the whole Bicol region during the months of November and December (Laud, 2001).

The annual average rainfall at Pili, Camarines Sur, where is the recording station located closest to Naga City is 1,166 mm. Even though annual average rainfall seems to be low, monthly average rainfall or rainfall intensity during a typhoon event will provide the clear picture of potential flood conditions in Naga city. The highest annual average monthly rainfall is 323 mm (November) and maximum rainfall intensity during a typhoon event could be reached up to 400mm within 24 hours. The highest monthly temperature experience in this area is 31^{o}C (May and June), and the lowest monthly temperature is 25^{o}C (January).

3.1.4. Topography

The central business district of the Naga city lies between 1.00 to 5.00 meters above mean sea level and rising west to east towards Mount Isarog. Within the city limits there is a considerable extent of agricultural lands having elevation under 2m and those low lands act as retention ponds during flood events. As a result of low land reclamation, natural terrain of the floodplain has changed a lot especially in the vicinity of Naga city.

3.1.5. Soil condition

The study area mainly consists of alluvium deposits, pyroclastics, limestone and volcanic flows. Alluvium deposits are mainly lying along Bicol River floodplain and surrounding low land areas. These alluvium deposits are transported during heavy rainfall events and deposited along active river channels. In the flat terrain at the foot of the Mt. Isarog, deposits of pyroclastics flows and volcanic debris could be seen. In addition cliff forming limestone is a very prominent geographic feature of the study area.(Laud, 2001)

Heavy deforestation is taking place in the slopes of Mt. Isarog; as a result tributaries of the Naga River starting from the mountain transport huge sediment load. Also during the monsoon period, the soils are close to saturation, whereby any soil disturbing activities in the higher slope will greatly enhance soil erosion. Therefore there is a potential to increase the flood level in future due to the heavy sedimentation of riverbeds. This problem was recognized even at municipality level. The authorities reallocated several families to avoid deforestation but the damage is not only produced by illegal occupation but also loyal forces opening routes in the ongoing battle against insurgents hidden nearby.

3.2. Secondary data collection

Fieldwork focussed on the collection of secondary data sources scattered over various public and private organizations. Two out of three weeks were spent to trace existing topographic and hydrological data sources that we new that were available. Lists of organizations that may have required data were prepared with the help of an officer from Naga municipality having local knowledge. During the visits new organizations were included to the list for further tracing the required data sources.

In addition it was required to obtain GIS layers containing building footprints, road network and land use of the Naga city and surroundings. The entire GIS data set was found in the electronic data processing unit of the Naga municipality.

3.2.1. Topographical data[2]

In order to develop a better quality DTM particularly in an urban area, detailed topographical data is the key requirement. Before the fieldwork it was understood that Naga municipality or any other organization in the area did not have a detailed Naga city contour topography or equivalent. Therefore gathering existing topographic data scattered at different organizations was the main objective of the fieldwork plan in view of the lack of means of getting the whole lot by our action.

Initially it was intended to visit all the infrastructure development and maintenance organizations (i.e. drainage, irrigation, roads, sewerage, water) within the city expecting to gather longitudinal profiles along infrastructure networks. It was understood later that the City Engineers office at Naga municipality maintains all other infrastructure networks except main roads and irrigation canals. As expected, it was possible to collect 12 A0 sheets containing 0.25m contours and over 600 spot heights from a proposed drainage rehabilitation project in 1981 with scale of 1: 1000. The entire Naga city area had been surveyed during the project in 1991. However out of 42 sheets only 12 sheets were traced from the City Engineers office. Initially it was expected that Department of Highway might have longitudinal sections (LS) along main roads however it was unable to find single LS along main roads, what it was astonishing since this means that all longitudinal roads are built without a drainage survey.

National Economic and Development Authority (NEDA) the executing agency for foreign founded projects in the Bicol region had three A0 sheets containing 1m contours with scale of 1: 4000 covering Naga city south. It has been prepared under Bicol watershed development project funded by Asian Development Bank (ADB) in 1991. There we found the most important data set, the Naga and Bicol River cross sections including a longitudinal section along centre line of rivers.

3.2.2. Hydrological data

During the fieldwork it was intended to collect stream flow discharge and river water level variations at Naga and Bicol River during typhoons with small time interval like one hour. Even though it was possible to identify water level variations during several typhoons at Bicol River corresponding discharge measurement were not available, mainly to the impossibility of establishing a secure $Q=f(h)$ relation in an area of strong inter-tidal effect. Moreover there were not any records related to water level or discharge measurements obtained at Naga River since no gauging station was established along Naga River in the past. However modelled (MIKE 11) Q vs. H relation for Bicol River at downstream of Naga River was fond for 1.25, 10 and 25 year flood events. This development was acquired during the recent 2003 project carried out by Nippon Koei Co. Ltd and NEDA as local partner.

Water level variations during several typhoons at 15-minute time intervals were identified at Camaligan gauging station (13◦ 37’17”, 123◦ 09’ 54”E) located 1.6Km downstream from the confluence of the Bicol and Naga Rivers. In addition water level variation records during another three typhoons from 1978 to 1982 were identified at river gauging station located at Mabulo (13◦ 37’ 00”, 123◦ 10’ 56”E) about 600m upstream of Bicol River from the confluence of Bicol and Naga Rivers. However from 1982 onwards this gauging station was not operational.

[2] Some of the paragraphs in this thesis are intended to local authorities in Naga in order to help them in the collection and archiving of the available data valid for hydraulic modelling. This description is one of them.

Selected water level records identified during the fieldwork are shown in the Appendix A1.

3.2.3. GIS data

Before the fieldwork the base map of the area was created using:

- A KVR (Russian) image taken in 1991 having 2m resolution and
- 1: 50000 digital toposheet with 5m contours covering the entire Bicol watershed

During the fieldwork several GIS layers in ArcView shape file format were obtained from the Electronic data processing unit of Naga municipality including building footprint, and road centreline layers. Both shape files had been updated to represent year 2000 condition. Therefore it was a quite satisfactory data set for the modelling the present condition. Attribute data other than the road width were unavailable.

Available at the Naga municipality was the Master Plan for year 2000 – 2010 in digital form with updated land use (2002). Details of all ArcView shape files obtained from the Naga municipality are included in the database created at the end of this study.

The original coordinate system of these shape files was GCS_WGS_1984. All these layers were later transformed into Philippines zone IV projected coordinate system with the help of ArcToolbox™ of ArcGIS™ in an effort to standardize the coordinate system of all layers.

3.3. Primary data collection

Recording historical flood levels within the city limit, identification and measurement of transversal hydrologically important structures along Naga River and urban land covers for surface roughness estimation were the primary data types expected to be obtained from the initial fieldwork plan. However this was extended to primary land levelling survey due to the non-availability of secondary elevation data.

3.3.1. Topographical data

At the end of the second week of the fieldwork it is understood that all secondary elevation data sets already collected do not adequately cover the proposed modelling area. Therefore it was required to carry out a field levelling work within the city centre with the intention of obtaining a complete and homogeneous spot height distribution through out the study area. The area without secondary data is shown as a semi-transparent polygon over the 2m resolutions KVR Image in the Figure 3-2 below.

There was another setback in the secondary elevation data sets collected from different sources. They had not referenced to the mean sea level (MSL) or any other common reference. Therefore in order to integrate all these different elevation data sets into a common reference, it was essential to perform a field levelling work, to agree in a common datum. Hence the land-levelling work of no data area was further extended so that area of levelling work overlaps the existing data sets.

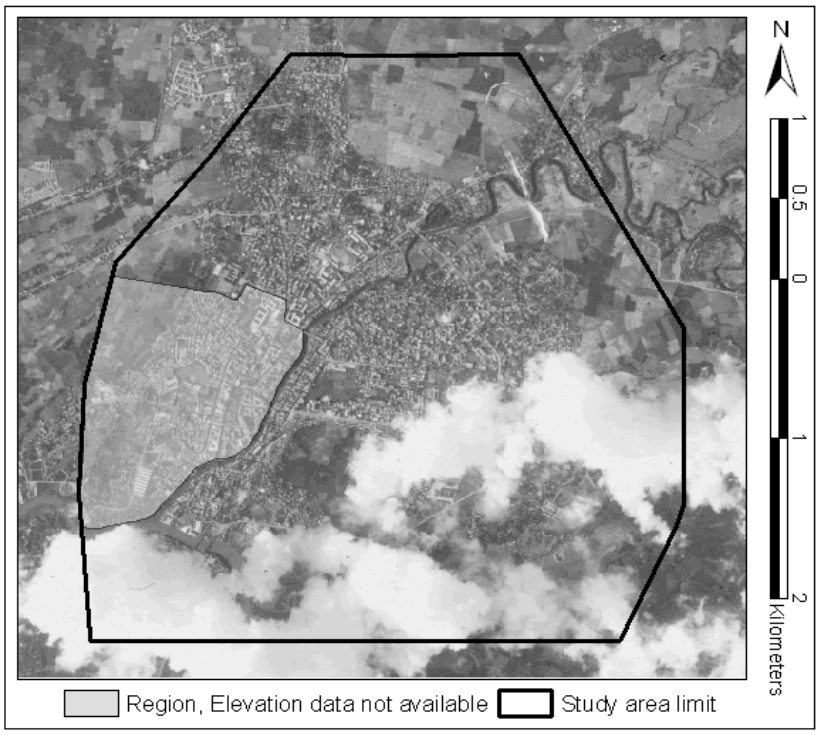

Figure 3-2: Elevation data gap zone within the study area

3.3.1.1. Simple and rapid land levelling example

The total extent of the required levelling area was about 2Km by 1 Km rectangular section as shown in the Figure 3-2 above. It includes the Naga city central business district too. Therefore most of the streets that required spot heights were full of traffic and quite busy during the daytime. Hence any survey work will be time consuming and tedious in similar area due to the congestion.
The levelling work was carried out with manual adjusting Dumpy level, Levelling staff and a hand held Gamin 12XL™ Global Positioning System (GPS), only elements at hand. It required a minimum of two skilled persons. While one person was observing the staff reading, the other person who is standing with the staff could record the position of the spot height using the GPS[3]. By this method it was possible to cover about 5km along busy streets per day having over 100 spot heights. In fairly flat streets the distance between two spot heights was taken at 100m – 200m apart and in sloping streets the points were taken at close intervals like 10 -20m apart.

With the introduction of GPS it was not required to obtain any tape or angular measurement for locating the position of spot height as we do in traversing. Therefore this approach allows a surveyor to cover wider area within a short duration. The second advantage of this method is that all the GPS waypoints could be instantly downloaded to a computer in tabular format and afterwards a GIS point layer containing spot height locations could be generated instantly. It is very helpful to examine the distribution of acquired spot height over the study area to identify any positional errors due to GPS signal variations; so wrong positioning can be redone. It is useful for finding areas where further spot heights are required and to organise the remaining levelling task.

[3] GPS was only used to record point location (X, Y) in this research.

With this method elevation accuracy could be obtained up to 1mm similar to typical optical levelling applications. However positional accuracy of spot location will depend on the accuracy of the GPS unit and amount of signal received by the GPS at a specific location. In general open areas without any dense canopy cover it was able to achieve $\pm$ 5m or better accuracy. Overlaying a point map of spot height over a high-resolution image of the area could make a quick accuracy check. If all the spot height were taken at specific side of streets it should be represent once overlay two layers.

This rapid, simple to use and low cost spot height acquiring technique is useful for small urban areas where there are not sufficient elevation details to run 2D hydrodynamic models or for any other applications where precise positional accuracy of spot locations are not essential.

3.3.2. Hydrological data

Dimensions of bridges, main culverts, streams and major embankments were noted down with sketches and positions of them were recorded using a handheld GPS as a series of waypoints.

It was required to obtain historical flood water levels within the Naga city during typhoons for model calibration. These were obtained by interviewing dwellers of the inundating area and observing recorded flood levels on walls, bridge abutments etc. The position of the recording point was obtained as waypoint using the GPS.

The reliability of this data set is questionable due to the contradicting statements made by different dwellers at neighbouring houses. Also it was not possible to find flood level referring to same flood event on a specific date, people normally remember the biggest event according to his own experience and refer to it. For example while Mr A is referring to typhoon Ruping in 1982 Mr B will refer to typhoon Pepang in 1979. The other limitation in the approach is that some people wanted to exaggerate the actual flood condition and just indicate very high flood levels that will never match with other records. Despite that this description is not very technical, we are aware in this research that most of the flood levels recorded during urban floods by the local municipal agents was obtained by consultation to the local people, so available hazard maps cannot be taken as irrefutable proof.

4. DTM generation

4.1. Introduction

For 2D hydrodynamic modelling a DTM is the key input data layer. As long as the input DTM is representing the actual terrain, model validation and calibration remains feasible and final inundation extent could be fairly accurate. According to (DHI, 2003), "DTM must represent variations less than 0.1m to obtain a good representation of the overflows in the streets."

Overland flow in an urban area primarily conveys along the roads. Buildings and other structures change the flow direction. Therefore in 2D modelling accurate representation of buildings and roads within the DTM is crucial. Since several elevation data layers were used for the final DTM generation, the initial DTM was constructed as a Triangular Irregular Network (TIN).

Since in Delft FLS and SOBEK hydraulic models used in this research can be specified terrain elevation in raster format, DTM in TIN was converted into raster. Furthermore, manipulation of different elevation models required in the data assembly is convenient in raster format. Finally each elevation model was assembled in raster calculator and process of assembly is shown in Figure 4-1 below.

4.2. Data used for DTM generation

Six different data sources were used to generate the initial DTM.

- 0.25m contour lines at south of Naga city, two A_0 sheets in 1: 4000 scale
- 1m contour lines in rest of the city area, six A_0 sheets in 1: 1000 scale
- Spot heights in the above two contour data sets
- Spot height along roads from the Naga city Drainage Development Project 1981, twelve A_0 sheets 1: 1000 scale
- Longitudinal and cross sections of Naga and Bicol river as spot cross section heights, eleven A_0 sheets with 1: 1000 scale
- Spot heights obtained during the fieldwork within the city centre with 1cm vertical accuracy.

All these paper maps were scanned and georeferenced with the KVR image that has already converted to Philippine Zone IV projected coordinate system. ArcGIS, ArcMap 8.2 version was used for goreferencing and subsequent all GIS operations.

As it can be seen from this description, the real accuracy of the generated DTM might not reach the required 0.1 m for urban modelling stated previously. In view of time and resources limitations during the field work and physical impossibility of getting such accuracy, I must warn here that my results might not be getting the precision required for vulnerability studies and remedial structural designs, but for the purposes of hazard mapping this DTM accuracy falls within required parameters, validating my data input.

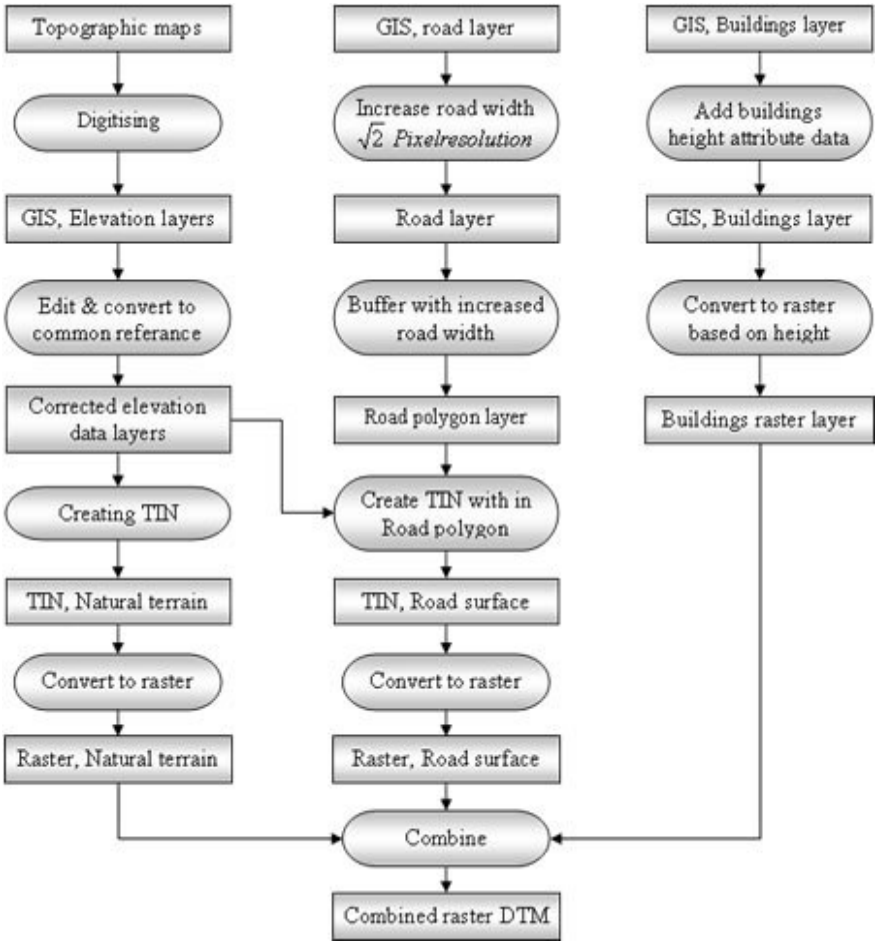

Figure 4-1: DTM assembling process

4.3. Digitising and arranging data sets in a geodatabase

The work of data cataloging in a research of this magnitude is not a minor task and has to be described in order to allow reproduction or tracking. This lack of description is the main drawback in many common projects regarding the future modeling updates. SLARIM[4] project main objectives to whom this research makes a contribution, explicitly mention the requirement of data cataloging.

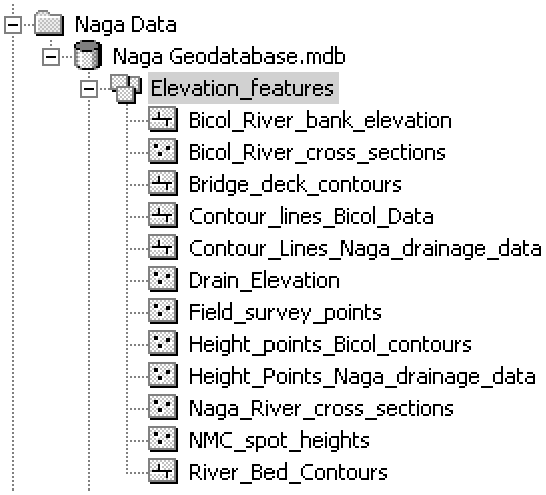

Figure 4-2: Structure of the geodatabase

In order to organise different elevation data sets an ArcMap geodatabase was created before the digitising. Within the geodatabase all elevation features were stored separately in a feature dataset. Inside the "Elevation features" dataset separate shape file were created for individual data source con-

[4] Strengthening Local Authorities in Risk Management, internal ITC project

tour lines and spot heights. Creating separate feature data sets for different category of data sets are quite useful in handling large databases. In general it improves the efficiency of any analytic task. A convenience of this approach is that all the shape files in one-feature data set automatically get the co-ordinate system of the feature data set. Since it is not necessary to assign coordinate systems to individual shape files, it saves lot of time. The structure of the geodatabase, feature class and shape files are shown in the Figure 4-2 above.

Creation of separate feature class for individual data sets was especially helpful when it was required to transform different data sets having dissimilar vertical datum. Also when building the TIN DTM it is possible to choose required elevation features for generating specific DTM like river bed without bridges etc.

4.4. Assembly of different data sets

Except for the Bicol River contour data set that is digitised from hard copy maps of Bicol River basin flood control and irrigation development project, all other data sets did not have any Meta data related to their vertical reference. Therefore it was required to check the vertical reference of each data set before they combine and use to generate the DTM. Alerted on this situation during the field work we extended the field levelling survey so that all the secondary data sets overlap the field levelling area at known points, as mentioned above. For example there were five bridges within the Naga city limits crossing the Naga River and at least one spot height were available in each data set on a bridge deck. Then it was possible to check all the data sets vertical reference only after all five bridges deck level were surveyed.

After digitising each data set, the bridge deck level was compared with the corresponding deck level of the field levelling data. It was found that except Naga city drainage project spot heights all other data sets were within 10cm accuracy. However about 1.2m deviation was observed in Naga city drainage project spot heights. Therefore this data set was compared with all other data sets and it was observed average surface is 1.1m above the other data sets. After this analysis it was clear that even this dataset was useful since the problem was in the datum and not in the relative heights measurements. Therefore the Naga city drainage project spot heights were lowered by 1.1m in order to bring all the data sets in to a common reference.

Also during the comparison of data sets it was noted that road levels obtained from field survey are in average 20cm above the secondary data set's road elevation. The reason behind this deviation was understood after a meeting with the road maintenance authorities. Road surface elevation is continuously rising and changing the road surface from bitumen to concrete in order to reduce the damage to the road surface during frequent floods events. This information indicates the importance of water energy in the area, so this parameter will come to the picture further during the analysis.

4.5. Density of elevation data

Density of available data sets for DTM generation within Naga city is shown in the Figure 4-3 right. It was observed that density of the data was quite low in Western part of the city compared to the rest of the area. However data distribution was quite homogeneous in the remaining parts of the city. This problem improved after additional spot heights and contour lines, which were incorporated by using fieldwork observations. The objective was to obtain a homogeneous and dense elevation dataset since the DTM was generated using Triangulated Irregular Network (TIN) technique.

The model study area was decided by considering urban floodplain extent as shown in the Naga city disaster mitigation plan 1999, density of available data sets and software limitation explained in above section 2.3.6.1

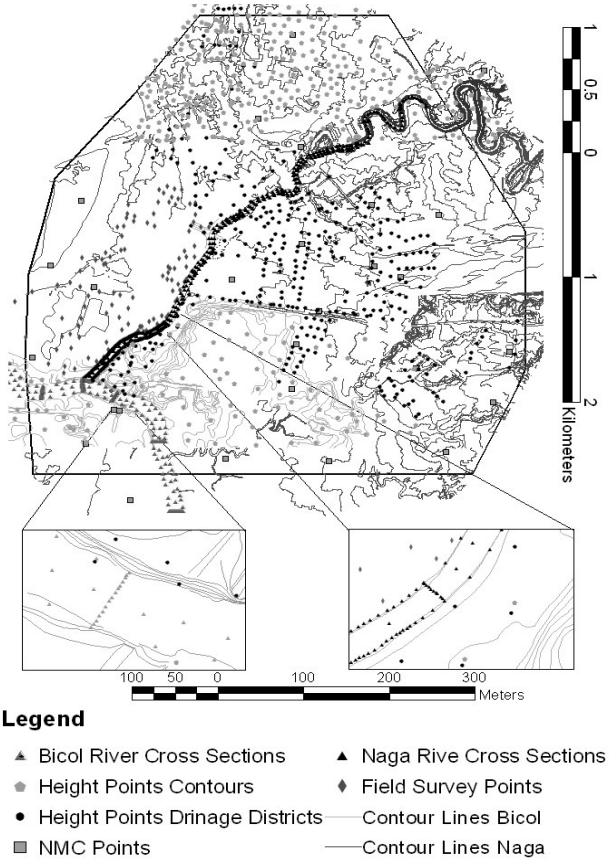

Figure 4-3: Elevation data distribution

4.6. Representation of river bed

Hard copy maps having riverbed cross-sections and longitudinal sections were scanned and digitised in ArcMap to create a point map containing spot heights of the riverbed. The distance between two cross sections is about 300m and that of two points with a cross section varies from 2m to 5m. Its distribution is shown in the Figure 4-4-a below.

However, it was not possible to obtain a satisfactory representation of the riverbed using this point data layer alone. Resulting TIN created only using those riverbed spot heights is shown in Figure 4-4-b above. Since the representation is not satisfactory several techniques were used to interpolate and reduce the distance between cross sections and river edge spot heights before generate the DTM using TIN. Since distance between river edge spot heights and cross sections spot heights are not evenly distributed with a river reach any of the interpolation methods did not provide satisfactory representation of riverbed using spot height alone. Therefore riverbed contours were drawn by manual interpolation of existing riverbed spot heights. TIN DTM constructed using interpolated riverbed contours are shown in the Figure 4-4–c and it was considered satisfactory for hydraulic modelling.

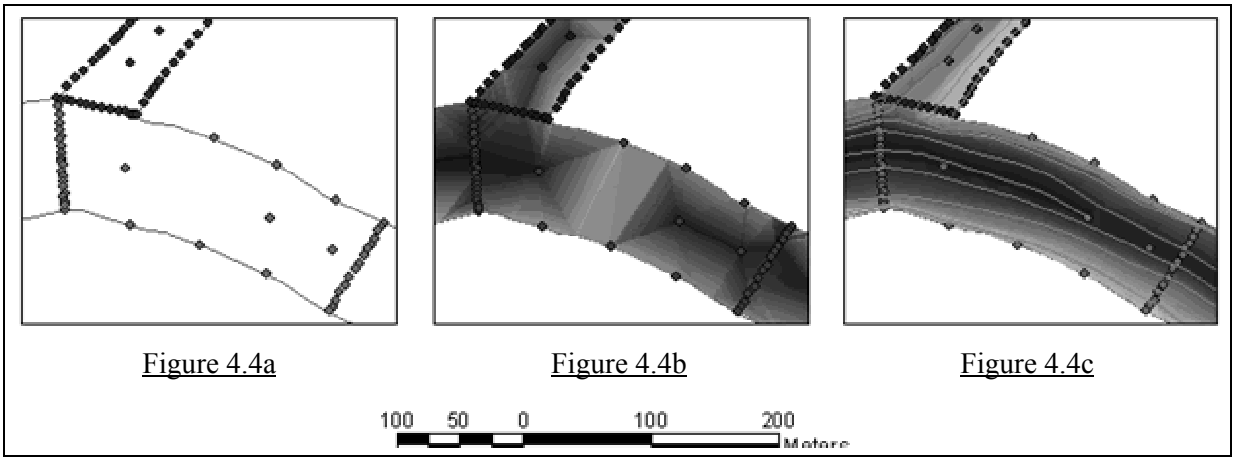

Figure 4.4a Figure 4.4b Figure 4.4c

Figure 4-4: Representation of riverbed: Confluence of Bicol and Naga Rivers

4.7. DTM of natural surface

In order to obtain flexibility during the analysis of different scenarios it was decided to develop a separate DTM's for the natural surface, road surface and building footprints. All three were finally assembled to generate the input DTM for the hydraulic model.

For the natural surface, the bridge deck spot height and contours were removed from the TIN generation. In addition spot heights obtained during fieldwork were reduced by 20 cm so that subsequent road level increase was removed from the DTM.

ArcGIS, ArcMap 8.2 version has the flexibility to select any number of separate feature classes having elevation data (i.e. contours, spot heights) to make a TIN for the study area. It allows the introduction of break lines for interpolation as hard lines or soft lines. The study boundary is then given as a polygon feature class and it will act as a clip layer or the cookie cutter to create the TIN only within the clip layer. Once the TIN surface is created it was carefully examined to avoid artificial elevated areas and sinks. Several sinks and elevated areas were identified by visual observations and corresponding input spot heights were corrected using the field experience. Additional points have been input in order to obtain reasonable triangulation during the TIN generation.

The DTM created, as a TIN surface cannot manipulate with other elevation models (i.e. roads and buildings) Moreover the TIN should be converted to raster format before input to the Delft FLS model. DTM's in raster format are highly flexible crossing and overlying operations. Due to above reasons the TIN DTM of natural surface was converted to raster format initially with a 5m grids however later it was changed into 7.5m due to the software limitations and long model run time. Both these aspects have been elaborated in section 2.3.6.1 above and section 5.4 below respectively. TIN DTM and its 7.5m-raster representation of the natural surface are shown in the Figure 4-5-a and 4.5-b respectively.

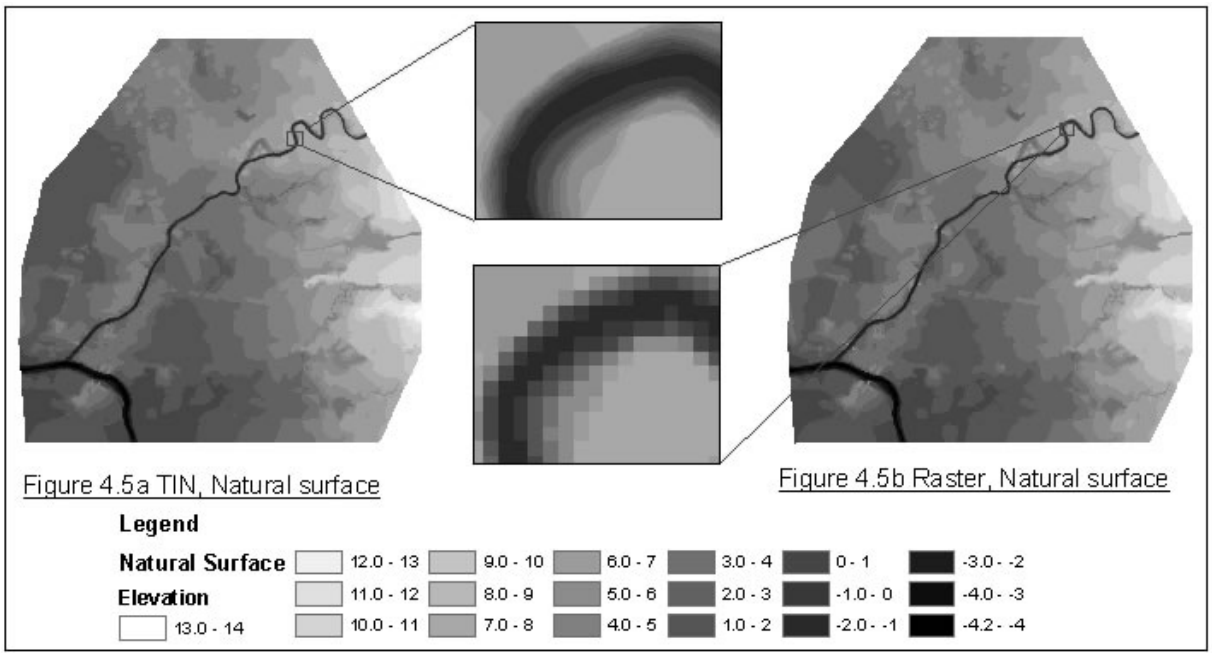

Figure 4-5 TIN and raster natural surface DTM

4.8. DTM of road network

ArcView shape file containing road centreline and road width as an attribute was obtained from the electronic data processing unit of Naga municipality. A polygon layer-representing road width was created after buffering from the road centrelines. Then TIN DTM in this road polygon was created in similar way as the natural surface DTM. In this case while contours and spot heights were assigned as mass points, the road buffer was assigned as clip layer to limit the triangulation within the road width. Even though the DTM is limited to road width all the elevation data sets were used for the triangulation. However contours representing river bed and drain spot heights were not used for TIN generation in order to avoid influence of low elevation areas to the road surface. This triangulation process was time consuming. ArcGIS, ArcMap 8.2 version took about two hours to generate 125Km long road TIN surface having 1634 road segments. Finally this TIN DTM was converted to raster DTM having grid cell size of 5m and 7.5m.

However both 5m and 7.5m raster road elevation models were not satisfactory in view of the requirement of road continuity for 2D hydrodynamic modelling as expressed in the section 4.10 below. Initial roads TIN and DTMs representing raised road surface with 7.5m and 5m-raster grids are shown in Figure 4-6-a, 4.6-b and 4.6-c respectively.

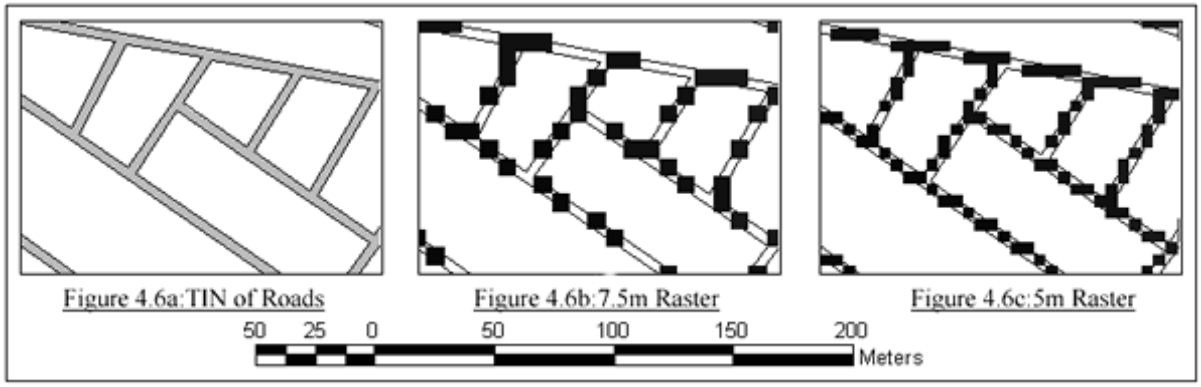

Figure 4-6: Representation of road surface elevation

4.8.1. Raising road elevation

The road elevation represented in the DTM generated above is not indicative of the present ground elevation of the road network. The reasons for this deviation are:

- All the available secondary elevation data sources were obtained before 1991.
- Provincial public works and highways have decided as a policy to raise road surface and/or change the road surface material from asphalt to concrete for safety and durability reasons. Raising the road level or changing the road surfacing is a good solution for reduction of maintenance cost.
- During the fieldwork it was noticed that most of the roads within the city are at higher elevation than the natural ground surface. It was up to 50 cm in recently developed areas.

Therefore by considering the fieldwork observations it is decided to increase all roads elevation by 20cm in the initial road DTM. Raster calculator was used to increase the road level of the previously prepared road DTM.

4.9. Buildings height representation

During a flood event in a densely developed area, buildings and structures present in the terrain will primarily decide the direction of the overland flow. Therefore accurate representation of building footprints as an obstruction to the flow in the input DTM is essential in hydrodynamic modelling.
Even though it was possible to obtain building footprints from Naga city as an ArcView shape file, building height information was unavailable. Since exact height of the building is not very crucial for the model, arbitrary building heights were decided based on the land use of the city.

The arbitrary height attribute was used to convert building footprint feature class into a raster layer representing building height, as a pixel value. This raster layer was added to the natural surface DTM to get a terrain elevation including the building height information. Three separate raster files representing building heights were created for 5, 7.5, and 10m grids in order to explore the model results variation with pixel resolution. Figure 4-7-a, 4.7-b and 4.7-c show building footprints within the study area and its 5m and 7.5m representation with close up view.

Figure 4-7: Raster Representation of Building footprints

4.10. Selection of optimum pixel resolution

In reality overland flow during a flood event mainly convey along roads. Therefore this phenomenon should be represented in the hydrodynamic model too. In Delft FLS model water can flow from one cell to the other neighbouring four cells but no diagonal flow is possible. Therefore in order to make sure continuous flow along roads, grids representing the road network should be connected to each other alongside but not diagonally. If two raster cells are connected diagonally flow path will be blocked in the model. Figure 4-6-a and Figure 4-6-b in the section 4.8 above represents the same road segments with pixel size of 5m and 7.5m respectively.

These figures show that some of the pixels are not connected each other and some of them connected diagonally. Therefore there will not be any flow through these points in the model. This is common in both 5m and 7.5m grids indicating that none of the above road DTMs represents the actual flow condition and they are not suitable input for the Delft FLS model.

Width of the roads within the Naga city varies from 12m to 2m. Roads having less than half of pixel size could not be represented in the raster format. Even though the road width is exactly equal to the pixel resolution if it is not running parallel or perpendicular to the grid coordinate system it is not possible to represent the road using continuous grids connected along side. Therefore in order to make sure continuous links of grids connected side-by-side minimum road width should be greater or equal to $\sqrt{2} \times Pixel\ resolution$. In this way roads having less than 7m in the raster layer need to be increased up to 7m in order to obtain continuous grid cell representation. Even when the road width increases up to 7m, effective roads width for overland flow is not more than 5m. It is clearly visible in

the Figure 4-8 below. Similarly road width in 7.5m raster layer was increased up to 11m if the actual road width is less than 11m. Thus a satisfactory (i.e. according to the model requirements) representation was obtained in the both cases by increasing the road widths. It is shown in Figure 4-8a and 4.8b respectively for 5m and 7.5m pixel values.

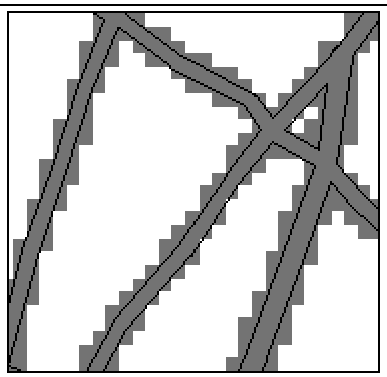

Figure 4.8a: 5m Raster

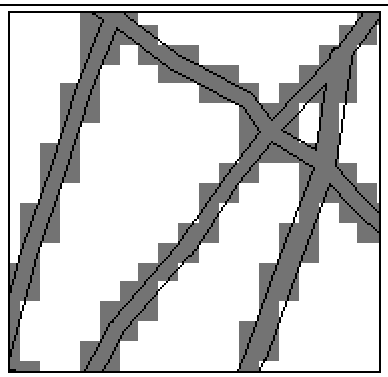

Figure 4.8b: 7.5m Raster

Figure 4-8: Modelling friendly road raster representation

The reduction of raster resolution to less than 5m provides better representation of road width. The problem is that the maximum number of pixels that the Delft FLS model stands is 497 by 497. Therefore lesser pixel resolution will limit the study area to a smaller extent.

One aspect that should be mentioned here is that despite this road representation is satisfactory from the "flowing" point of view, it produces a systematic increase in "dead areas" that do not participate in the conveyance but only in the storage. Since in this case, actual road width has increased by $\sqrt{2}$, increase in the dead area makes favourable in representing the actual road widths.

The analysis of dead area effect is complex since the problem has to be isolated from other effects. This could be eventually approach by modelling one street that flows following a raster line or a column and then the same road twisted diagonally after the pixel size is increased according to the text. However the effect of such a model does not seems to match the complexity of the real case (Naga city) to be incorporated as a fact.

Since the objective of this thesis is not the detailed performance of the hydrodynamic model but the evaluation of hazard maps, the continuity consideration overrules the extra storage effect despite the warning[5].

Though pixel resolution has an effect on representation of building footprints it is not crucial with respect to the hydrodynamic modelling. If we use 5m-raster-cell size it is possible to represent any building its area higher than 2.5 by 2.5m^2.

[5] It could be possible to evaluate the difference between D-FLS and a tin based 2-D model of finite differences. The model is available at ITC but it was not tested due to time constraints.

4.11. Combined elevation model

Three different elevation surfaces are generated as explained above with the intention of obtaining flexibility to change the elevation of one feature without influencing the others. At the end preparing individual elevation models all of them were joined to make a combined DTM representing the urban features in a single grid file.

Raster calculator and reclassification functions of ArcMap do this operation. A flow chart showing the whole process is given in Figure 4-9

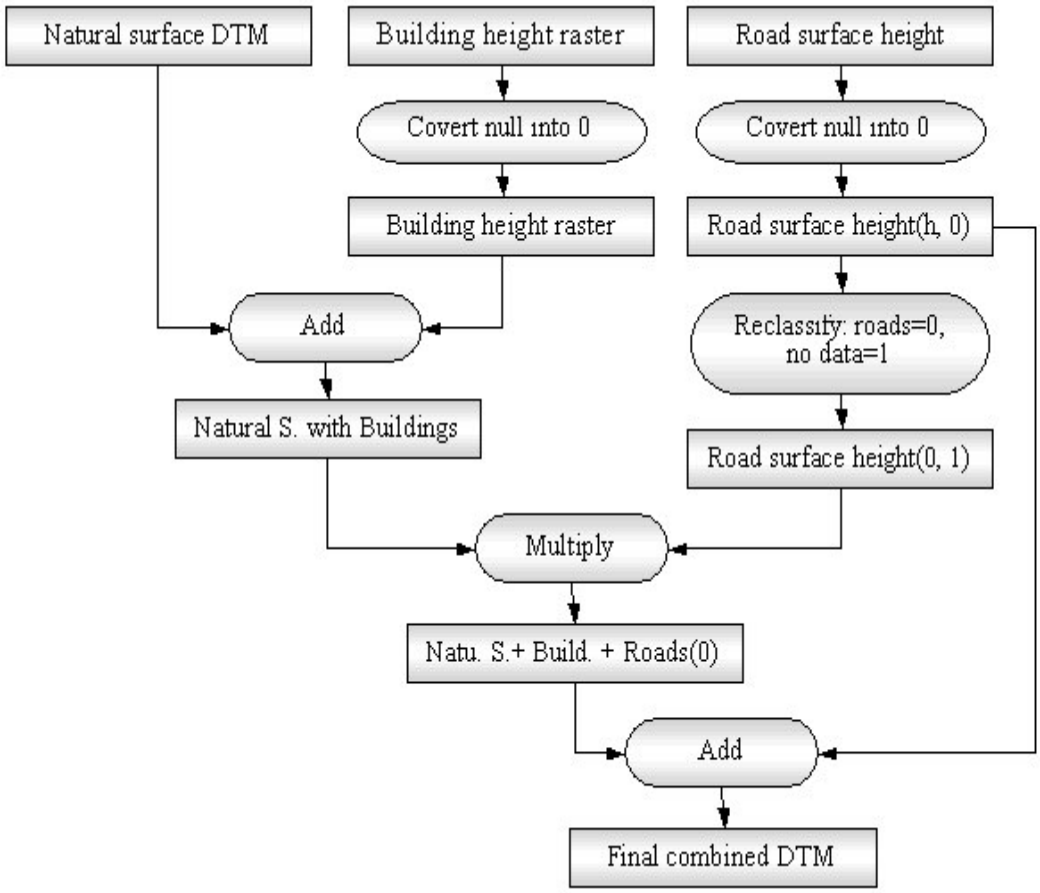

Figure 4-9: DTM assembling process

The step that has to be done carefully in this process is the representation of roads in the combined DTM. As explained above, all the road segments have to be represented as continuous grids in the final DTM. Therefore in order to avoid encroachment of pixels representing buildings into roads, the order of the joining is crucial. First the buildings were overlaid with the natural surface and later the roads raster layer was overlaid with the previously prepared combined layer. The resulting final DTM with the three DTMs used for the combination is shown in the Figure 4-10 below.

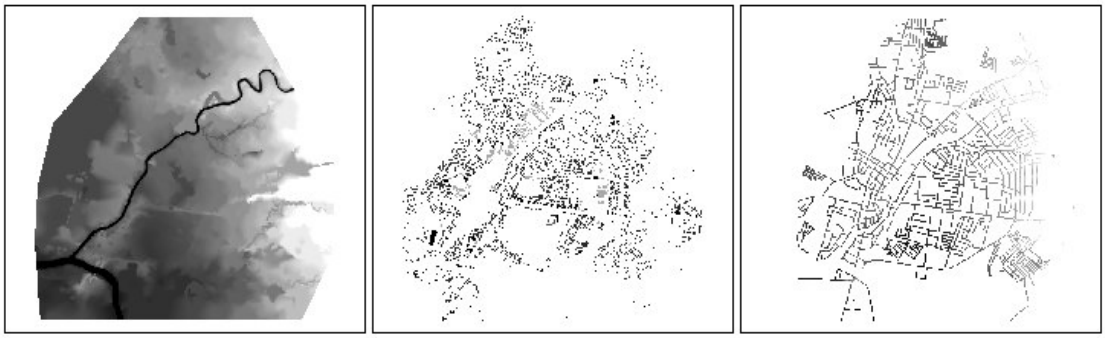

Natural surface DTM | Building footprint height | Road surface elvatiom model

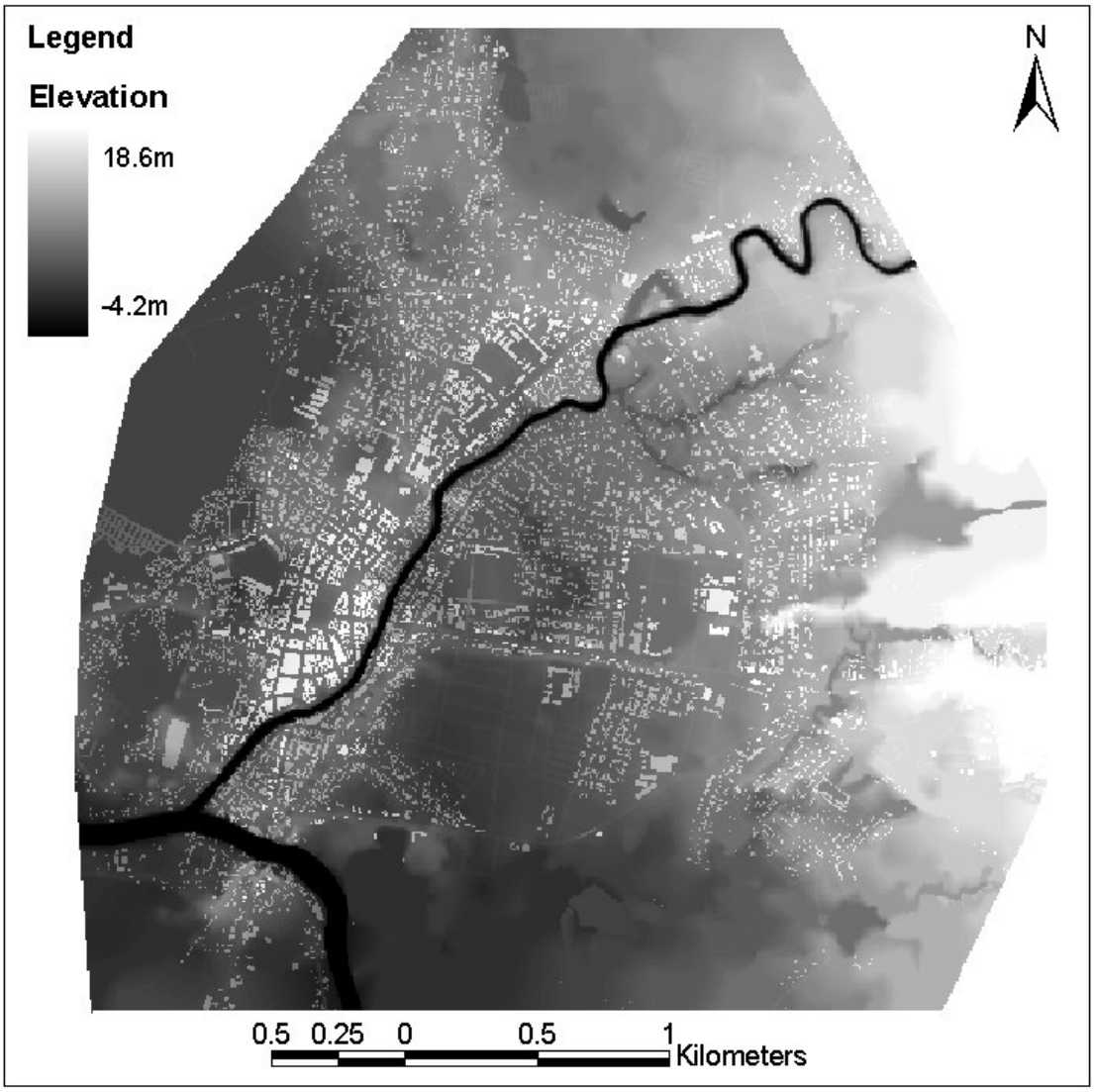

Figure 4-10: Assembled DTM for input to the model

4.12. Accuracy of DTM

Since all the field survey spot heights were used for the DTM generation it was unable to carry out any numerical test on the DTM. As an alternative natural surface DTM was converted into a hill shaded surface and visual observation was carried out to identify artificial perks and sinks. By observing the hill shaded surface it is only possible to make a relative check on the DTM to make sure that the different data sets properly refer to a common reference. In addition it was possible to identify and correct points having sinks and perks with respect to the surrounding surface. Once identify the location of the error, its data source and its attribute values can be traced. Then corresponding attributes can be replaced with an average surrounding elevation value in the attribute editor and require to generate the DTM again. These erroneous perks or sinks appears due to human errors during surveying, recording or while entering data. Figure 4-11-a represents a location of an erroneous perks and the same location after correction is shown in the Figure 4-11-b.

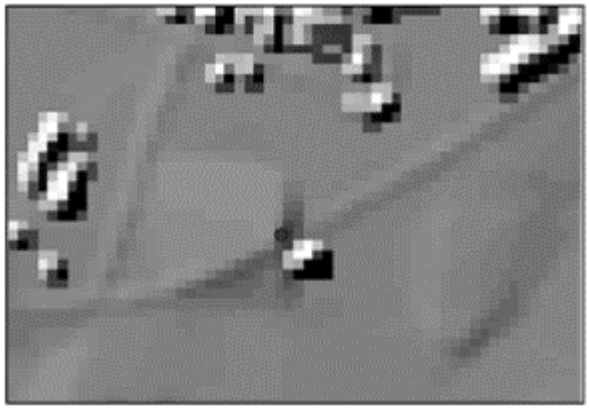

Figure 4.11a: Erroneous perk

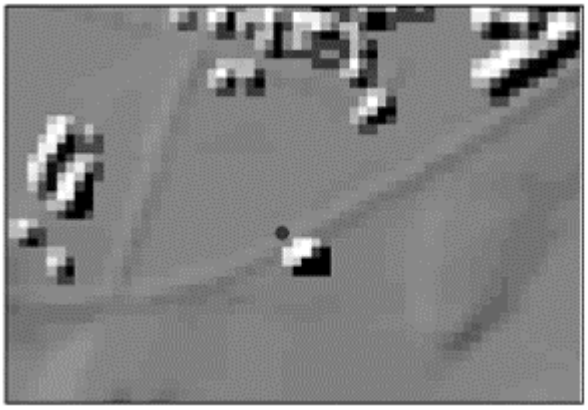

Figure 4.11b: After correction

Figure 4-11: Error identification using a hill shaded of DTM

In addition several attempts were made to check the accuracy of the DTM using the hydrological modelling extension of ArcView 3.3. Automatic sinks removal; watershed delineation and flow path generation was tried for the natural surface DTM to identify possible serious variations in the terrain. The procedure was supervised to be certain that sink removal did not carry out for the combined DTM in order to protect flow barriers created as a result of raised roads and buildings that represent the real case.

4.13. Development of DTMs with 5m and 10m spatial resolution

The key objective of this study was to evaluate the model performance for different grid cell size of the input DTM. A priori the smaller the pixel size the more accurate the calculations, but the objective behind these attempts was to find a compromise solution between feature representation, model accuracy and computation time in order to give recommendations on survey requirements from these findings.

The initial natural surface TIN was rasterised with 5m and 10m pixel to create additional two DTMs with cell size 5 and 10m. Similarly the building footprints vector layer was converted to raster by specifying cell size of 5 and 10m respectively to develop two building height raster surfaces. However

road surface DTM was created from the beginning since it was required to increase the road width by $\sqrt{2} \times Pixel\ resolution$ in order to get continuous raster surface as explained in the section 4.10 above. Therefore in 5m DTM, road widths less than 7m were increased up to 7m and for 10m grids it was increased up to 14m. Then TINs of the road surfaces were created within the road polygons. Then it was converted to a raster surface by specifying the corresponding grid cell size. Finally DTMs of natural surface, building height and road surface of 5 and 10m cell size were combined together and created combined 5 and 10m DTMs to input to the model. Combined 5m, 7.5m and 10m DTMs are shown in the Figure 4-12 below.

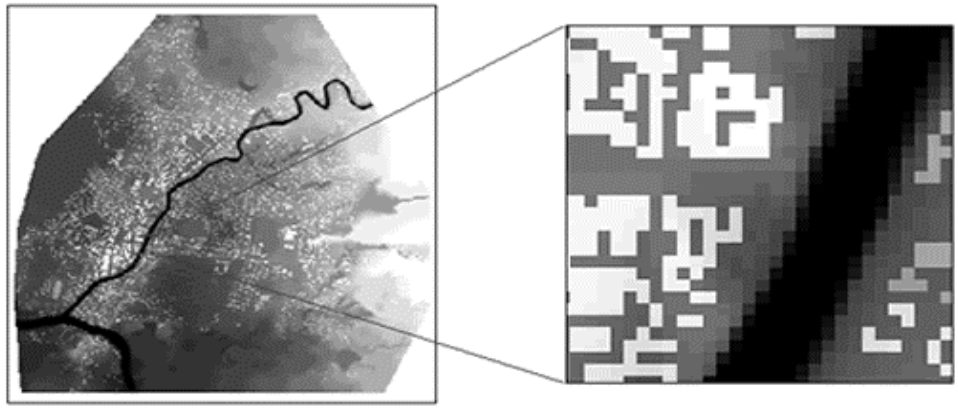

Figure 4.12a: 5m DTM

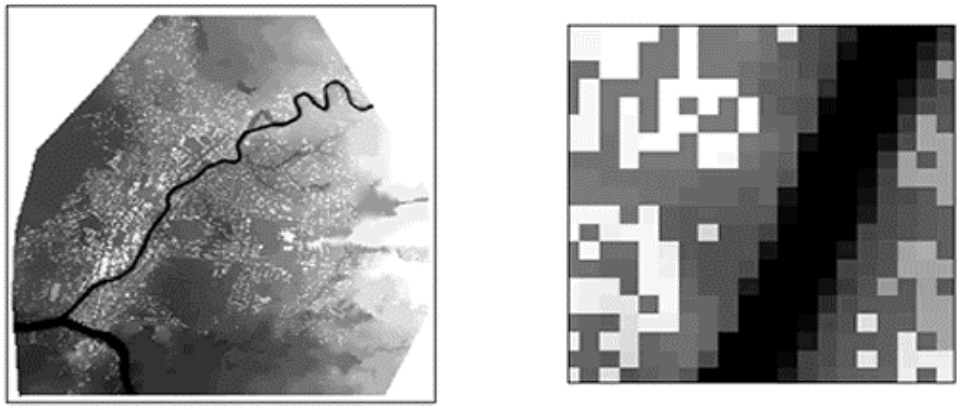

Figure 4.12b: 7.5m DTM

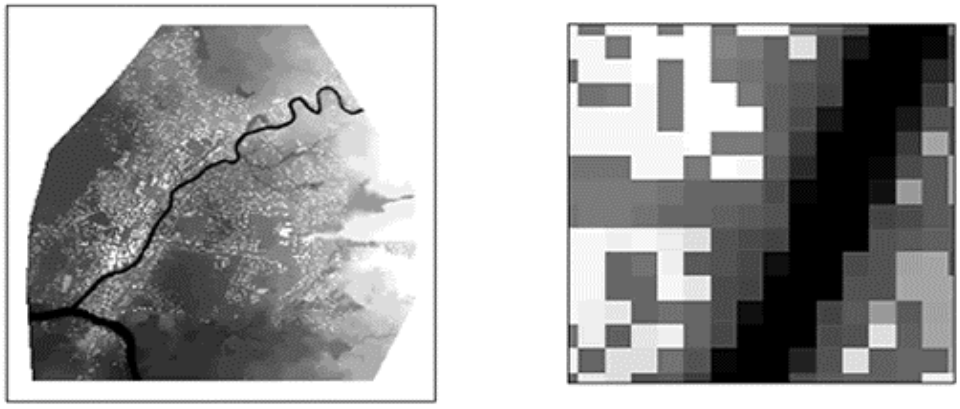

Figure 4.12c: 10m DTM

Figure 4-12: DTMs with different spatial resolution

4.13.1. DTM preparation for input to 2D models

These three combined DTMs were converted into ArcInfo ASC II raster format using the ArcToolbox of the ArcGIS software. Both 2D models (SOBEK and Delft FLS) accept the terrain elevation in this file format.
Procedure of inputting the DTM as well as the other parameter in to the model is described in the next chapter on Hydrodynamic modelling.

5. Hydrodynamic modelling

5.1. Introduction

This chapter explains the data input procedure for 2D models and describes the output results of the models. Delft FLS 2.47 was used for initial model runs. However, at the last stage of this research SOBEK was available which allowed including a 1D (Naga and Bicol Rives) component to the 2D model already developed. Among the nine simulation modules available in SOBEK, the overland flow module is identical to the Delft FLS model. Delft FLS as a stand-alone module typical 1D flowing features like rivers and canals could not be adequately represented. Therefore when modelling with Delft FLS, 1D Rivers streams etc have to be incorporated in the DTM. However with a low resolution DTMs it is quite impossible to represent a river or a canal in the DTM with required accuracy. With SOBEK, the other main limitation of delft FLS was eliminated since SOBEK accepts any number of pixels in the input DTM.

Combined channel flow and overland flow modules of the SOBEK are used for the modelling. In the 'channel flow module', river cross sections were entered at about 300m intervals. In the 'overland flow module' the DTM was input. With this approach it is possible to incorporate even small urban drainage lines in the model. However drainage lines were not incorporated due to non-availability of drainage layouts. However this study was aimed to identify inundation for more than ten-year flood events and most of the drainage paths do not function once river water level exceeds 0.5m from the M.S.L

.

5.2. Input data

In Delft FLS version 2.47 all input data has to be specified in the master definition file (*.mdf). However in SOBEK there is an advance graphical user interface (GUI) and several data input forms are available to ease the data input. In both models data requirement is the same except for river cross sectional details, which have to be specified in the case of SOBEK. Delft FLS master definition file used for simulating 7.5m DTM is given in the annexure A2.

5.2.1. Geometric parameters

In Delft FLS

Geometric parameters required for Delft FLS are:

- Pixel size (DX)
- Number of pixels in west to east and south to north (MMAX, NMAX)
- Centre coordinate of the pixel located at bottom left corner of the study area (Xo, Yo)
- DTM of the terrain.

Though there are nine methods available to input the terrain elevation, the most convenient method is Arc info ASCII file format. Since the DTM was generated from ArcGIS it straightforward to convert the raster grid file into ArcInfo ASCII format using the ArcToolbox. Null values must be specified in pixels representing the boundaries of the study area. Finally the edited DTM was input to the model just by specifying it name in the master definition file. The input geometric parameters of the master definition file of Delft FLS model are shown in Figure 5-1 below.

```
********************************* DELFT-FLS Master Definition File (*.mdf) ***
* Trial 2 Naga River
********************************* GEOMETRY PARAMETERS ************************
MAIN DIMENSIONS                   MMAX   NMAX
                                  488    489
GRID                              DX     X0          Y0
                                  7.5    518927.75   1505195.75
COMPUTATIONAL GRID ENCLOSURE

HEIGHT                            ARC-INFO naga_dtm.asc
```

Figure 5-1: Input geometric data in master definition file of Delft-FLS

In SOBEK

Geometric data input and editing is easier in SOBEK with its Windows based user interface. It has the facility to add several GIS shape files as background layers to facilitate the data input. NETTER is the data input and editing interface of the SOBEK. It provides two separate menu bars to input and edit 1D feature like rivers, drains and 2D floodplain as a 2D grid layer.

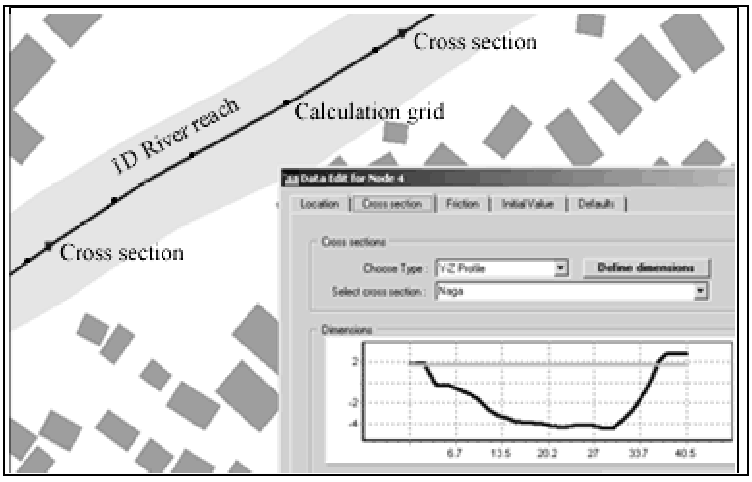

Figure 5-2: 1-D network with cross sections in SOBEK

First the 1D river system or channel network is defined in the in the NETTER using 1D nodes, later those nodes are connected as a network using "connect node" option. The resulting straight-line river network has to be reshaped to follow the real river geometry using "edit reach vector" option and additional close calculating points are incorporated (i.e. 100m apart) along all reaches. River cross sections along reaches can be input using inbuilt icon and specify the corresponding cross sectional dimensions. The Figure 5-2 shows a 1D river reach, two cross sections and several calculation grids along

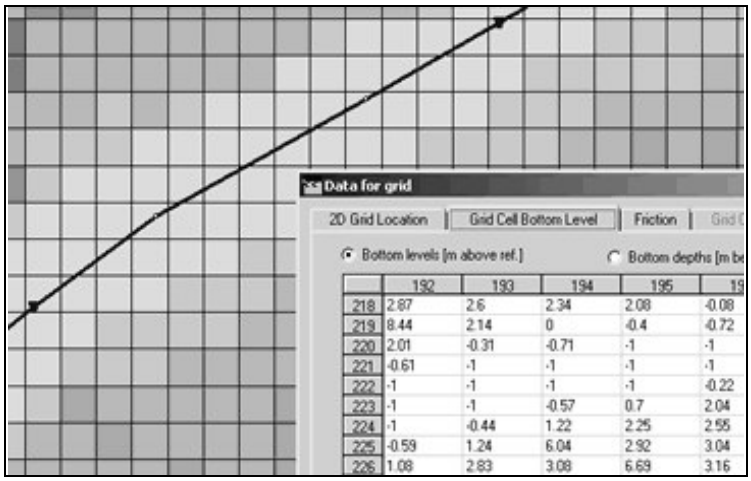

Figure 5-3: 1-D network & 2D grids and grid cell editor

the reach. At the background of the network two GIS layers containing building footprints and Naga River are shown.

Then ArcInfo ASCII DTM can directly input to the model using the "2D grid" tools. The NETTER is equipped with user-friendly grid value editing facility in the grid cell editor. The Figure 5-3 above shows the imported 7.5m Naga DTM with the river network as 1D feature. The small window within the figure shows the pixel values of each cell. At this stage each cell values can be edited in manually using the grid cell editor. This is especially useful when it is required to edit the DTM for various simulations or to create null pixel values along the boundary of the study area. SOBEK 1D node structure for river network is shown in appendix A4.

5.2.2. Initial flow conditions

In both Delft FLS and SOBEK there are two basic techniques available to initialise the water level in the model and start the simulation. These are known as "cold" and "hot" start. "Cold" start specifies zero initial velocity and constant water level at specific grid points within each river reach. In FLS those grid cells representing initial conditions have to be specified in the master definition file using column and row number (M, N) of each grid cell. In this case three points in each river reach were specified zero water level. However the program allows entering global initial value for whole system or local values for each reach. These points were located at upstream of Naga and Bicol Rivers and downstream of Bicol River.

Then the program automatically fills the study area up to the specified water level and starts the simulation from that level onwards. However, initial computation time to reach the initial water level can be saved using "hot" start. This approach specifies a "restart file" which is automatically generated at the end of each successful model run. This file provides the initial velocities and water depths to start the computation again.

```
********************************* INITIAL CONDITIONS ************************
INITIAL WATERLEVEL                M    N    ZETA0
                                  421  373    0    Naga
                                  140   2     0    Bicol_up
                                    4   89    0    Bicol_down

RESTARTFILE
```

Figure 5-4: Inputting initial water levels into Delft-FLS

In SOBEK initial water level and discharge can be specified in each network reach locally or global value can be specified for the entire network at once. In this case water levels of zero were specified to start the computation in all three reaches.

5.2.3. Boundary conditions

Boundary conditions simulate the action that external flow or water energy produces over the modelled system. There are several options to specify boundary conditions in both models. They are water level, velocity, discharge, or as a rating curve. For this model a flux (discharge) files were specified for Naga River and time series water level was specified at Bicol River upstream. A rating curve was

specified for down stream of the Bicol River. Flux in north and east direction is positive while south and west direction is negative. Data and methods use to generate those rating curve and flux files for ten-year return period flood event are explained below.

5.2.3.1. Rating curve of Bicol River down stream

Bicol River meets San Miguel bay after running about 30km from Naga city. Furthermore the bed level of Bicol River at the progressive of Naga city is about 4m below mean sea level (MSL). Therefore Bicol River near the Naga city is affected by tidal influences since no critical section occurs between Naga and Bicol bay. As a result, in the past any rating curve was not developed for the Bicol River in the proximity of Naga city. Ombao is the nearest location having a rating curve in the Bicol River. It is about 40km upstream of Bicol River from Naga city, and tidal influence is not affecting at this progressive.

There were two options available to obtain an approximate rating curve for the model.

- Mike 11 model outputs given in the Nippon Koei report of year 2003.
- Delft-FLS model developed parallel to this study for Bicol River down stream from Naga city.

Limited Mike 11 model results were fitted with a curve and used in the initial model runs. The resulting rating curve is shown in Figure 5-5.

However just at the last stage of the research it was possible to obtain a rating curve exactly for the downstream boundary from Delft FLS model developed for the Bicol River down stream from Naga city under another study. It was used for the calibration of the model and shown in the Figure 5-19 below

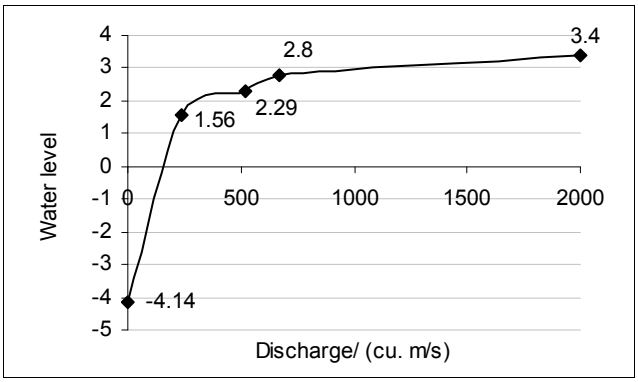

Figure 5-5: Mike 11 model results at Camaligan station, Bicol River

Source: (Nippon_Koei, 2003b)

The importance of the lower boundary condition when simulating sub critical flow systems like the Bicol is decisive. In this particular case the downstream boundary of the model is affected by tides. The event producing the flooding at Naga (typhoons) has a random nature and it is not related with the tidal fluctuations. The worse scenario occurs when the flood wave arrives to Naga just at the moment that the backwater effect produced by a high tide at the San Miguel Bay reaches a maximum, and this has a random nature. During typhoons the strong winds may dramatically increase the natural height of the tidal harmonics, or dramatically reduce it depending on the main wind blowing direction. Naga has a long history of typhoons, and few events were catastrophic. The initial hydraulic status of the rivers immediately before these events was variable, but the overall evaluation indicates that alert rises in any situation when the river reaches a certain water height. If the storm comes under this condition, even when the event has a relatively low return period, then a flooding has a high chance to occur.

The duration of the flood is intimately related to the storm duration. This explanation supports the hypothesis of establishing high and variable water level at the downstream boundary of the model certainly related to but not attached to tidal fluctuations.

Figure 5-6: Level of alerts in the Bicol River Basin.
(Camaligan is the closest station to Naga city)

5.2.3.2. Naga River time series discharge

The non-availability of any discharge measurement in the Naga River is the major limitation of this modelling attempt. It was not possible to model any rainfall runoff model for the Naga watershed without having observed discharge measurements in the Naga River at Naga city.
There were two alternative approaches found to identify an input hydrograph to the Naga River upstream boundary.

- Mike 11 model hydrograph for ten year rainfall event prepared by Nippon Koei Co. Ltd in 2003 for ten-year return period. It is shown in Figure 5-7a.
- Using a parallel study conducted by another student to develop rainfall runoff model for the Naga watershed. Ten-year hydrograph developed in that study is shown in Figure 5-7b.

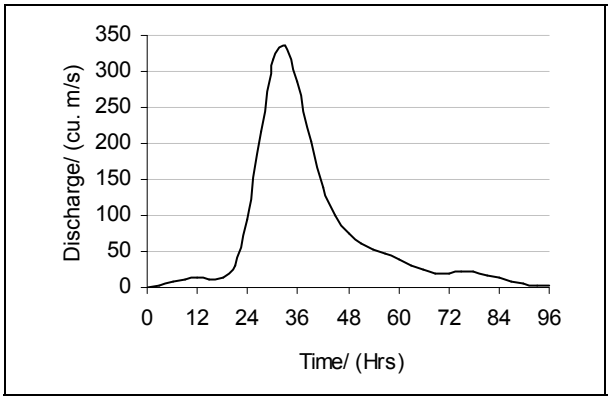

Figure 5-7a: Mike 11 model of ten year hydrograph
Source: (Nippon_Koei, 2003b)

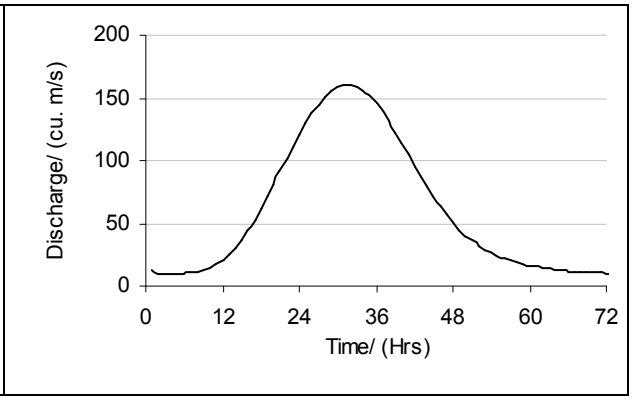

Figure 5-7b: Hydrograph of HEC-HMS model developed at ITC
Source: (Wijetatne., 2004)

Both the hydrographs are based on model results and not calibrated with observed records. However, considerable deviation was observed in two approaches.

In the Nippon Koei study they have considered total extent of Naga watershed as 88 Km^2 while in the second study it has considered as 58 Km^2. Also ten-year rainfall event used for the second study has based on 1991 HEC1 model design rainfall while that of Nippon Koei used was unknown. Furthermore "recent rainfall events seems to have altered the statistical

properties of the extreme method projections" (Nippon_Koei, 2003a). Therefore higher design rainfall may have been used by the Nippon Koei study by considering these recent extreme events.

Due to the time constraints, this study was used only first hydrograph developed by Nippon Koei consultants as input to the 2D model.

5.2.3.3. Approximation of Bicol River upstream time series water levels.

During most of the typhoon events time series of water level were recorded at the Camaligan station. Since Mabulo gauging station[6] at Naga city is not operational since 1982, the exact boundary conditions at the upstream of the Bicol River were unavailable. However, the distance between Camaligan station[7] and Bicol River upstream model boundary was about 1.7Km. Locations of both river-gauging stations are shown in the Figure 5-8. Therefore for the initial model simulations water level records measured at Camaligan station were used as boundary conditions of Bicol River upstream. This approximation results in an underestimation of water levels in the Naga city. Therefore during the calibration of the model this approximation was corrected using initial model results.

Input time series water level at Camaligan station recorded during typhoon Ruping in 1982 is shown in the Figure 5-9. Due to the extensive computation time the simulation was limited to the rising limb (i.e. up to 96 hrs) of the water level, since this simulation was intended to verify the downstream boundary condition.

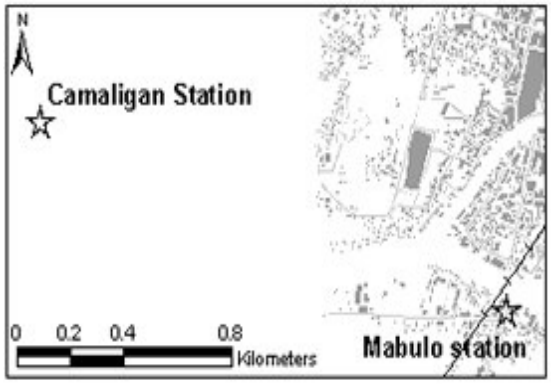

Figure 5-8: Locations of river gauging station at Naga city

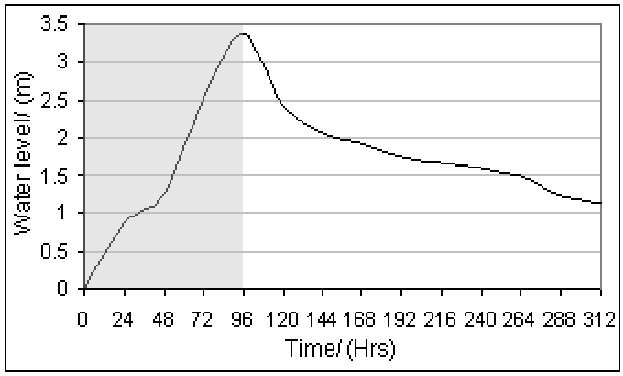

Figure 5-9: Bicol River time series water level at Camaligan station for typhoon Rufing

[6] Location 13º 37' 00" N, 123º 10' 56'E
[7] Location 13º 37' 17" N, 123º 09' 54"E

5.2.3.4. Transformation of Camaligan station water level to Bicol upstream boundary

First, the water level variation at two points in Bicol upstream and downstream were obtained form the initial model run which was simulated using Camaligan station water levels. The resulting water level vs. time plots for these two points are shown in Figure 5-10. The plot shows agreement in the initial approximation. However during the calibration Bicol river upstream water levels were adjusted by adding 2cm to the Camaligan station water levels. This value was the average water level difference between Bicol upstream boundary and Bicol downstream boundary.

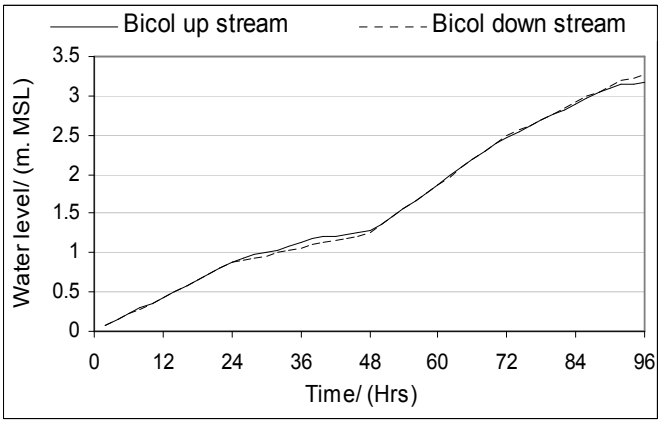

Figure 5-10: Water level variation in Bicol down stream and upstream

5.2.3.5. Boundary conditions in Delft FLS

Time series water level in Bicol upstream was specified as "*.lev" file and time series discharge was specified in Naga River as a flux files with extension "*.flx". For Bicol downstream a rating curve was specified with extension "*.qh". In the model, the grid cells representing any of these open boundaries should either be vertical or horizontal. The locations of the boundary cells were specified using column and row number representing the starting and ending boundary cells. Description of boundary conditions in the master definition file of FLS is shown in the Figure 5-11 below.

```
********************************* BOUNDARY CONDITIONS ***************************************
OPEN BOUNDARIES                   M1   N1   M2    N2    TYPE  FILE TIME-SERIES
                                  317  280  317   280    5     naga10.flx
                                  103  1    108    1     2     bicol10.lev
                                    3  62    3     73    8     9    62    9   73   -1   Qh_bicol10.qh

BREAKING DAMS                     M    N    TO    FILENAME

PUMPS
```

Figure 5-11: Input file for Boundary conditions in Delft FLS

5.2.3.6. Boundary conditions in SOBEK

A 2D grid cell boundary or a 1D network boundary can be used to input boundary conditions in SOBEK. 2D grid cell boundary is useful when sufficient hydrological data is not available to specify the boundary conditions.

In that case "2D boundary node" containing time series water level can be specified. However if there is sufficient hydrological boundary data in the 1D network "1D boundary nodes" can be used at 1D reaches. In this case 1D boundary nodes were added at Naga River upstream, Bicol River upstream and Bicol River downstream end.

Similarly to FLS, Naga River upstream boundary was assigned ten year hydrograph while Bicol River upstream was assign the time series water level corresponding to Typhoon Rufing. The boundary node at the end of Bicol downstream was assigned with rating curve shown in Figure 5-19 in page 54 below. The Bicol River 1D boundary node with its time series water level is shown in the Figure 5-12.

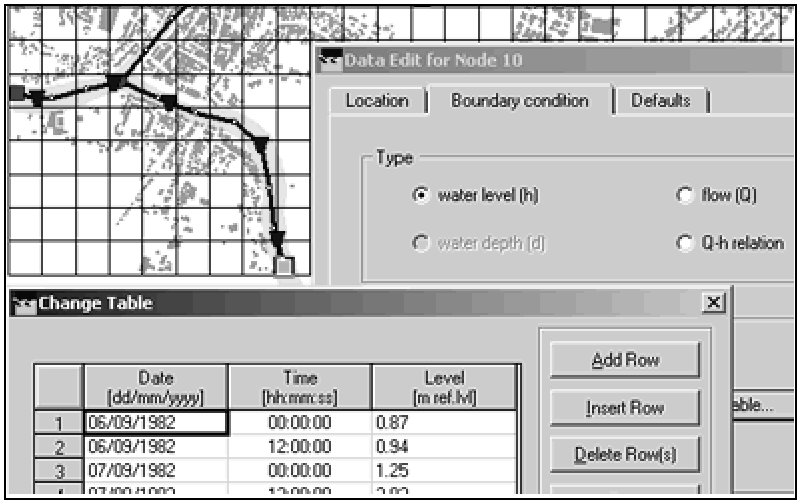

Figure 5-12: Boundary nodes and input screens of boundary data in SOBEK

5.2.4. Simulation time frame

In FLS three parameters use to specify the time steps and duration of the simulation. They are computational start time (TSTART/ hrs), end time (TSTOP/ hrs) and computational time step (DT/ s). In this case 0 hour, 96 hours and 10 seconds were assigned respectively. By default all model input and output information is in hours except DT. A good computational time step should be decided by considering that: $V_{\max} \times \frac{DT}{DX} < 1$.

Where:

- V_{max} is the maximum expected computed velocity.
- DT is the computational time step and
- DX is the grid cell size.

In SOBEK these parameters can be specified in the setting blocks of the channel flow and overland flow modules.

5.2.5. Bottom friction

In the both models there are several options available to incorporate bottom friction of the flood plain as well as channel network in case of SOBEK. It is possible to specify roughness as Manning's, Chezy's or Colebrook parameters. Also flexibility is given to input constant roughness value for whole flood plain or varying roughness for each grid cell using ArcInfo ASCII grid file.

There are several procedures to improve roughness estimations based on simple RS techniques and land cover maps. However the available imagery was inappropriate for this attempt due to cloud cover and lack of ground truth. The impact of roughness in the model is considerable and it has to be investigated more in detail. For this thesis floodplain roughness was specified based on land use and a reclassification from standard tables as it is normally done in studies of this magnitude and purpose.

First the land use map of Naga municipality was reclassified into four classes as residential, commercial, Agricultural and open lands. Then Roads and building footprint layer was overlaid with the land use map and another two classes were prepared for roads and buildings. Subsequently following roughness coefficients (Manning's n) were assigned to a new attribute field in the land use map.

Roads	0.025
River	0.03
Commercial zone	0.032
Residential areas	0.035
Agricultural zones	0.040
Building foot prints	1.000

Source: (West_Sacramento, 2002)

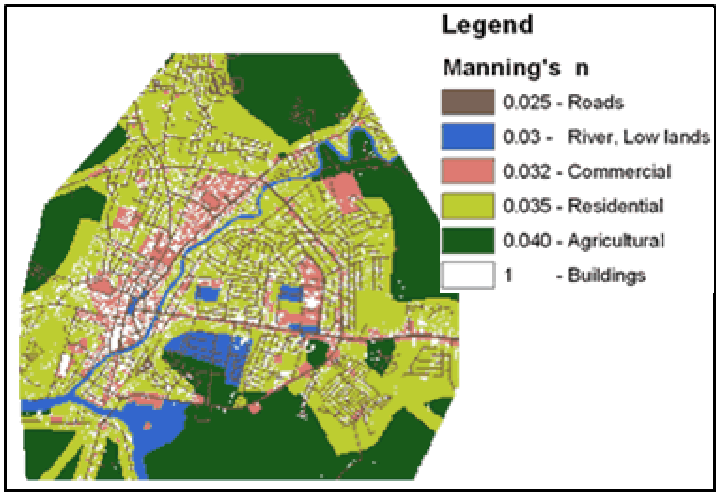

Figure 5-13: Hydrological roughness of floodplain

Building footprints were given very high roughness in order to make sure no flow through those cells. Then vector land use map was rasterised using the "Manning's n" attribute class. The resulting raster Manning's coefficient layer is shown in the Figure 5-13 above. Finally this layer was converted to ArcInfo ASCII raster format using the ArcToolbox of ArcGIS and then input to the model.

5.2.5.1. Channel friction in SOBEK

In the cross section data editor any number of roughness classes could be specified for each cross section. This allows the developer to specify different roughness classes for effective flow path and riverbanks separately based on site observations.

Since floodplain roughness has already been assigned at pixel level, single roughness coefficient of 0.030 was specified to the riverbed.

5.2.6. Output parameters

Both the models are capable of providing several output files at user specified time frames by specifying them in "output parameter" section. The following parameters can be pre-selected.

Discharge at sections – Discharge through a particular cross section is possible to obtain with time series. It is very useful tool to develop a rating curve for a particular station in the River.

History stations – At a history station calculated water levels are saved for each time step of simulation. It is helpful to observe water level variation at a particular point during a flood event, and to compare several scenario results.

Restart Interval – By default a restart file is created at the end of each successful model run. However time interval can be pre-specified when it is required to create a restart files during the simulation. Then each pre-specified time intervals restart file will be created and overwritten the previously cre-

ated file. The last restart file created could be used for next simulation if the computation fails before ending the complete simulation.

Quantities in map files – This allows the pre-selection of the map files to be saved during the simulation. Water depth (H), Flow velocity (C), Water level (Z) and velocity components (u,v) are the available map files for pre-selection.

Maximum quantities in map files – In addition to the selection of required map files at simulation time steps; it is further possible to generate files having maximum quantities of each output parameter at pixel level. For example if it is specified to create the maximum flow velocity file, the program will create a raster file containing the maximum flow velocities experienced by each pixel during the full simulation period. This information is very useful when it is required to prepare flood hazard map.

5.3. Program output

There are three basic output information produced at the end of each successful computation. They are:

- ASCII raster map files indicating spatial distribution of pre selected parameters (i.e. water levels, water depths, average and u, v velocities) at specified time intervals.
- History plots, graphs of selected parameters vs. time at pre selected stations.
- Animations using incremental water depth or velocity map files.

The resulting output information are similar in both Delft FLS and SOBEK, however SOBEK provides in addition 1D channel water depths and velocities. Also it has a GIS based Viewer to create required maps and convert resulting animations into AVI movie files.

5.4. Model computation time

Extensive computation time is a major constraint in 2D hydrodynamic modelling. Model run time in FLS as well as SOBEK is directly proportional to number of pixels in the DTM and maximum computed velocity. In Delft FLS with 488 by 489 pixel in the 7.5m DTM took about five days to simulate 96 hours flood event in a 1200 MHz Pentium processor. However the same processor for 10m DTM spent only 14 hrs to complete the computation.

It was unable to compare difference in computation time between Delft FLS and SOBEK since SOBEK simulation were carried out with 2.8Ghz process. However in general SOBEK takes higher computation time than DELFT FLS. The resulting computation times are shown in table 5.1 below.

	10m DTM	7.5m DTM	5m DTM
Total number of pixels	366*367	488*489	732*734
Computation time in 2.8Ghz processors[8]/ (hrs)	15	54	132

Table 5-1: Computation time in SOBEK in a 2.8Ghz processor

5.4.1. Depth of inundation

The model simulations were carried out for ten year return period representing four-day typhoon event and output results were obtained at one-hour intervals. Therefore 96 ASCII raster water depth files were resulted during a single simulation. First these files were converted to ArcGIS grid file format using ArcToolbox and later they were georeferenced in order to overlay with the other GIS layers for analysis. The resulting water level file (after 40 hours of simulation) overlaid with hill shaded urban terrain is shown in the Figure 5-14 above.

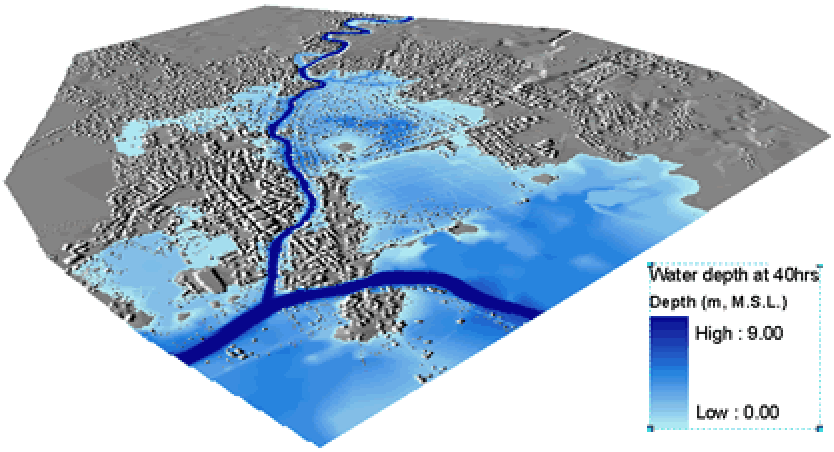

Figure 5-14: Depth of inundation after 40 hrs of simulation

5.4.2. Flow velocity variation

Similarly to the depth of inundation, the average velocity of floodwater also computes at every time step of simulation and record as ASCII raster file format. Therefore it is possible to examine the velocity variation with time within the floodplain once velocity files are converted and overlaid with the study area.

During the analysis these velocity files were combined with the corresponding wa-

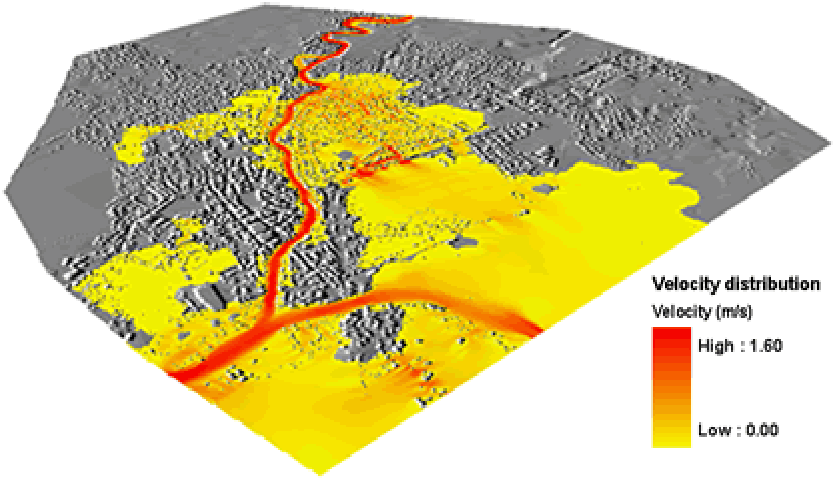

Figure 5-15: Velocity of floodwater after 40 hrs of simulation

[8] These computation times valid only for the DTMs of this study, it will change considerably with the terrain slope. Lower the time for flat terrains.

ter depth files and created energy maps for flood hazard mapping. The velocity distribution after 40 hrs of simulation is shown in the Figure 5-15 above

5.5. Delft FLS vs. SOBEK

The main difference between the two models with respect to data input is; SOBEK provides window based graphical user interface and several data input forms make the data entry easy and accurate. Network validation and flow model checking options prior to simulation will obviously save lot of time by pointing out errors. Otherwise computation will be crashed during half way of simulation. Also GIS based NETTER of SOBEK is a convenient interface for data entering and output result viewing. Inundation depth and water level variation within the channel network can directly be animated in NETTER. Also it has a facility to record the animation as an AVI movie file and view the movie file in any media player. However compared to Delft FLS, SOBEK is quite complex to learn within limited time since it is made up of combining several flow models.

	Delft FLS	SOBEK
Computation time	Lower	Higher
Window based graphical interface	No	Yes
Network validation and check before simulation	No	Yes
Limitation on number of input cells	Yes (497 * 497)	No

Table 5-2: Comparison of Delft FLS vs. SOBEK with respect to data input

5.6. Model validation and calibration

Model calibration was conducted with the ten-year hydrograph of MIKE 11 model as shown in the Figure 5-7 above. Resulting maximum inundation extent was compared with inundation maps prepared by Naga municipality based on observed flood levels in the Naga city. Even though those flood maps were classified according to “High” “medium” and “low” flood hazard categories, it does not specify corresponding water levels. Naga municipality inundation extent maps are shown in Figure 5-16. Since these observed inundation extent maps were already categorized into 5, 10, 20 year return periods, it was possible to compare the model simulation of ten-year flood event with the corresponding observed inundation extent map. Observed inundation extent corresponding to ten year flood event is shown in Figure 5-16 below. Calibration of the model in terms of flood boundary conditions was hampered due to following reasons.

- The exact rainfall event that has developed the above maps is unknown.
- Rating curve of the Naga River used for the model simulation is not tested. Therefore discharge data used for simulation is very rough.
- Computation time restricted the several simulations trials.
- The model did not incorporate the inflow coming to the city through small creaks located at North West of the study area.
- Bicol River water levels corresponding to the ten-year discharge of Naga River also approximated in these simulations.

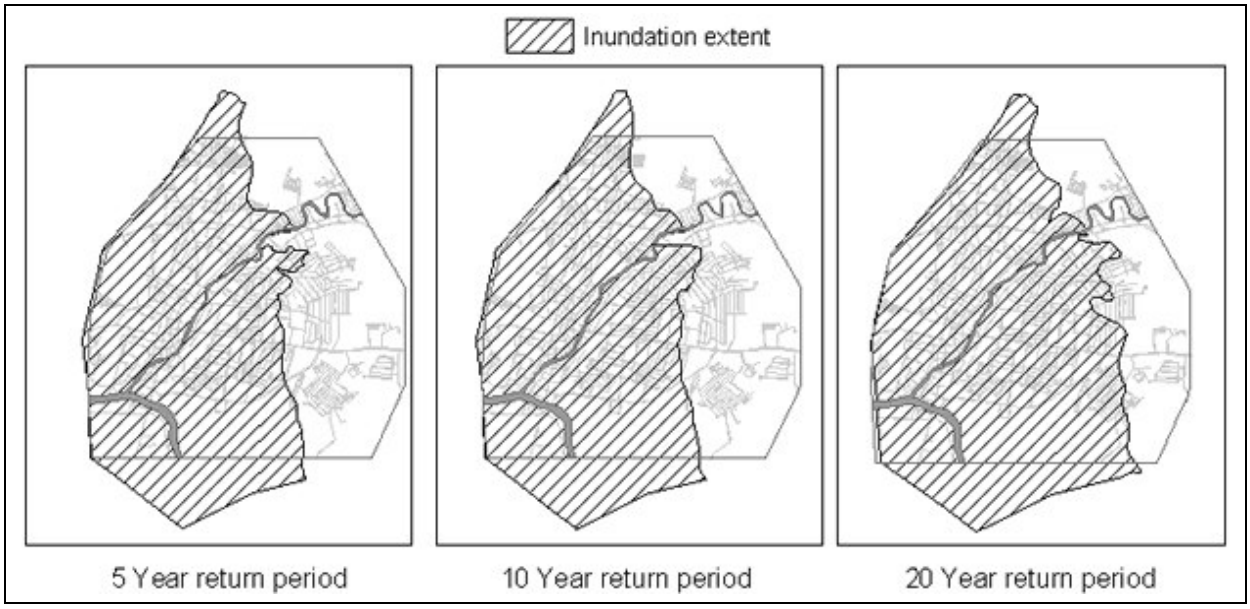

Figure 5-16: Inundation extent maps prepared by Naga municipality

Source: Electronic data processing unit Naga municipality

Three trials were decided by changing the Manning's roughness of the floodplain. The Manning's roughness coefficients used for each simulation were given below.

Land use	Initial run	Trial 1	Trial 2
Residential	0.035	0.032	0.038
Commercial	0.032	0.028	0.035
Agricultural	0.04	0.035	0.042
Open land/ River	0.03	0.025	0.032
Roads	0.025	0.022	0.028
Buildings	1.00	1.00	1.00

Table 5-3: Manning's roughness coefficient used for calibration of the model

5.6.1. Comparison of inundation extent

Each trial simulation inundation extent was compared with the existing Naga municipality observed inundation map of ten year return period. Maximum inundation extent corresponding to the Trial 02 is shown in the Figure 5-17 below.

Considerable deviation was observed in North of the city. Though the observed records shows inundation in north of the city, model results depicts trickle in that area. Reason for this variation was investigated with the 2D model developed for the Bicol downstream and observed that this area inundates due to the flow coming from the Bicol River downstream in the direction of the arrow shown in the figure 5.13 above. Since west of the city is belt of low lands excess water flow of Bicol runs to north of the city through this belt. Since model area of this study is limited to the city, it was unable to represent such a flow in this model.

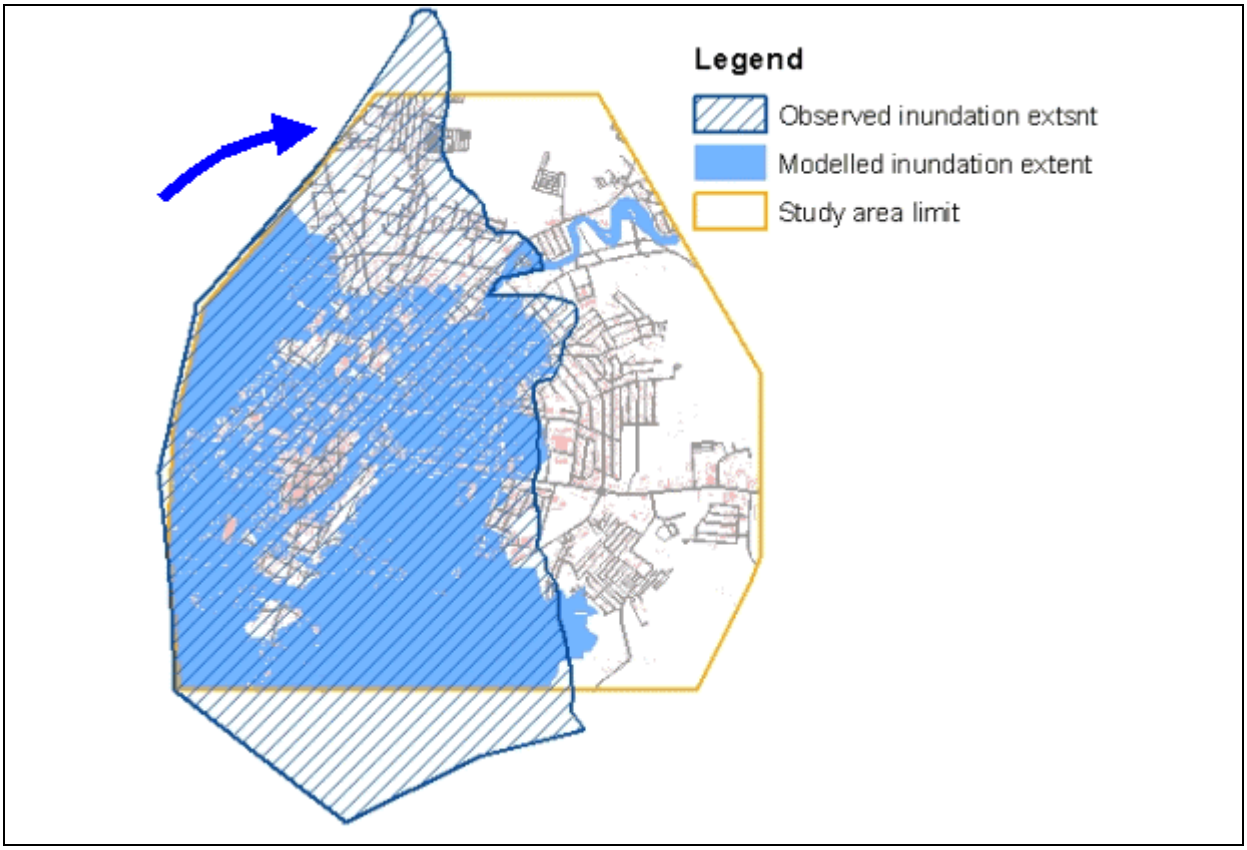

Figure 5-17: Observed and modelled inundation extents for ten year return period flood event

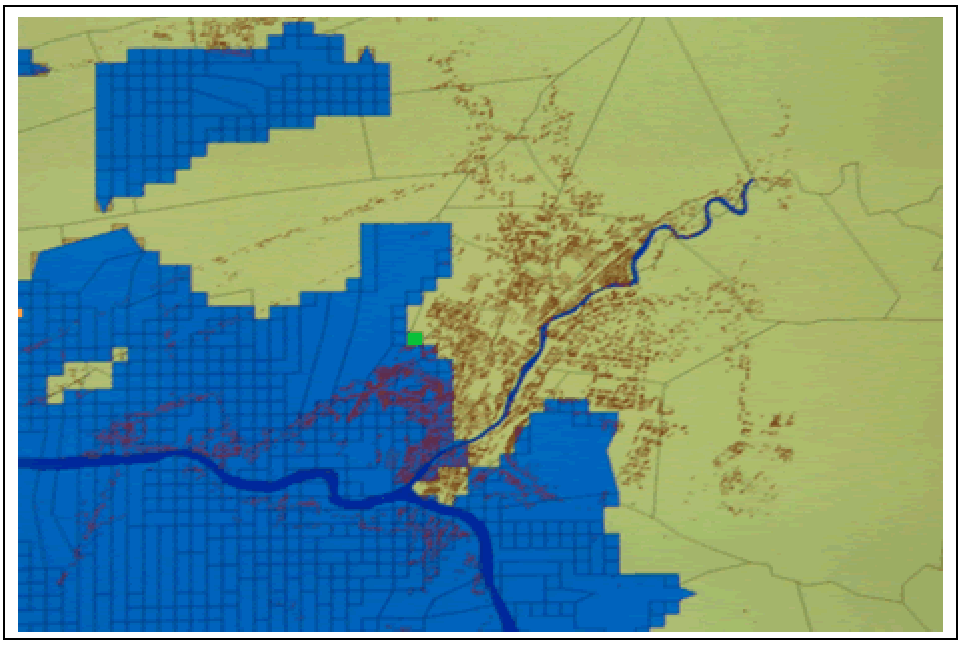

Figure 5-18: Screen picture of the Mike 11 model results prepared by Nippon Koei

In addition observed record shows the city centre has inundated during ten year return period flood event however, according to the model results isolated spots of the city do not inundated during the flood event. Observed records consist of single polygon of the inundation extent and do not depict any high lands in the city as none inundating areas. Therefore during the preparation of inundation extent

map their intention may not be to identify none inundated points within the main polygon of the flood plain. Therefore the deviation in the city centre may be occurred due to low precision in the observed data set.

In contrast the rating curve used for Bicol River downstream was not based on field measurements and derived from the 2D model developed for the Bicol River down stream. Therefore any errors in the rating curve will change the model results considerable. Therefore sensitivity of the rating curve was analysed and given in section 5.7 below.

In Figure 5-18 above Mike 11 run produced by the Nippon Koei consultants is presented. It shows inundation extent resulting from Bicl River overland flow and has not paied much attention on Naga River. The focussed of Nippon Koei modelling work mainly on the Bicol river basin since their objective was the development of a feasibility study on bank protections in the Bicol river. In this model, the Naga river was kept flowing at module rate while the Bicol River was loaded with the runoff produced by a typhoon in the upper catchment (Mayon volcano), the most common flooding mechanism for the basin.

Several aspects of that Mike 11 and Sobek run were different: Mike 11 was done for the Bicol basin and not restricted to Naga, the grid resolution was coarser, and mainly the boundary condition were completely different since the event to be simulated did not consider heavy rainfall in the upper Mount Isarog catchment.

Comparing the inundated areas given by the two models, is clear that the flooding in the Naga center is not produced by a Bicol discharge although severe flooding by the Bicol occurs close to the confluence. The flooding pattern highlighted by the left and right water tongues sourrinding Naga is identical in both simulations. The main difference is that Sobek model, loaded with an extreme event coming from the Naga river, succeds in detecing the vulnerable areas close to the city center, which pass undetected in the Mike 11 model.

5.7. Sensitivity of the model

Sensitivity of the model was analysed by varying output discharge while maintaining the water level same as initial condition. In this case discharge was changed by $\pm 10\%$ in the discharge vs. water level relation (rating curve) developed to the Bicol River downstream. Resulting rating curves after making changes in discharges are shown in the Figure 5-19 below.

Therefore another two simulations were conducted by inputting the above two rating curves as boundary conditions. The resulting inundation extent at every hour was compared with inundation extent obtained from the initial simulation. Figure 5-20 below shows inundation extent variation with time for initial discharge, 10% increased discharge and 10% decreased discharge from the initial flow of the Bicol River downstream boundary.

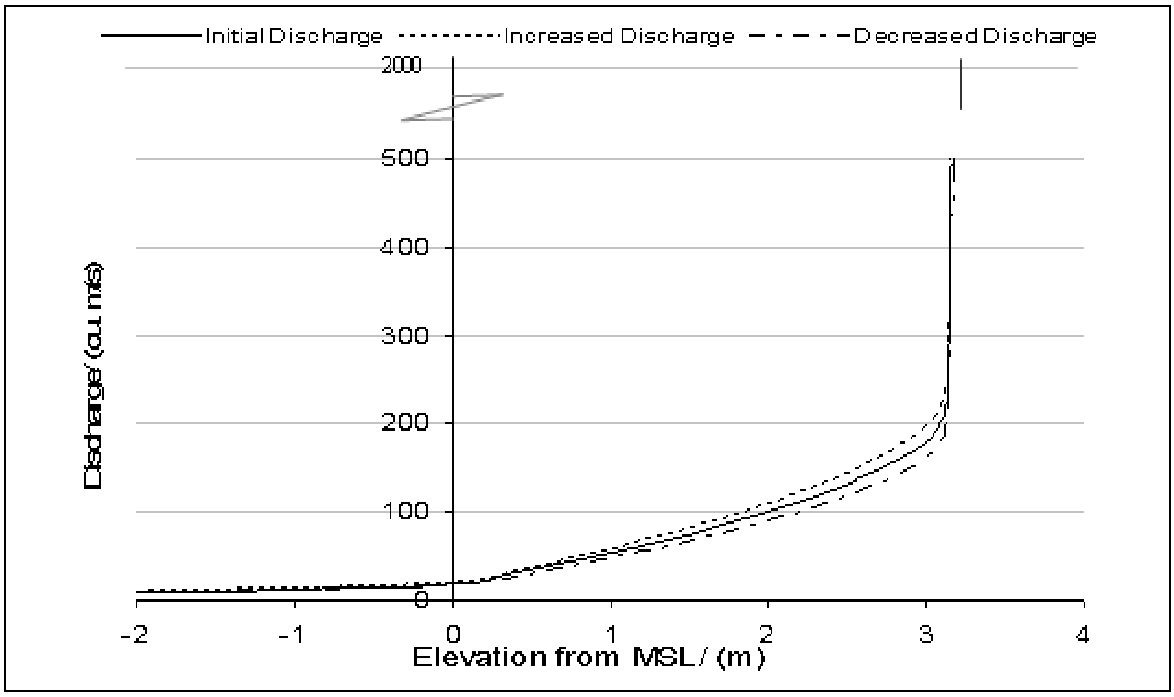

Figure 5-19: Bicol River downstream rating curves after changing the discharge by ±10%

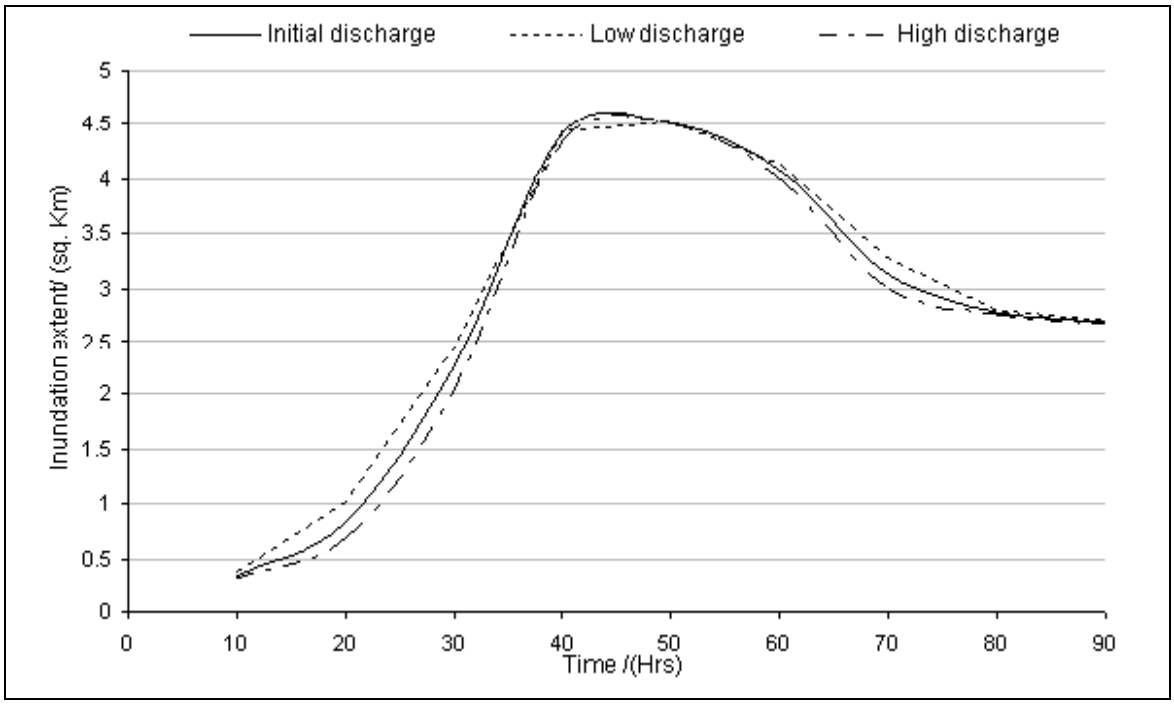

Figure 5-20: Sensitivity of the model with the change of Bicol River down stream discharge

Clear variation of the inundation extent was observed with the change of discharge vs. height relation at the Bicol River down stream. For example by increasing 10% in the initial discharge of the Bicol River downstream while maintaining same the water level, distinct reduction was observed in inundation extent through out the simulation period. Average inundation extent reduction was 5% (i.e. equivalent to 0.24 Km^2) with compared to the inundation extent corresponding to the initial rating curve shown in the Figure 5-20 above.

Similarly, with the decrease of discharge while maintaining the initial water level, corresponding inundation extent noticeably increased as compared to the inundation extent resulted from the initial rating curve. In this case increase was 6% (i.e. equivalent to 0.29 Km2).

Therefore this analysis concludes that inundation extent in the Naga city is very sensitive to the downstream boundary conditions of the model. That is discharge vs. water level relation at the Bicol River downstream (i.e. Camaligan station). Though several rating curves have developed in various studies, those cannot be calibrated and validated to use as reliable boundary conditions without having observed discharge measurements.

5.7.1. Tidal effects at Bicol River downstream

Rating curve at the Bicol River downstream is very much affected to the tidal movements of the San Miguel bay. It was clearly observed from the discharge vs. water level relation resulted from the 2D model developed for the Bicol River downstream. In this model tidal fluctuations were able to incorporate in the model by inputting water level variations at San Miguel bay. The resulting rating cure from this study was shown in the Figure 5-21.

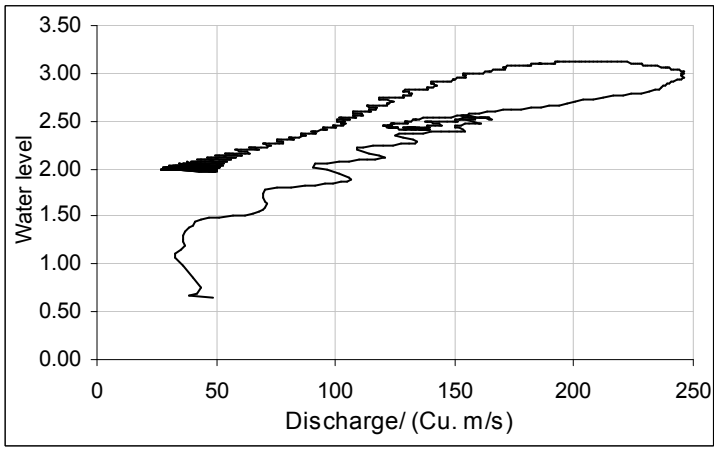

Figure 5-21: Rating curve resulted from the 2D model of Bicol downstream for Camaligan station

Source: (Otieno, 2004)).

Due to the fluctuation of bay water level two rating curves have resulted for rising limb and the falling limb of the hydrograph. The curve indicating the lower water level represents the rising limb while the other represents the falling limb. 50 – 100m^3/s discharge variation was observed at the same water level. In addition considerable zigzag pattern was observed in the rating curve representing the rising limb of the hydrograph. That is due to the daily water level fluctuation in the bay. Therefore it is very clear that discharge of the Bicol downstream is very sensitive to the tidal fluctuations and cannot generate an exact relation for discharge and water level using the models alone.

Since both the above relations were limited to a discharge of 300m^3/s, both of them were unable to apply in the detailed urban model. Therefore above curves were combined with the Nippon Koei Mike 11 model results give in the Figure 5-5 above. During to the curve estimation between two data sets daily tidal level fluctuation (zigzag pattern) were automatically removed and rating curve given in the Figure 5-19 above resulted. Therefore in this study water level variation due to daily tidal movement were not incorporated. However, more important water level fluctuation due to the typhoon winds has been incorporated in the upstream boundary of time series water level.

However in future developments of this model it is important to incorporate daily tidal fluctuations in the downstream boundary. Only monitoring and analysing long-term discharge measurements can reach successful boundary conditions including daily tidal fluctuations.

6. Model applications

6.1. Low land reclamation and urbanization

Naga city is expanding very fast and to cope up with the increasing population and economic expansion most of the low-lying agricultural lands within the city and its suburbs are converted to residential or commercial land use. These low-lying agricultural lands are located in close proximity to the city and serve as a natural flood detention area easing the flood level in the city.

The first step of this development process is the reclamation of the lowland up to or just above the elevation of surrounding area. As a result, most of the retention ponds within the city will be reclaimed parallel to the city expansion. Locally this process is recognised as an economic development or increase of investments in the area. Therefore in most cases no detailed studies are carried out to identify the adverse effects that might happen to the neighbourhood due to the low land reclamation. The aim of this analysis is to identify the impacts of such a development work on future flood events in Naga city and explore the model sensitivity for small terrain changes.

6.1.1. Present land use and Naga city Master Plan within the study area

Summarised land use classes within the study area as at year 2000 are shown in Figure 6-1a. In addition to that the recommended land use classes in the master plan proposed by the Naga city government for period of ten years (From 2000 to 2010) is given in Figure 6-1-b for comparison purposes. This master plan indicates the recommended land use within the city especially for future development activities.

Figure 6-2-a, shows the reclassification of the present land use under developed and non-developed categories. Figure 6-2-b indicates the proposed development and protected agricultural lands under the master plan year 2000 - 2010.

An important information is obtained by intersecting the above two layers mentioned in Figure 6-2-a and 6-2-b. That is the area to be developed (agricultural or open lands in year 2000) under the proposed Naga city master plan year 2000-2010. The resulted proposed development area is shown in the Figure 6-2-c below.

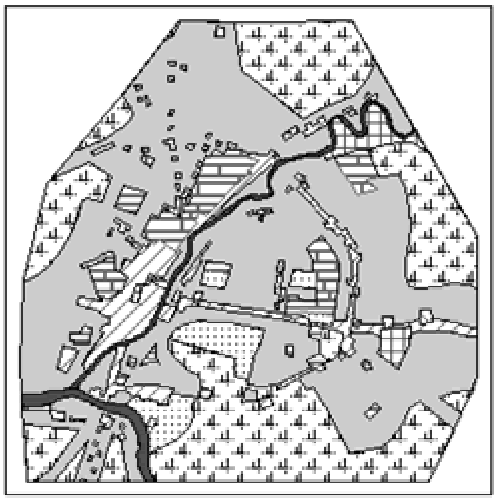

Figure 6-1a: land use year 2000

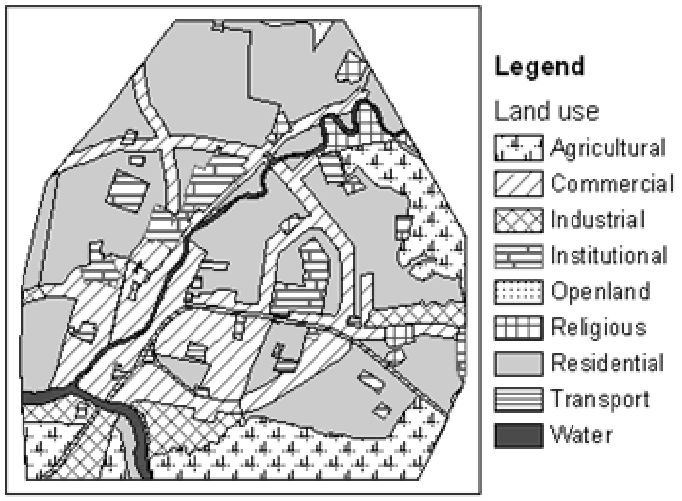

Figure 6.1b: Master plan year 2000- 2010

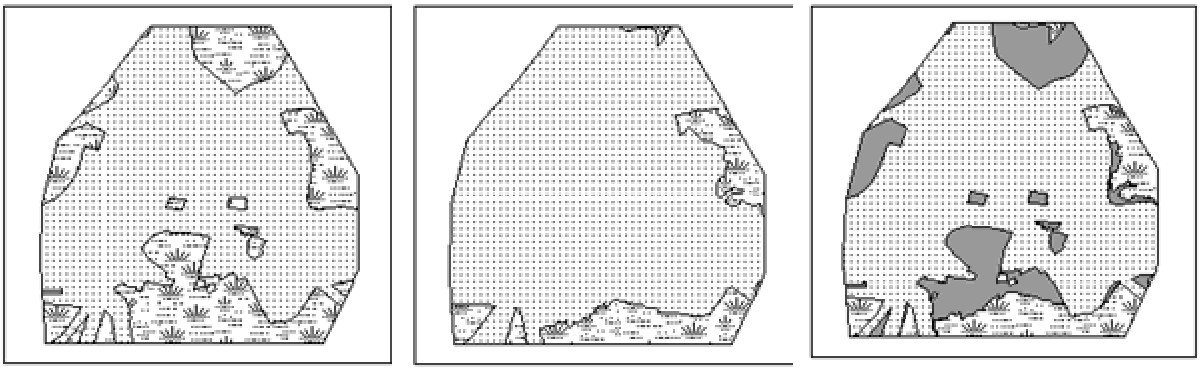

Figure 6.2a: Developed and none developed area in year 2000

Figure 6.2b: Developable and protected area under Master plan

Figure 6.2c: Proposed development area under master plan

Figure 6-2: Proposed development area under the master plan year 2000-2010

Most of the proposed development areas as shown in the Figure 6-2-c are classified as agricultural land in the year 2000 land use map. It is also evident that the area identified in the Figure 6-2c marked is non-developed land from the KVR image taken in 1991. Also by comparing the proposed development area with the natural surface DTM it can be identified that the area to the south of the city is a distinctively low land with elevation varying from 0 to 2m MSL. The average elevation of this area is less than 1m. The above conditions give rise to an ideal situation for the Naga city planners to explore the effect due to the development of low lying agricultural lands during a future flood.

6.1.2. Scenario on reclamation of southern low lying area

Proposed low-lying development zone situated to the south of the city is shown in the Figure 6-3-a. It is assumed that the proposed area to be developed is raised to the average elevation of the surrounding

area in order to obtain proper local drainage conditions. Initially a buffer of 100m was created around the proposed development area and average elevation of the buffer zone was calculated as 2.8m. The buffered area is shown in the Figure 6-3-b.

Then proposed development area was raised up to 2.8m in the previously created natural surface DTM. The resulting DTM was combined with previously created buildings and road surface elevation models. Then the combined DTM was input to the SOBEK model with same boundary conditions and initial conditions as given in the above ten-year return period flood event. Model results were compared with that of present condition at different potentially affected areas.

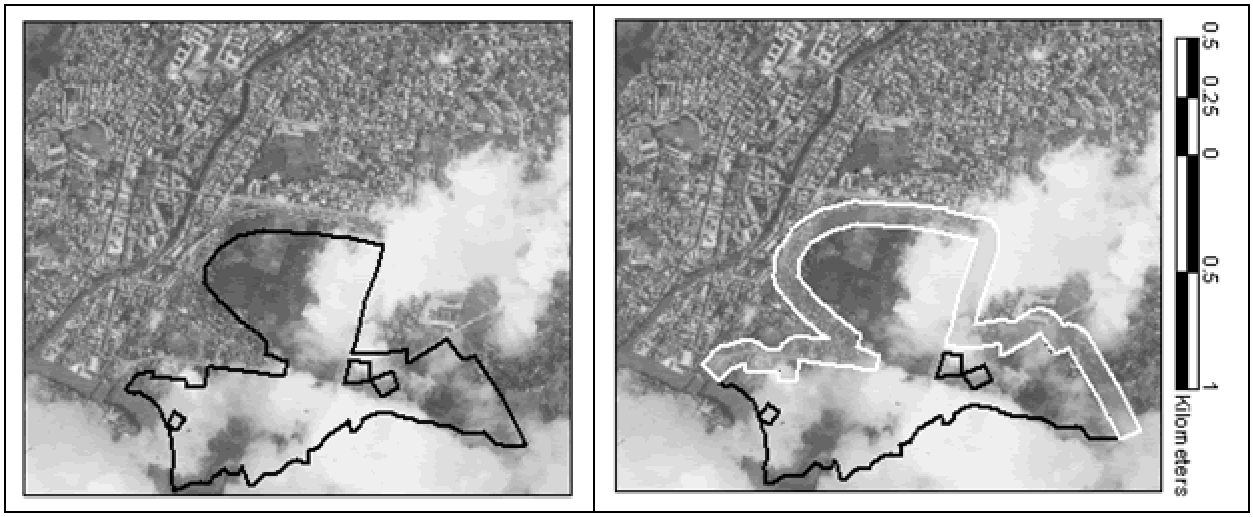

Figure 6-3a: Proposed low-lying development zone

Figure 6.3b: 100m buffer of the development zone

6.2. Resulting effects due to the proposed developments

Following analyses were made using the resulting inundation depths and flow velocities to identify the effects due to the above proposed reclamation scenario.

- Increase in inundation depth and extent within the centre of city
- Total increase of inundation extent within the entire study area

6.2.1. Increase in inundation depth and extent within the centre of the city

It was identified that city centre is mostly affected due to this reclamation work from the resulting flood propagation movies. Then time series average inundation depths and total inundation extents were calculated for the city centre identified above. The identified affected area in the city centre is shown in the Figure 6-4. Then resulting average inundation depths and total inundation extents obtained from this scenario were compared with the previous simulation of the model for present condition of the terrain. The comparison is shown in the Figure 6-5a and 6.5b.

Figure 6-4: Potential affected area in the city centre

A maximum increase of 13cm was observed in the inundation depth once the proposed development area is reclaimed up to 2.8m (that is equivalent to the elevation of surrounding area). In addition 9% (equivalent to 9ha) increase in inundation extent was observed within the city for ten-year flood event due to this proposed development scenario.

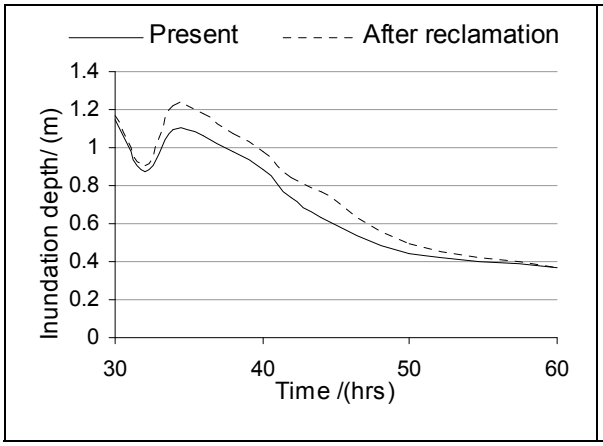

Figure 6-5a: Inundation depth variation due to the proposed reclamation

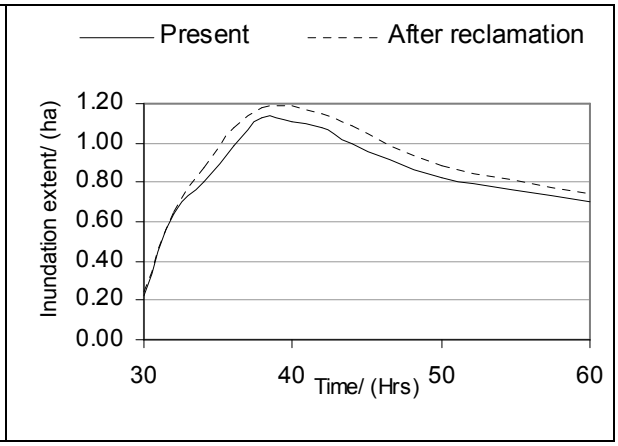

Figure 6-5b: Inundation extent variation due to the proposed reclamation

6.2.2. Total increase of inundation extent within the entire study area

Then total inundation extent variation within the entire study area was calculated due to the proposed development plan. Resulting inundation extents for present condition and after reclamation for a flood event having a ten-year return period is shown in the Figure 6-6a and 6.6b respectively. Increase of inundation due to the reclamation was observed through out the city. The increase was calculated as 0.25 Km^2 and it is equivalent to 5% as compared to present conditions. Figure 6-7 below shows the potential inundation areas due to the proposed development activity.

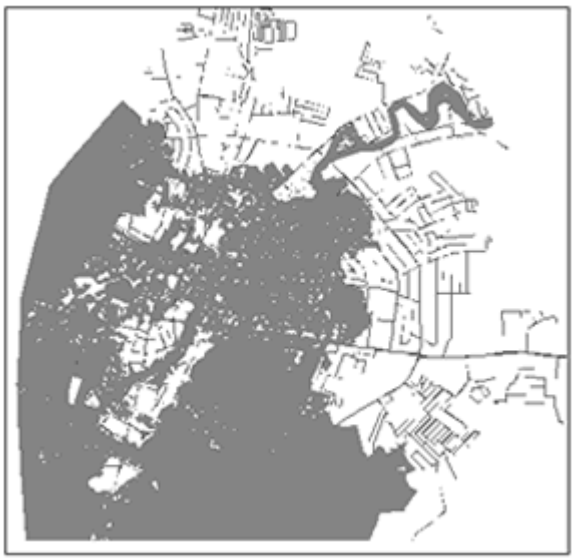

Figure 6-6-a: Present inundation extent

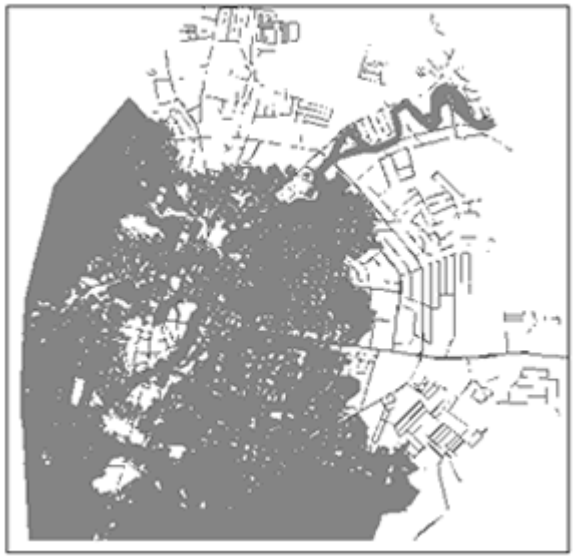

Figure 6.6-b: Inundation extent after reclamation of the development zone

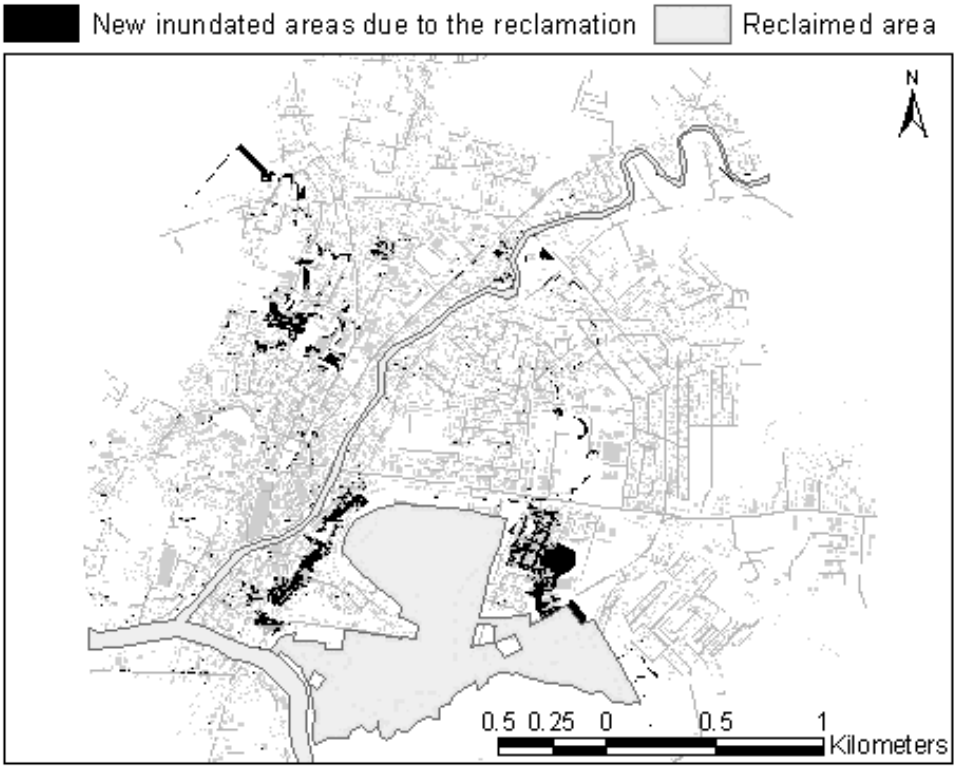

Figure 6-7: Potential new inundation areas due to the proposed developments

This scenario analysis concludes that effect of the above proposed development activity further aggravate the present floodwater level and the inundation extent within the city centre as well as the entire Naga city. However overall effect to the entire city is lesser compared to that of the city centre as shown in the Figure 6-4 above.

This analysis further revealed that the model results are sensitive for small terrain changes in the DTM. Therefore the model can be used for exploring the large-scale development scenarios such as EIA studies related to individual structure or large-scale reclamation projects.

Therefore the model can be used for analysis of various development scenarios to explore their effects on future floods. It is useful to investigate the effects of the raising road network as explained in the section 4.8.1. Also exploration of changes in overland flow due to the increase of rive bed elevation is also important since high sediment deposition had taken place during the last two decades in the San Miguel bay and Bicol River downstream due to the deforestation of Naga upper catchment (Adolfo, 2003).

7. Flood hazard mapping

7.1. Introduction

In the past flood hazard maps were primarily based on extent of inundation. According to the Federal Emergency Management Agency (FEMA) specification on determining flood hazard on alluvial fans (FEMA, 2000) they considered a 100 year flood zone extent . This was mainly due to the probabilistic methods and 1D-modelling approach that they have selected to develop flood hazard mapping.

Additionally, in FEMA specifications they have incorporated site observation based sediment erosion and deposition zones during the flood hazard mapping. However, determination of active erosion and deposition zones using fieldwork observation alone is a quite tedious and time-consuming task.

With the development of 2D hydrodynamic models for riverine flood simulations, it was possible to create flood hazard maps incorporating inundated depth classes. At present it is a quite popular technique to visualise depth of inundation. Moreover, 2D model results provide further opportunity to develop more meaningful hazard maps by incorporating additional hazard parameters. In an attempt to identify potentially hazardous areas threatened by flood effects not only by water depth but by erosion and water permanence, this study proposes the generation of combined hazard maps by combining three factors.

7.2. Factors influencing flood hazard

Even though flood hazard is a multi-dimensional phenomenon, it is conventionally assessed and mapped only considering its spatial (area) distribution. Though 100-year inundation map is useful for planning and flood insurance activities it may not be very useful for flood risk assessment. Once the depth of inundation is incorporated it is more practical for risk assessment work. Also spatial extent and depth of inundation are the most popular parameters use for flood hazard mapping in today's context. However, it is quite useful to combine with other parameters that adjust the level of hazard to hazardous situations where water depth is not all the concern.

Since in a flood risk assessment study the amount of damage is a function of duration of inundation, it is critical to know how long floodwater remains in the area. It is equally applicable to a cropland or business premises. In both cases loss of income is directly proportionate to the duration of inundation of that area.

Physical damage to properties during a flood event is closely related to the amount of energy contain in the floodwater. The extent of soil erosion also primarily depends on velocity of water. However velocity of floodwater alone does not give the real danger of floodwater. In a 10cm of water depth with 1 ms^{-1} velocity, wading is possible for an able person however in a 1m of water depth with the same velocity it is quite difficult. In contrast, low water depth at high velocity floodwater has the en-

ergy to damage light structures and foundations.(USDL&WC, 2001) Therefore an energy map of floodwater represents the amount of damage or the level of hazard better than the velocity of floodwaters or depth of inundation alone.

Current development of 2D hydrodynamic modelling helps to incorporate these additional parameters for better representation of the hazard. Maximum velocity and impulse (water depth * flow velocity) maps generated by (Alkema, 2003) for the 1997 Oder flood are a good example for incorporating new parameters in flood hazard mapping. However it is further possible to introduce new hazard parameters and create multiple-parameter hazard map representing several hazard parameter in the same map. In this study, defining flood hazard as a function of following parameters generated the hazard maps.

$$Flood\ hazard = f(Depth\ of\ inundation, Duration\ of\ inundation, Kinetic\ energy\ of\ \ flood\ water)$$

Where,

Depth of inundation is the maximum inundation depth experienced by each pixel during the simulation.
Duration of inundation specifies how long each pixel was under water during the flood event.
Kinetic energy determines the maximum energy experienced by each pixel during the whole simulation period.

7.2.1. Maximum depth of inundation

This is the most common way of representing the level of flood hazard. It gives a clear picture of the hazard and it is perhaps the most helpful map for urban planning.

Delft FLS as well as SOBEK creates a depth of inundation file at every specified time step and a maximum water depth file at the end of the simulation. Therefore once converted the maximum water depth file into raster, inundation depth based hazard map is ready. However it can be reclassify in to hazard classes or combined with the other hazard parameters to generate meaningful hazard classification. In this study inundation depths of 0.8m and 1.2m are considered as upper limits for low and medium hazard levels respectively. The cut-off level for defining the hazard classes are subjected to several aspects including end requirements of the maps, study area as well as individual perspectives. Figure 7-1a and Figure 7-1b show the inundation depth levels and corresponding hazard classes for ten year return period flood event[9].

[9] Ten year hydrograph given in (Nippon_Koei, 2003a) report used to generate these maps

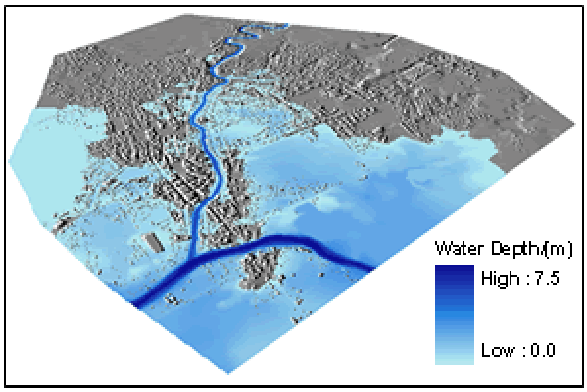

Figure 7-1a: Inundation depth variation

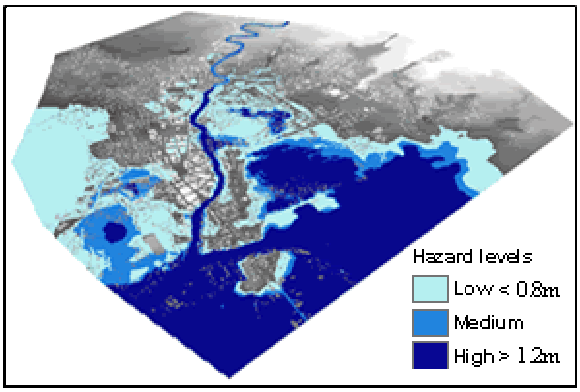

Figure 7.1b: Hazard classification

7.2.2. Duration of inundation

Duration of inundation is an important parameter for flood risk assessments, mainly in the evaluation of transport blockades and access to emergency services. However it has not been considered in many flood hazard studies may be due to the cost involved of its estimation. Hazard zonation could be estimated from ground survey by geomorphological interpretation supported by levelling, but flood duration requires hydraulic modelling and the effort to achieve an accurate model is normally hampers by the cost. Moreover in most of the cases the hydraulic modelling requires so many data and expertise that is not feasible to be carried out in view of the locals.

The flood duration on pixel basis is not a direct output from the model results. In this case it was derived using a time integration of the 96 inundation depth files created for each time step (one hour) of simulation. First all 96 ASCII files were converted to raster grid format. Then, undefined pixels (value -999) indicate cells those were not undergone by floodwater. Pixels representing inundated area have corresponding depth of inundation as its pixel value. The 96 raster files were reclassified into binary raster files representing 1 for pixels gone under floodwater and 0 for pixels not affected by floodwater. Finally the 96 binary raster files were summed up to get the duration of inundation map. The final map represents pixels value 0 to 96. For example pixel values 96 represents areas inundated through out the simulation while pixel value 50 represent areas inundated only 50hrs during the flood event. Resulting inundation duration map is shown in the Figure 7-2a below**.** In this case each hazard levels was established with respect to the duration of the flood event T (i.e. 96 hrs). That is if the simulation was conducted for a ten year four day flood event then T is equal to 96 hrs. If an area gone under water less

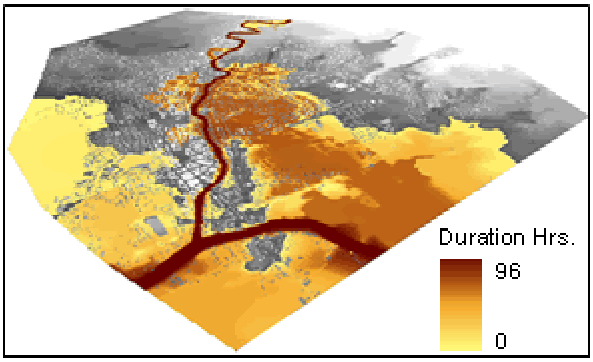

Figure 7-2a: Inundated duration

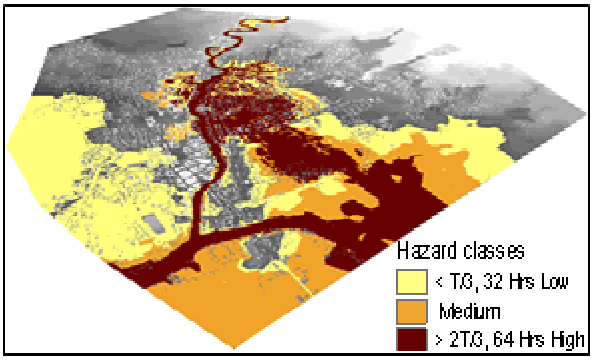

Figure 7.2b: Hazard classes

than one third of the simulation period ($^1/_3$T), it was classified as "Low". Similarly "High" hazard zone was delineated as if an area gone under water over $^2/_3$T period. The corresponding flood hazard map is shown in Figure 7-2b. However there was a limitation in the duration of inundation map since at the end of the simulation it was observed that several scattered isolated spots did not dried out. This was caused by the fact that local drainage network was not incorporated with the model.

7.2.3. Maximum energy of flood water

In this study we refer to the "energy term" as limited to the kinetic energy of floodwater. Since kinetic energy is a function of depth of inundation as well as velocity of floodwater the hazard map generated from this parameter is expected to be a better representation of the hazard "flood" as compared to maps shown above in terms of risk assessments.

The creation of the maximum kinetic energy map for the whole simulation period is quite cumbersome work. However it can be generated by manipulating velocity and depth of inundation files created at each time step of simulation.

Kinetic energy ($E_{k,(i,j)t}$) of floodwater at (i, j) pixel after "t" hours of simulation could be expressed as

$$E_{k,(i,j)t} = \frac{1}{2} m_{(i,j)t} V^2_{(i,j)t}$$

$$E_{k,(i,j)t} = \frac{1}{2} (Pixel\ \mathrm{Re}solution)^2 \times \rho_w \times [Depth\ of\ inundation]_{(i,j)\,t} \times [Velocity]^2_{(i,j)\,t}$$

Where $m_{(i,j)t}$ is mass of floodwater column in pixel (i, j) after "t" hours of simulation and ρ_w is density of floodwater. During floods ρ must not necessarily be equal to 1000kg/m^3. Water is heavier during mudflows. This approach allows increasing the hazard (energy) by adjusting the density of the flowing element. For this study we accept $\rho = \rho_w = 1$, although it is well known that during some flooding with origin in Mount Isarog, water came heavily loaded with sediments.

By substituting the corresponding inundation depth and velocity raster maps in to the equation 6.2 above, 96 kinetic energy maps were created for each hour of simulation.

Then next step was to create the maximum energy map out of the resulting 96 energy maps. For example in this case it was required to com-

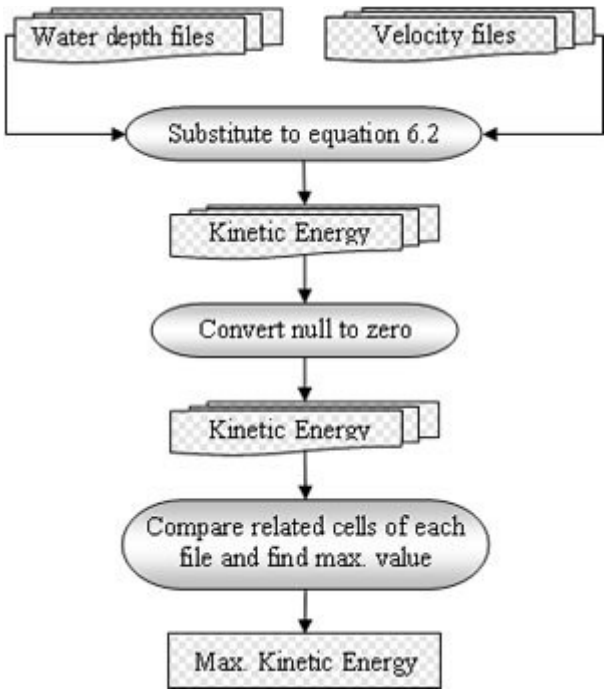

Figure 7-3: Process model for generating maximum kinetic energy

pare each (i, j) cell of all 96 energy maps and find the maximum energy of (i, j) cell and write that maximum value in a new raster file. The process model for generation of maximum kinetic energy map is shown in the Figure 7-3 above. The maximum kinetic energy map is shown in the Figure 7-4a above. Upper limits for "Low" and "Medium" hazard level were calculated as 45KJ and 22.5KJ respectively. These limits of hazard classes were calculated for water column of one square meter base area and details on the calculation of these limits are explained in the section 7.3. Limiting velocity and inundation depths to calculate the cut-off energy levels were obtained from hazard classification of US department of land and soil conservation. It is shown in Figure 7-5**.** According to this classification 1.2m-floodwater depth with 1.4m/s velocity is classified as "High" hazard zone. Details of this classification are given in appendix A5.

Flood hazard categories based on maximum energy of floodwater are shown in Figure 7-4b. Hazard zone corresponding to medium hazard level was disappeared in this area due to the selection of high velocity cut off limit (i.e. 2m/s) for high hazard level.

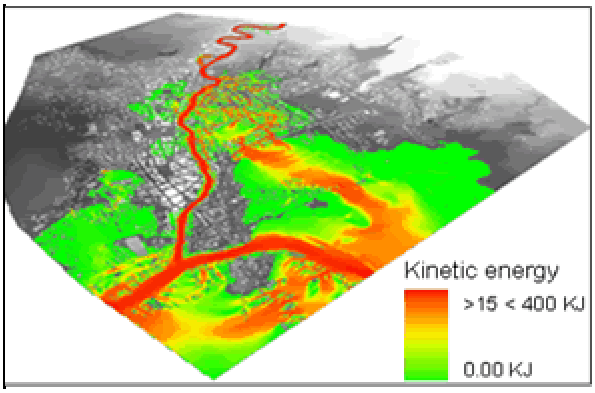

Figure 7-4a: Maximum kinetic energy

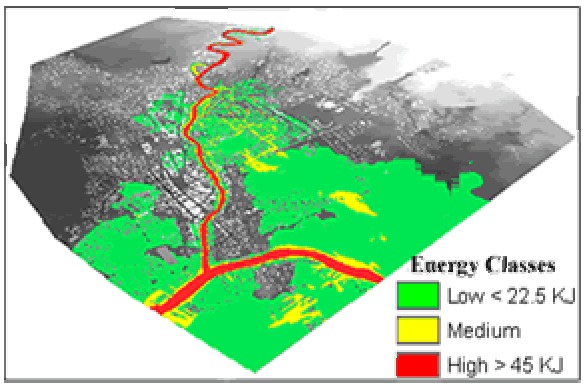

Figure 7-4b: Kinetic energy hazard classes

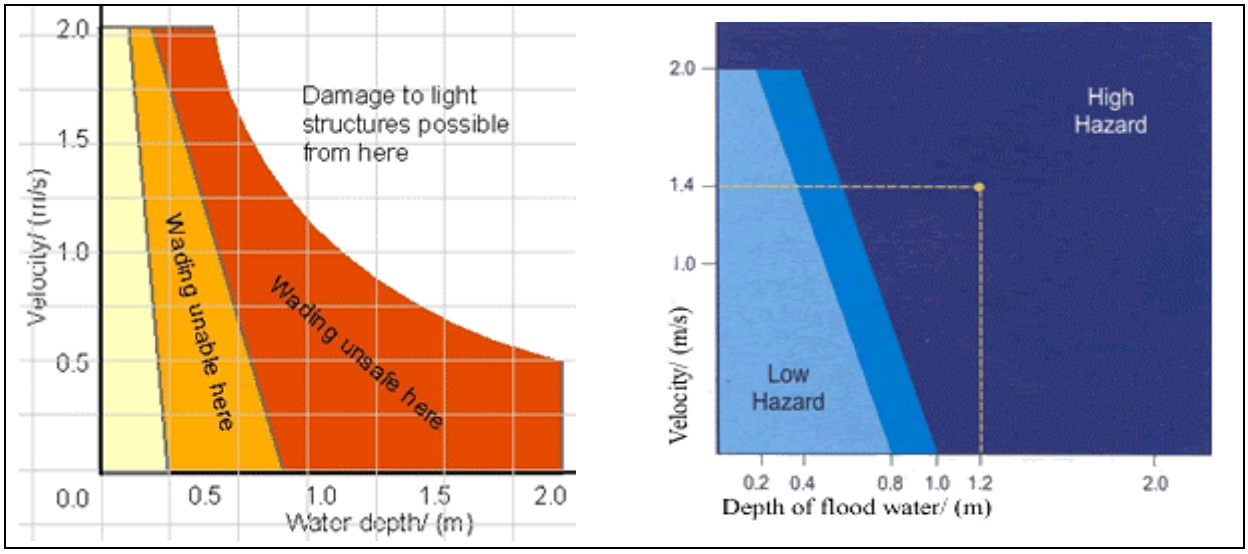

Figure 7-5: Flood hazard classification

(Source: US department of land and soil conservation)

7.3. Combination of hazard parameters

It was attempted to combine above parameters and derive a multiple-parameter flood hazard map representing depth, duration and flow kinetic energy of inundation. Even though depth of inundation is already included in the kinetic energy it counted double in the combination since the energy term here is limited to kinetic energy alone. Also it is not possible to represent water pressure, up thrust due to water depth or flowing debris effects from kinetic energy alone. In addition even the energy of floodwater is zero (i.e. in stagnant water) if the water depth is over 1.5m it is a quite impossible for wading and even possible to drown.

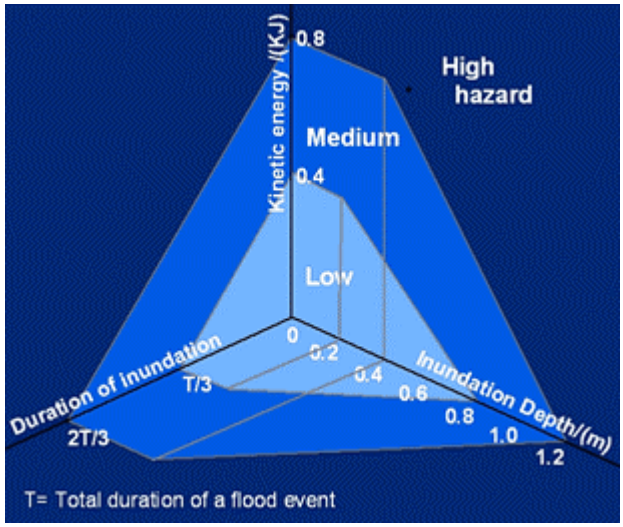

Figure 7-6: Flood hazard classification

Therefore in the final hazard map all three parameter were combined and the resulting combined hazard map was classified in three categories as "High", "Medium" and "Low" based on hazard categories as shown in Figure 7-6**.** Derivation of upper and lower limits for each flood hazard category is explained below.

Initially, limiting hazard level for each parameter was decided based on past literature as well as site conditions. Cut off kinetic energy values were calculated based on limiting water depths and velocities given in the hazard classification of US department of land and soil conservation. For example an upper limit of "low hazard" was marked as 2m/s of velocity and 0.2m of water depth. Therefore corresponding kinetic energy could be calculated for a water column of unit area (1m by1m) and 0.2m deep as follows;

D=0.2m, V=2m, ρ_w=1000kg/m^3, Base area= 1m* 1m

$$Ke = \frac{1}{2} m V^2$$

= 0.5 *1*1*0.2*1000*2^2 J = 0.4KJ

However in this study all the hazard parameters were available in 7.5m by 7.5m pixels. Hence kinetic energy of a water column having 7.5m of base area could be calculated as;

= 0.4*7.5*7.5 KJ = 22.5 KJ

Therefore energy corresponding to upper limit of low hazard level is 22.5KJ for 7.5m pixel. Similarly lower limit of high hazard level could be calculated as 45KJ. This is the same as saying that the pixel size is used as scaling factor for the limits given by the US department.

Cut off inundation depths corresponding to hazard levels given in US department of land and soil conservation is realistic for urban applications. Therefore the upper limit of the low hazard zone was selected as 0.8m. However, lower limit of high hazard zone was changed from 1m to 1.2 m in this study, since cut-off limit of 1m for medium hazard category is inadequate for an area experiencing heavy

floods. In contrast these limiting values depend on perspectives of individuals, study area as well as the end requirement of the hazard map.

7.3.1. Kinetic energy vs. depth of inundation

Kinetic energy vs. inundation depth was plotted in 2D Cartesian space and each zone corresponding to hazard categories was delineated as shown in the Figure 7-7 Reclassification of each pixel into raster maps of maximum kinetic energy and maximum water depth requires equations corresponding to the different hazard zones. They were calculated using the equations of limiting lines given below.

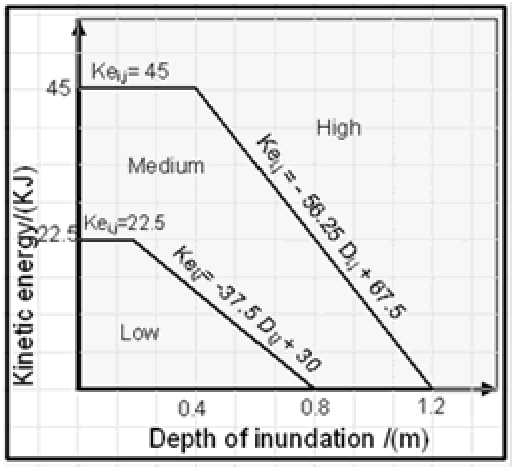

Figure 7-7: kinetic energy vs. depth of inundation

Once corresponding raster maps were substituted to $Ke_{i,j}$ and $D_{i,j}$ in the following equations, it is possible to delineate the hazard zones corresponding to kinetic energy and depth of inundation. Then combined hazard map with respect to above two parameters was created. All raster computations were done in ArcGIS raster calculator and equations used for the calculations are given in annexure A7.

$$Low\ Hazard\ Zone = \left\{\left(Ke_{i,j} < 22.5\right) \cap Ke_{i,j} < \left(-\tfrac{22.5}{0.6} D_{i,j} + 30\right)\right\}$$

$$Medium\ Hazard\ Zone = \left\{\left(Ke_{i,j} < 45\right) \cap Ke_{i,j} < \left(-\tfrac{45}{0.8} D_{i,j} + 67.5\right)\right\}$$

$$High\ Hazard\ Zone = \left\{Total\ inundated\ area - \left(Low\ hazard\ zone + Medium\ hazard\ zone\right)\right\}$$

Where, $Ke_{i,j}$ and $D_{i,j}$ are representing Kinetic energy and water depth in (i, j)th pixel respectively.

7.3.2. Duration of inundation vs. depth of inundation

It was decided to use T/3 and 2T/3 as cut off duration of inundation corresponding to upper limit of low hazard and lower limit of high hazard zones respectively. Where, T represents total duration of the flood event. In this case T is equal to four days (i.e. 96 hrs) and corresponding hazard map represents ten year return period flood event.. Duration of inundation vs. depth of inundation plot was shown in Figure 7-8. Similarly, equations of low and medium hazard zones corresponding to above two parameters were derived and given below.

$$LHZ = \left\{\left(T_{i,j} < \tfrac{T}{3}\right) \cap T_{i,j} < \left(-\tfrac{T}{0.6} D_{i,j} + \tfrac{2T}{3}\right)\right\}$$

$$MHZ = \left\{\left(T_{i,j} < \tfrac{2T}{3}\right) \cap T_{i,j} < \left(-\tfrac{T}{0.6} D_{i,j} + \tfrac{4T}{3}\right)\right\}$$

Where, $T_{i,j}$ represents duration of inundation undergone by (i, j)th pixel and T represents total duration of the flood event. Above two equations were used to derive raster maps corresponds to low and medium hazard zones. Deducting above two raster maps from the total inundated area, high hazard zone was delineated.

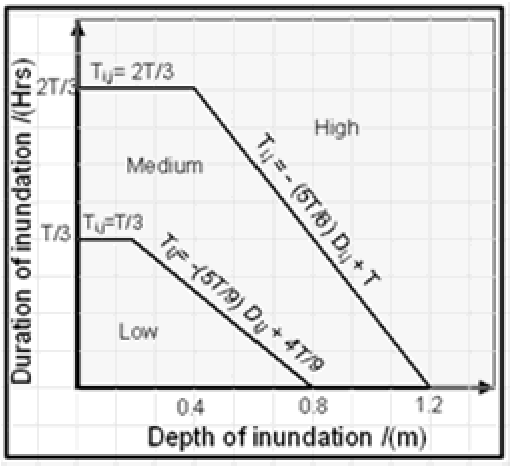

Figure 7-8: Duration of inundation vs. depth of inundation

7.3.3. Kinetic energy vs. duration of inundation

Using the above derived limiting values, plots of kinetic energy vs. duration of inundation was drawn and shown in Figure 7-9. Each hazard zones were delineated as follows.

$$Low\ Hazard\ Zone = \left\{Ke_{i,j} < \left(-\frac{135}{T} T_{i,j} + 22.5\right)\right\}$$

$$Medium\ Hazard\ Zone = \left\{Ke_{i,j} < \left(-\frac{135}{T} T_{i,j} + 45\right)\right\}$$

Where, $T_{i,j}$ represents duration of inundation undergone by (i, j)th pixel and T represents total duration of the flood event.

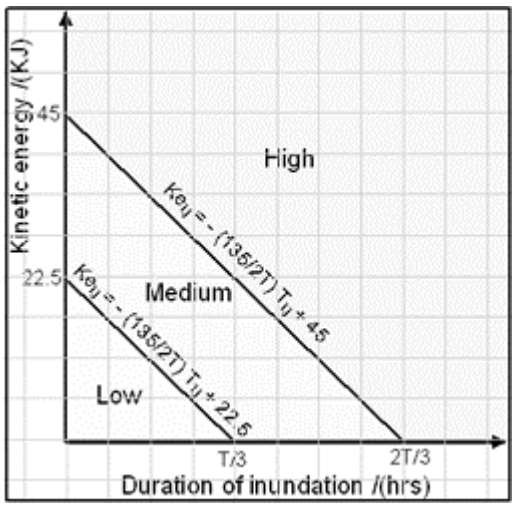

Figure 7-9: Kinetic energy vs. duration of inundation

7.3.4. Multiple-parameter hazard map

Finally the resulting three raster maps corresponding to the three relationships were reclassified on a 3-D space graph based on hazard classification defined in Figure 7-6 above. Reclassification was done following an exclusive criterion.

If all three individual maps represented low hazard then those areas were classified as low. If at least one map represents medium while others are low then those regions were reclassified as medium. Finally if in at least one individual map the area represents high hazard then those pixels were classified as high hazard. The final multiple-parameter hazard map generated based on the above classification is shown in Figure 7-10. For convenient comparison, hazard map prepared based on water depth alone is shown in Figure 7-11b.

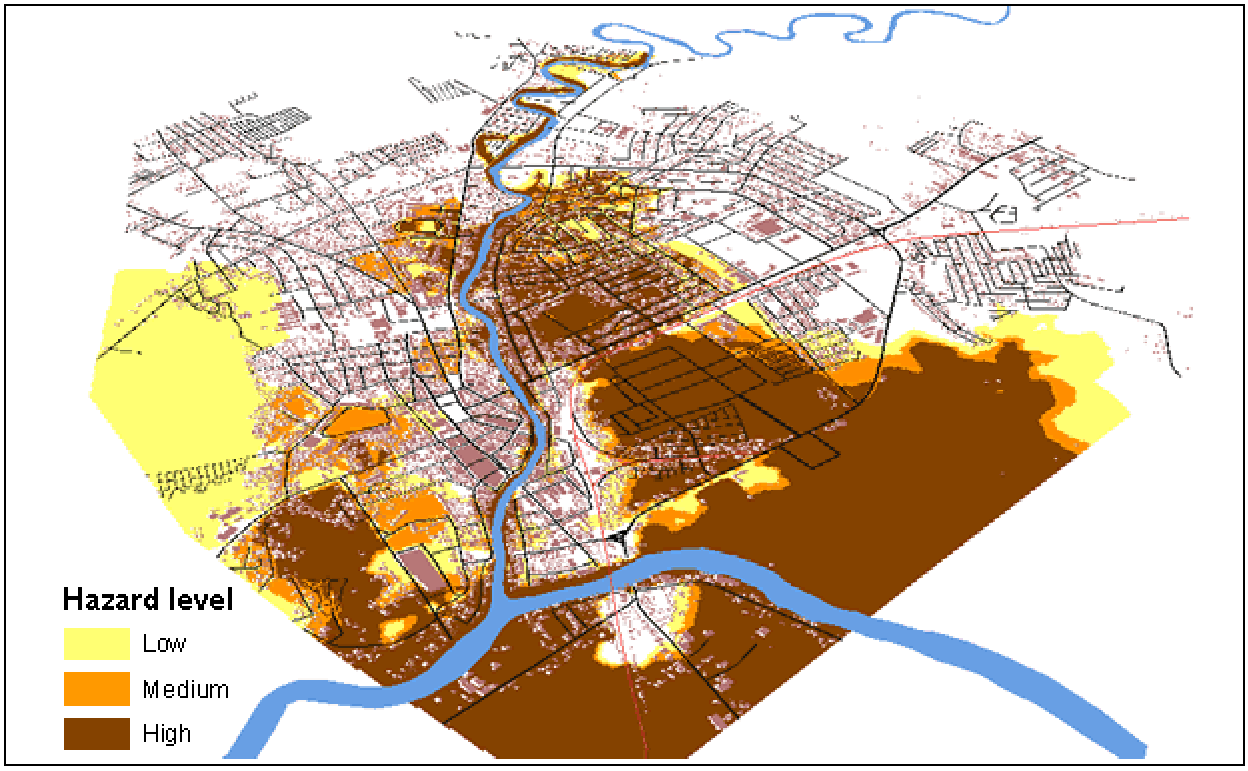

Figure 7-10 : Close up view of Naga city flood hazard map

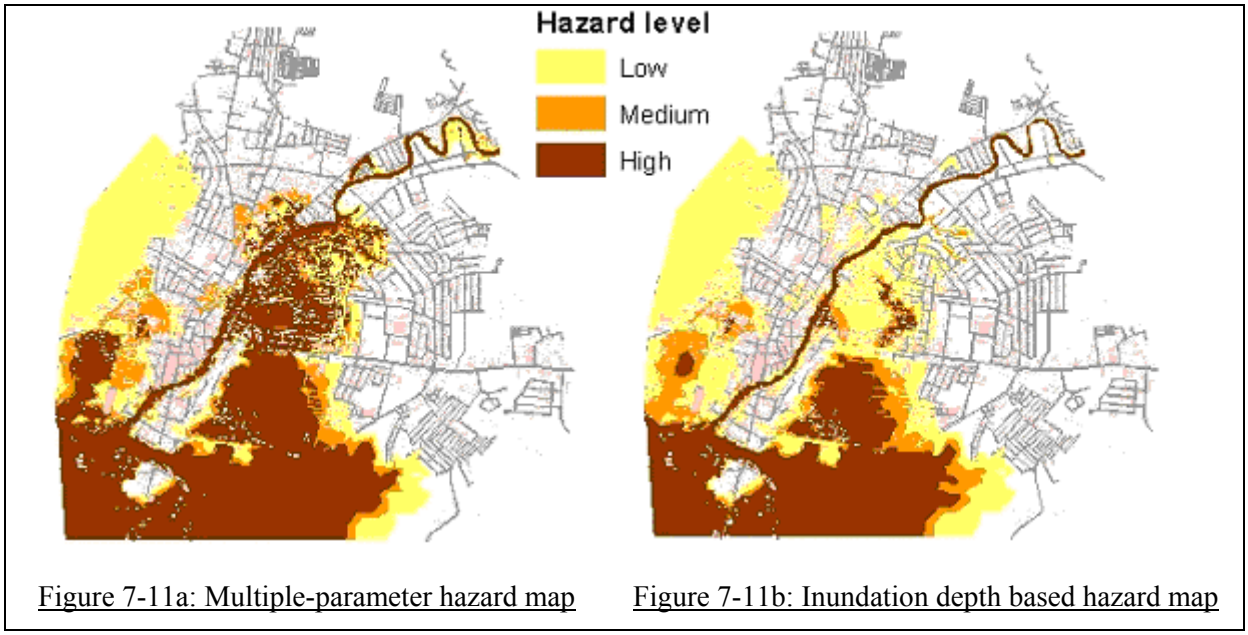

Figure 7-11a: Multiple-parameter hazard map

Figure 7-11b: Inundation depth based hazard map

Figure 7-11: Comparison of conventional inundation based hazard map with multiple parameter hazard map

Comparison was made with conventional hazard map prepared based on inundation depth and the multiple-parameter hazard map. First both raster maps of hazard classes were converted from raster to vector and area of each hazard zone was calculated. Figure 7-12 shows the total area of each group and percentage deviation between the two hazard maps.

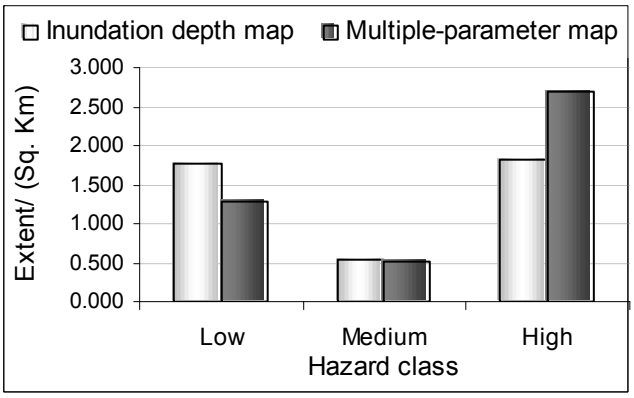

Figure 7-12a: Extent of each hazard classes in conventional and multiple-parameter approach

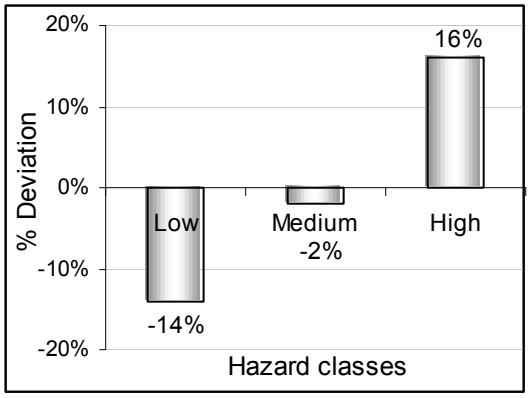

Figure 7.12b: Percentage deviation in two approaches

A 16% increase in high inundation zone was observed in the multiple-parameter hazard map compared to that of inundation depth based single parameter conventional approach. In the conventional approach, areas where inundation depths less are than 0.8m were classified as low hazard. However in the multiple-parameter approach it will further check for energy level and duration of inundation. If at least one parameter is higher than the "low" hazard level it will classify as medium or high hazard.

Therefore by combing several hazard parameters reliability of the hazard class delineation can be improved.

8. Analysis of results and discussion

8.1. Introduction

This chapter discusses four main outcomes of this research. First it reviews the types of data used, their collection methods and their advantages and limitations. The next section discusses on the optimum pixel resolution for urban feature representation in the DTM. Then it focuses on model results and its variations with spatial resolution. Finally it, examines the advantages and limitations of additional hazard parameters used for deriving a multiple-parameter hazard map.

8.2. Topographic Data for DTM

Reliability of model results is primarily based on the accuracy of DTM. Therefore a good elevation data set of the terrain is the prime requirement, and the final modelling result will directly link to the accuracy of the DTM regardless of any other important land parameter surveyed for the purpose. Even though there are newer technologies available to obtain terrain elevation, they are costly and require advanced post processing skills. Conventional survey to prepare a contour map of the study area with required accuracy will consume several months and the cost of the survey itself must not be ignored.

This is one of the major obstacles faced by municipalities with scarce resources during the preparation of flood hazard maps, which are essential for urban planning. Therefore this study was focussed to identify alternative secondary elevation data sets, which were prepared in the past for various infrastructure development projects.

8.2.1. Where is alternative data available?

In general most of infrastructure development projects require detailed topography of the project area during their design phases. Therefore isolated detailed topographic maps are available in the organizations responsible for development and maintenance of those projects.

The above concept was found to be true in the fieldwork by identifying six isolated elevation data sets covering different parts of Naga city. All these data sets were collected by NEDA, the organization responsible for foreign funded projects in the area, the Municipal engineer's office, the Road development and maintenance authority and the Irrigation department. In other cities similar data sets can be identified from water supply, telecommunication, drainage authorities and private construction consulting organizations. These types of isolated elevation data sets are useful for developing high resolution DTMs since generally those are large-scale detailed maps.

Note: The crucial effort of collecting, organizing, compiling, checking and making this information available in straight forward formats is a responsibility of the local authority as part of their plans for the security and well-being of the taxpayers. Regardless any other outcome of this thesis, it should be clear that on the municipal authorities lies the obligation of accounting with this planning information

keeping it ready and up-to-date for use mainly in those riverine towns frequently affected by serious floods. This study proves that in most of the cases this information is not unavailable, but is dispersed and difficult to find and compile. Municipalities must be aware of its essential rolls in acquiring the information they need to confront floods, understanding that despite their limited resources it not a matter of funds but centralization of the information into readily formats.

8.2.2. Inherent problems of this approach

Since these elevation data sets have been created for different objectives, several limitations are inherent in them. Primarily, each data set could be referred to different elevation references (datum). If any Meta data is not available it may not be possible to combine this data with any other data sets. In that case control survey is required to transfer them into a common reference level (i.e. Mean sea level). Datum mismatching is the most common problems of DTM data assembly, together with misleading coordinate systems.

The other limitation, in most of the cases is that the alternative data sets are not covering the entire study area. As a result, an additional survey will be required to cover the data gap areas. Simple spot height collection technique used in this study is appropriate to cover small areas where additional data is required. It is also useful as a control survey to transfer isolated data sets in to a common reference.

8.2.3. A spot height collection technique; its advantages and limitations

A simple levelling instrument was used to get spot elevation data while the location of the data points was recorded in a hand held GPS. This method is fast since it does not require any tape measurements. Vertical accuracy of spot heights can be obtained up to 1mm as conventional levelling survey. However positional (i.e. coordinates of the elevation point) accuracy may depend on the GPS signal level. During the fieldwork it was possible to obtain up to $\pm 5m$ accuracy except under dense canopy cover and along streets where several high-rise buildings were located[10].

This method is speedy and not laborious. It was possible for two skilled persons to obtain about 100 elevation points within eight hours covering about one square kilometre extent along roads. Therefore this method is cheap and convenient for filling data gaps and as a control survey. Also it is simple to adopt it in any medium scale city with available resources.

However, specific terrain features (i.e. roads, embankments) cannot be represented in the DTM using these elevation points alone. Therefore this method does not replace the standard plani-altimetric survey and it should be limited only for filling data gaps and should not be used to obtain elevation data for the entire study area.

8.2.4. Applicability of alternative data for flood modelling

In general the topographic maps available in infrastructure development and maintenance organisations are large scale and useful for creating detailed DTMs. Therefore resulting DTMs adequately rep-

[10] The (x, y, z) accuracy of GPS is expected to increase in the very near future with the addition of the new Galileo constellation and ground base DGPS services. Moreover, with the increase of the satellite density the problem of "radio wave shadows" causey by high buildings is to be dramatically reduced.

resent terrain features required for 2D flood modelling. Though it was not possible to conduct a fine calibration of the model results, preliminary inundation maps generated by the model for Naga city matched with the observed inundation extent maps. Therefore these alternative elevation data sets proved sufficient for 2D hydrodynamic modelling requirements applied to applications in hazard mapping.

It has been also found that those areas lacking dense and homogeneous elevation data had deviated from the observed inundation maps. Once again, it is crucial to assure homogeneity and density data distribution when creating DTM using scattered elevation data sets. Also if the model output is going to be used for investigating river dynamics with respect to specific structures, then the precision here described might not suffice.

8.3. Optimum pixel resolution for urban feature representation

This optimum pixel resolution discussion is limited to urban feature representation in the DTMs as an input for 2D hydrodynamic modelling.

In ArcGIS, vector to raster conversion process for polygon features, is based on the centre of the raster cells. "Each cell on the resulting raster data set from the conversion process is assigned the value of the feature that passes through the centre of the cell" (ESRI, 2003) Therefore to guarantee the polygon feature representation in the raster layer at least single cell centre should be within the polygon. It is represented in Figure 8-1. As a result with the increase of the pixel size the resulting raster layer deviates from actual shape and position of the real features.

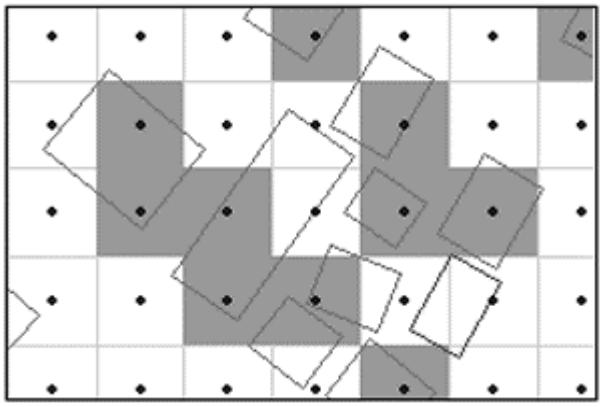

Figure 8-1: Representation of polygons after rasterisation

Looking at the resulting raster structure in the Figure 8-1 above, it is a good suggestion to rotate the original vector file to match the square pattern of the city with rows and columns of raster and conduct the rasterisation. By rotating the above vector file about 50^{o} degrees clockwise most of the deviations in occurring due to rasterisation can be avoided. It is a good solution for a small area, along few street or even cities designed by Spanish in the world with all streets originated from Cartesian X,Y axis. However it is not practical for most of the cities in the world as well as the Naga city since they do not follow a specific grid pattern.

This description establishes the basis for the following discussion.

In urban flood modelling overland flow direction is affected by the urban features (i.e. roads and buildings). Therefore reasonable overland flow condition can be expected from the model only if the urban features are modelled in the DTM with required accuracy. Firstly, road network and structures

should be proportionate to their actual dimensions in the DTM. One may suggest that a DTM with 1m or less pixel size would represent them more accurately in the model. Though it is true, such a DTM is not appropriate for 2D hydrodynamic modelling since computation time increases exponentially with the number of pixels in the DTM. Also at present, some 2D models have a maximum limit for number of pixels in the input DTM (i.e. Delft FLS 2.47 can simulate only 497* 497 pixels)[11]. Therefore the identification of the optimum pixel resolution helps to compromise between computation time and urban features representation in the model.

8.3.1. Buildings

In general structures and building in the terrain obstruct the flow path and change the flow direction. Therefore it is crucial to establish building footprints within the DTM with required accuracy. However once building footprints are converted from vector to raster shape, size and orientation of the original building changes and several building blocks have merged each other and represent as a single large building block. Changes occurring to the building blocks were compared in the 5m, 7.5m and 10m raster representations. First each raster layer representing buildings was converted back to vector files for calculating areas and overlay with other layers. A comparison was made with the original building footprints and the resulting building blocks after rasterisation. Building blocks count, total building block area and overlaps area of the resulting building blocks with the original building footprints were used as parameters to identify the effect of pixel size on building footprint representation. The results are shown in the Figure 8-3a and Figure 8-3b below.

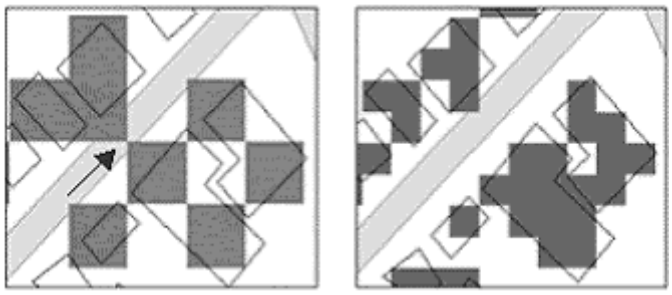

Figure 8.2a: 10m Raster Figure 8.2b: 7.5m Raster

Figure 8-2: Difficulties representing building footprints with higher pixel values

It was observed that the total area of building footprints remains almost the same with the change of pixel resolution. However the position of the building footprint has considerably changed from the original location with the decrease of pixel resolution. It was further observed that, overlaps between resulting raster building blocks and original building footprints were reduced with the decrease of pixel resolution. In the 5m raster representation overlap was 79% while it was 71% and 64% in 7.5m and 10m pixels respectively. Conclusively, with the decrease of pixel resolution of the building footprints layer the original position of the buildings varies considerably.

[11] This second limitation has resolved in the SOBEK 1D 2D model developed in year 2003.

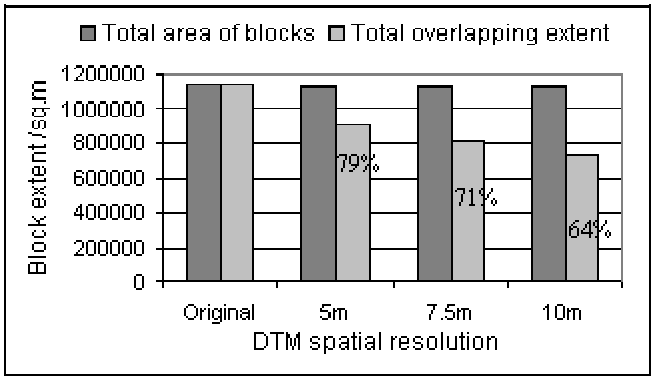

Figure 8-3a: Variation of total floor area and its overlapping extent with original building location against spatial resolution

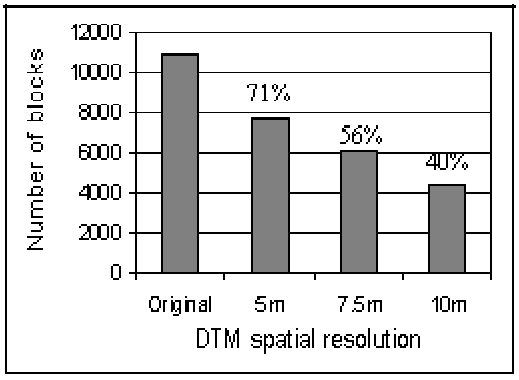

Figure 8.3b: Changes in total number of building blocks with pixel size

In addition it was observed that individual building blocks merge each other with the increase of pixel resolution. The original shape file contained 10911 individual buildings blocks within the study area. This was dropped to 7794, 6064 and 4406 in 5m, 7.5m and 10m raster representations respectively as it is shown in the Figure 8-3b above. This reduction took place due to merging of individual buildings with neighbouring blocks. As a result, with the increase of the pixel size, space between building blocks disappears and effective flow through those buildings could not be represented in the model. Thus the model deviates from the real flow conditions.

When the buildings are represented with 10m pixels it has the potential to block up to 14m wide road segments or equivalent space between building blocks. This is represented in the Figure 8-2a above. In this case the flow path will be obstructed at the point shown with the arrow. These obstructions can be eliminated from the combined DTM by adding a road surface elevation model at the end to the combined DTM. However, this is not applicable for spaces between buildings where there is no road segments. Therefore better overland flow could be achieved between individual buildings with lower pixel resolutions. It is advisable to use high resolution DTM when it is required to study changes in flow condition in individual buildings (i.e. EIA studies for infrastructure developments). However pixel resolution up to 10m is quite satisfactory for small-scale applications. Table 9-1in the conclusion chapter indicates optimum pixel resolution for various modelling applications.

8.3.2. Road network

Overland flow in general conveys along roads during a flood event. Therefore this phenomenon should be represented in the model too. Hence road network elevation as well as dimensions should be close to the reality for better results. Also during the model calibration road network plays a major role. Since overland flow carries along roads, inundation extent is more sensitive to roughness of road surface compared to any other land use type. Therefore fine calibration is feasible by varying Manning's roughness of the road network if the road surface is hydraulically connected using raster cells.

This could be achievable only if pixels, representing road surface are connected to each other along the sides but not diagonally. Figure 8-4a shows a raster representation of 7m wide roads using 10m pixels. Each cell representing road surface is not connected along side and as a result continuous overland flow cannot be obtained with this representation.

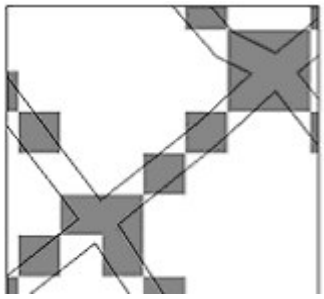

Figure 8-4a: 10m raster

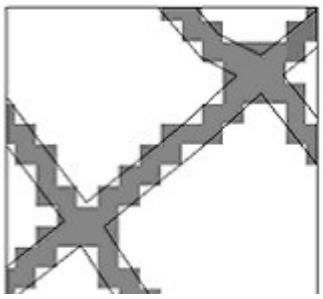

Figure 8-4b: 5m Raster

Figure 8-4: Difficulty of representing road surface as connected cells

Therefore in this case, pixel size should be reduced so that cells representing road surface are connected to each other along side as shown in the Figure 8-4b. This representation is possible only if the road width is greater than $\sqrt{2}(Pixel\ resolution)$.

In order to make sure continuous overland flow along roads in 5m, 7.5m and 10m DTMs, road widths less than $\sqrt{2}(Pixel\ resolution)$ were increased up to 7m, 10.6m and 14m respectively. Though it was increased up to 14m in the 10m DTM, effective flow width would be 10m. This procedure has undesirable effects; a representation of 2m wide footpaths as 10m in the 10m DTM will eventually results in considerable difference between the model and real conditions.

Therefore if the road surface is relatively different from natural terrain elevation, it is advisable to conduct detailed urban modelling with DTMs having pixel resolution below 10m. In contrast DTMs with pixel size less than 5m is quite hard to employ in small-scale studies since it will end up with extensive computation time.

8.4. Effect of DTM resolution on modelling results

Model results from the 5m, 7.5m and 10m DTMs were analysed to explore changes in both depth of inundation and flow velocities. Comparisons were made at specific point locations as well as selected areas in the flood plain under following four control levels.

- At selected points of the flood plain covering roads, rivers and open spaces.
- Entire inundated area at every 10 hrs intervals for average water depth and velocity.
- Whole inundated area for maximum average water depths and velocities.
- Selected built-up and non-built up areas at every 10 hrs interval for average values.

Initially 7.5m and 10m DTM were separately simulated in Delft FLS with same initial and boundary conditions. However 5m DTM did not run with Delft FLS since the number of pixels exceeded the maximum allowed. Therefore 5m DTM was simulated in new SOBEK model. Boundary conditions and SOBEK node structure used for the comparison are shown in the annexure A6.

In this analysis first, all the observations were made and later they were summarised in section 8.6 below and finally an attempt was made to explore the reason for each observation.

8.4.1. Depth of inundation with spatial resolution

8.4.1.1. Within selected points of the flood plain

During each step of simulation depth of inundation was recorded by specifying cross sections (or history stations in case of SOBEK) at suitable locations in the flood plain. In Delft FLS those points are specified in the master definition file, but in SOBEK, it can be done by adding "History nodes" during the network preparation. By doing so, at the end of the simulation it is convenient to compare water depth and flow velocities at those locations. Besides to the specified cross-sections additional points were selected within the floodplain where experiencing high velocity flow paths (i.e. along roads and spaces between structures). The resulting inundation depths and flow velocities were analysed at these locations to identify the model variation due to change of pixel size.

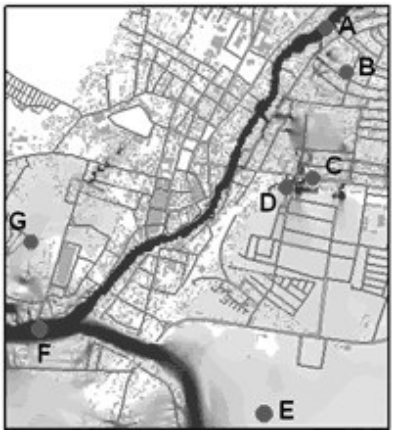

Description of points

A: Within the Naga River
B: Between buildings
C: Along a main road
D: Along a main road
E: With none built-up area
F: Within the Bicol River
G: Within low land area

Figure 8-5: Selected points for comparison of results

Depth of inundation vs. time was plotted from the simulation results obtained from 5m, 7.5m and 10m DTMs. The resulting inundation depth vs. time graphs for each point are shown in the in the Figure 8-6 below. Letters A to G refer to the point locations shown in the Figure 8-5 above.

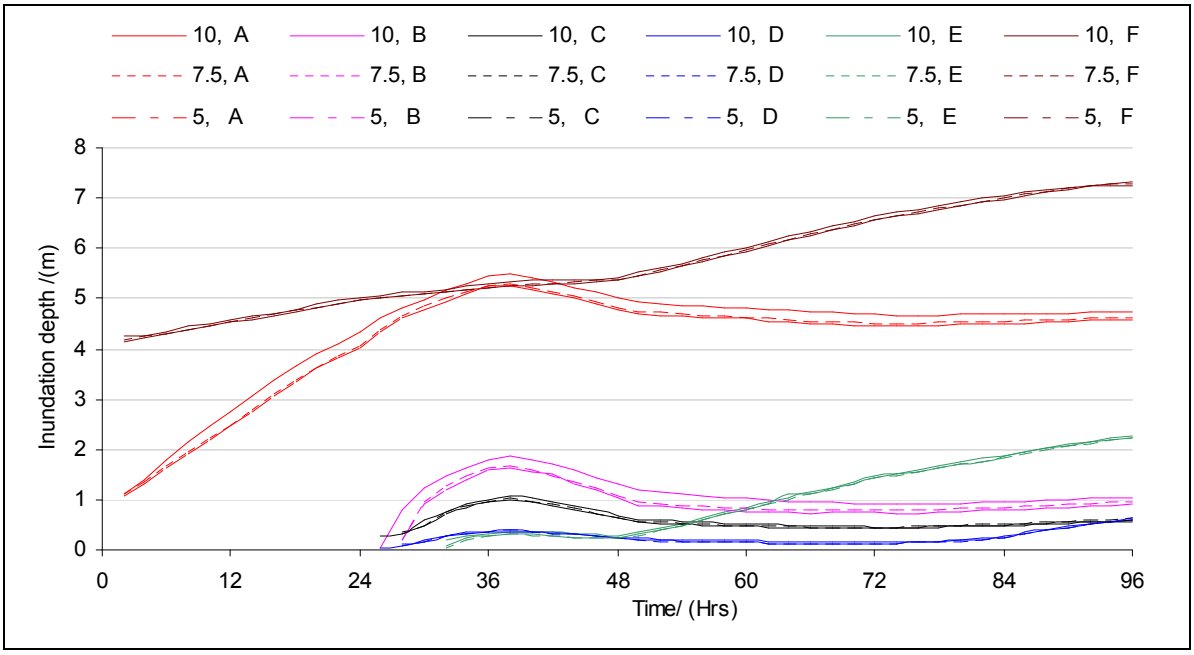

Figure 8-6: Inundation depth variation with pixel sizes 10m, 7.5m and 5m at specific points.

It was observed that inundation depth has little or no variation with 5m, 7.5m and 10m DTMs. However in location A and B shows about 17 cm higher water depth in 10m DTM with compared to 7.5m DTM. At the same points water depth variations with 7.5m and 5m DTMs were less than 2cm. Point B is located in between two buildings in highly built up area while A is located at the centre of Naga River. This change may be occurred due to the influence of difference in representation of rivers and structures in DTM with different pixel size for pixels flowing at higher speed. Detailed explanations for all these observations are given in section 8.6 below.

8.4.1.2. Average water depths at entire inundated area

Here average water depth was calculated within the whole inundated area at every 10hrs of the flood event. Current version of SOBEK has a limitation for recording the ASCII files at every time step for longer duration flood event simulations. Therefore two simulations were made to generate water depth files and velocity files separately. The resulting water depth vs. time variation for 7.5m and 10m model results are shown in the Figure 8-7**.** Corresponding 5m depths of inundations was just above 7.5m results and not included in order to obtain clear representation. However about 2cm higher water level was observed in 5m DTM compared to that of 7.5m DTM. Also an average 4cm (3%) water level drop was observed in the 10m DTM compared to 7.5m DTM.

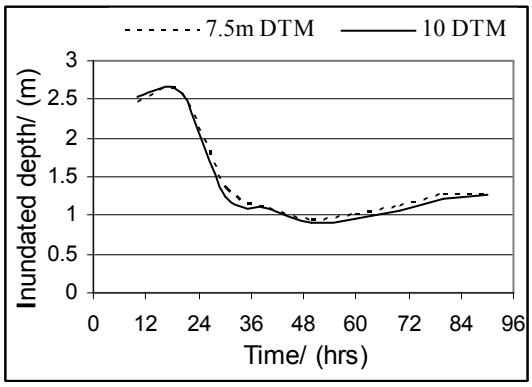

Figure 8-7: Average inundation depth variation with spatial resolution.

However these variations are not significant in flood hazard mapping or other modelling applications. Therefore simulation with 10m DTM is quite sufficient for flood hazard mapping based on depth of inundation.

8.4.1.3. Averaged maximum inundation depths

Thirdly, the maximum water depth experienced by each pixel during the whole simulation period was compared in 10m and 7.5m pixel levels. The average of maximum water depths of the 7.5m DTM was calculated as 1.295m while that of 10m DTM was 1.278m. The difference was just 1.7cm.

8.4.1.4. Average depths in built up and non built up areas

Finally, a further analysis was made to explore the water level variation within built up and none built up areas as shown in the Figure 8-8 with pixel size. Separate masks were prepared for each control area and the average water depth within each zone was calculated. The recorded average water depth variation vs. time for 5m, 7.5m and 10m DTMs within the built up area is shown in the Figure 8-9a**.** That of the non-built up area is shown in Figure 8-9b above.

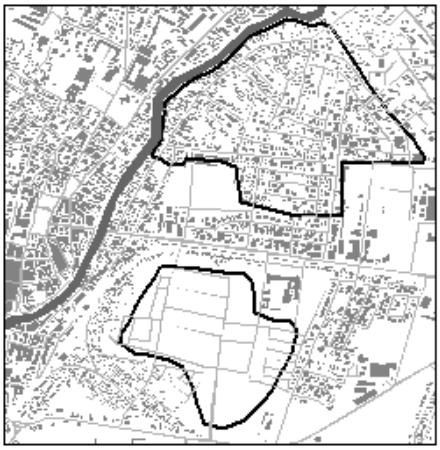

Figure 8-8: Built up and none built up areas use for the analysis

Though the average inundation in the entire inundated area was nearly the same for all the DTMs (see Figure 8-7 above), it was quite different in the built up area. About 20 to 15cm higher water depth was shown in 10m DTM compared to 7.5m DTM at built up area while distinct variation was not shown in none-built up areas.

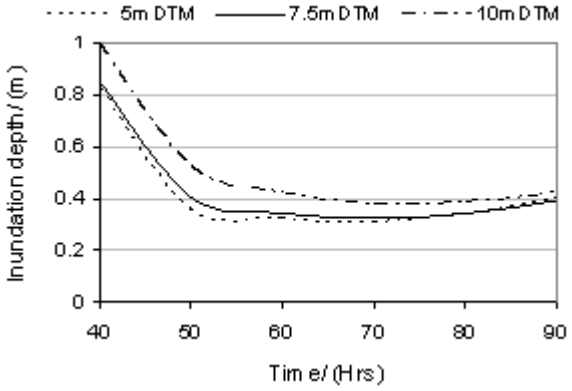

Figure 8-9a: Depth of inundation variation in built up area with spatial resolution

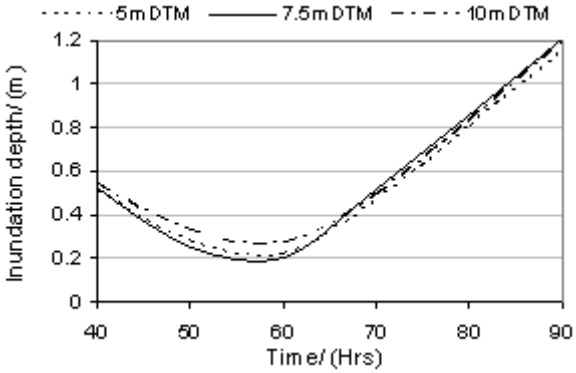

Figure 8-9b: Depth of inundation variation in non-built up area with spatial resolution

8.5. Velocity variation with spatial resolution

8.5.1.1. Within the selected points of the flood plain

Velocity vs. time was also plotted for simulation results of 5m, 7.5m and 10m DTMs for the same points shown in the Figure 8-5 above. In this case quite higher deviation was observed between the 7.5m and 10m DTM results. The resulting velocity vs. time plots for only five points were given in the Figure 8-10 for clarity.

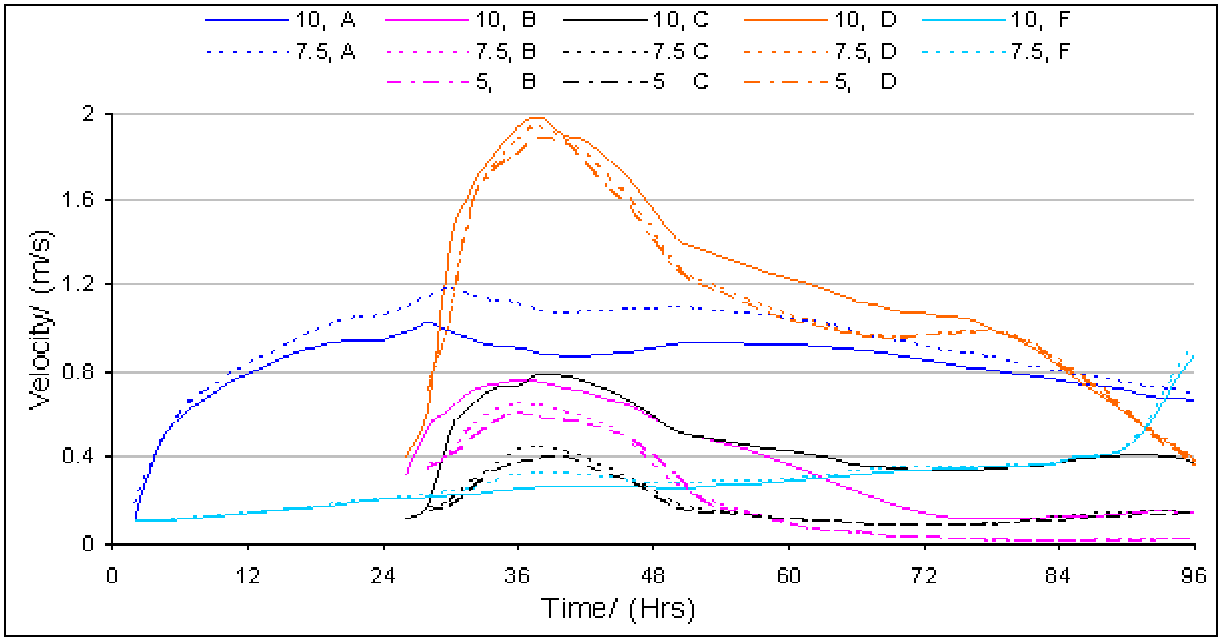

Figure 8-10: Variation of flow velocities with pixel resolution

In the 5m DTM results, points at Bicol River and Naga River were removed from the analysis since they were part of the 1D network in the SOBEK model. Therefore the velocity distribution at rivers was limited to 7.5m and 10m DTM.

In this case all points located in the flood plain show higher velocity in the 10m DTM while compared to that of 7.5m and 5m DTMs. Also 5m DTM shows the lowest velocity and little difference was observed between 5m and 7.5m DTMs. Therefore the flood plain velocity increases with the increase of pixel size.

However within the river reaches (i.e. at point A and F) 10m DTM shows low velocity as compared to 7.5m DTM. Therefore in river reaches velocity reduces with the increase of pixel size. In this case 5m DTM results were removed from the analysis since in SOBEK, rivers were modelled separately as 1D feature.

However before coming to the above conclusions further controlled studies were made at total flood plain as well as built up and none built up areas to explore the model results.

8.5.1.2. Average velocity within the flood plain and river

First average velocities of the entire inundated area and within the floodplain at every ten-hour interval were calculated in all DTMs. The resulting graphs are shown in Figure 8-11a and b below. In this case too 5m DTM velocities were removed form the analysis due to the same reason.

Within the floodplain, velocity of 10m DTM is higher than 7.5m DTM through out the simulation period. Also 7.5m DTM results are slightly higher than the 5m DTM results. Therefore it is can be concluded that with the increase of pixel size the velocity increases within the floodplain.

However within the river reaches a very clear velocity decrease was observed with the increase of pixel size. Therefore the observations made in the points A and F in the above section further confirm with this remark.

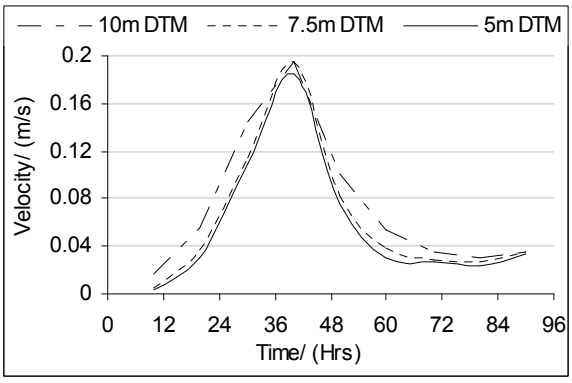

Figure 8-11a: Average velocity variation with pixel size within the entire flood plain

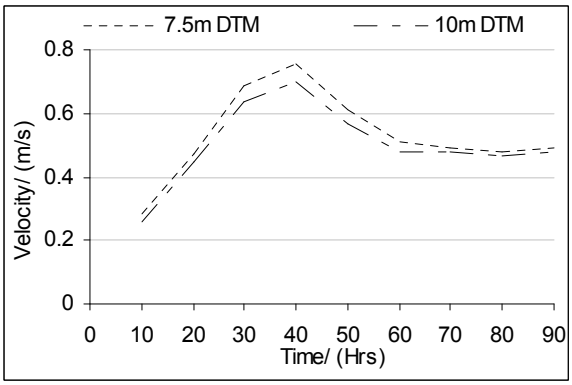

Figure 8-11b: Average velocity with pixel size within the Rivers

However to explore the velocity distribution further within the flood plain an additional analysis was conducted by selecting areas from the built up and none-built up areas.

8.5.1.3. Within built-up and non-built up areas

Velocity distribution within the built up and none built up areas were further analysed inside the masks shown in Figure 8-8 above. Average velocities within the masks were calculated at every 10 hr intervals for 5m, 7.5m and 10m DTMs and shown in the Figure 8-12a and Figure 8-12b respectively.

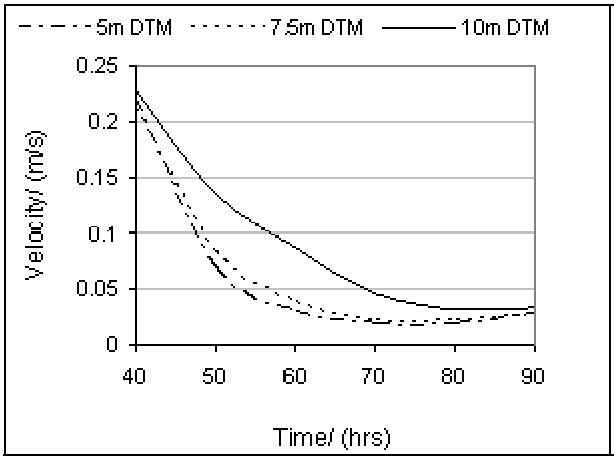

Figure 8-12a: Average velocity variation within built up area with pixel size

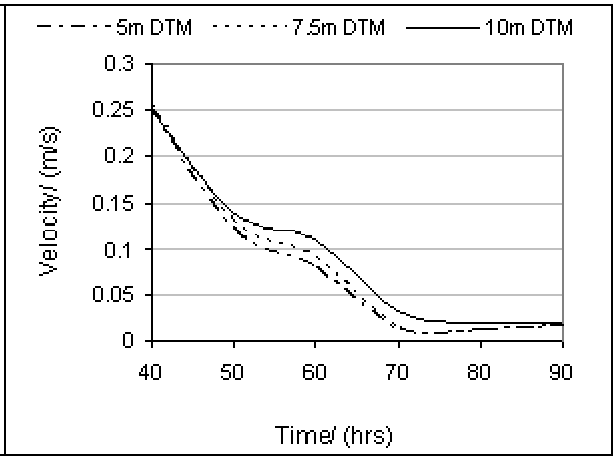

Figure 8.12b: Average velocity variation within none-built up area with pixel size

In built up area 10m DTM shows distinctly higher velocity variation (i.e. 28%) increase with compared to 7.5m DTM. The increase in 7.5m DTM with respect to 5m DTM was about 6%.

In none built up area 10m DTM shows about 18% velocity increase with compared to 7.5m DTM. Also velocity increase in 7.5m DTM compared to 5m DTM was 5%. Therefore further conclusion can be derived, as velocity increase with the increase of pixel size is higher in built up areas than none-built up areas.

8.6. Summary of findings and reasoning

From the above analyses following observations were made.

- Within the river reaches velocity reduces with the increase of pixel size
- Within the floodplain velocity increases with the increase of pixel size
- Velocity increase is higher in the built up area as compared to none built up areas with the increase of pixel size
- Within built up areas inundation depth increases with the increase of pixel size

It was found two reasons for these deviations and explained below.

8.6.1. Variation of DTM slope with the change of pixel size

Changes in velocity primarily depend on terrain slope, roughness or boundary conditions. As long as holding the roughness and boundary conditions constant if the velocity still changes it must be due to the terrain slope variations. Therefore further analysis was made to explore the terrain slope variation with the pixel size.

First maximum terrain slope of the whole study area was calculated for 5, 7.5 and 10m DTMs. Later initial TIN DTM was used to generate further raster DTMs with pixel size 15m and 25m to generalise the relationship between spatial resolution and the slope. The resulting terrain slope vs. DTM resolution is shown in the Figure 8-13a below. Very clear drastic reduction was observed in the maximum slope with the decrease of pixel resolution.

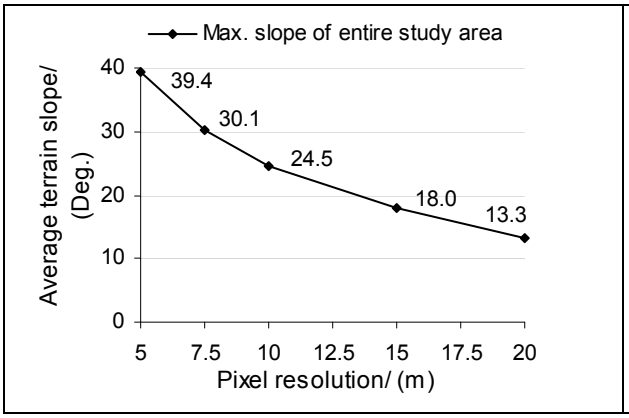

Figure 8-13a: Maximum slope variation within entire study area with pixel size

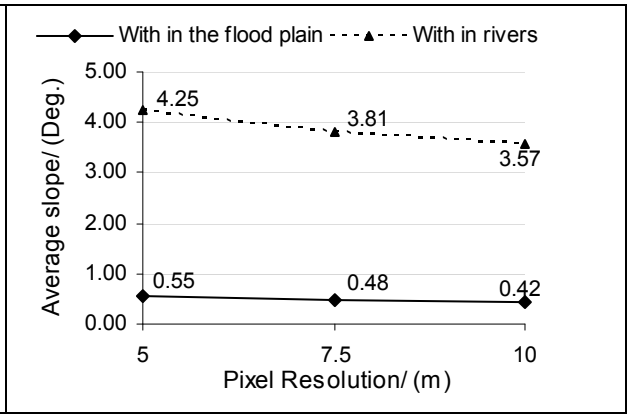

Figure 8.13b: Average slope of the flood plain and rivers with pixel resolution

In addition average terrain slope vs. pixel resolution was further analysed in following controlled areas.

- Flood plain
- River reaches

The resulting variation remains same for both the controlled sample areas. Therefore this terrain slope reduction with the increase of pixel size gave the clarification for the increased velocity in the flood plain as well as decreased velocity in the rivers with the increase of pixel size.

Along the river reaches water flows towards the downward slope. Then during the rasterisation if the slope of the river reduces resulting flow velocity will be reduced. This clarifies the above first observation; reduction of flow velocity within the river reaches with the increase of pixel size.

Though along river reaches water flows downward, during a flood event excess overland flow gushes towards upward direction during the propagation of the flood event. As a result if terrain slop deduces due to the rasterisation, the resulting overland flow velocity increases at this stage. Because resistance to the overland flow towards uphill is lesser if the terrain slope is decreased. This clarifies the second observation of higher velocity with the increase of pixel size within the flood plain.

However this strange slope reduction with the increase of pixel size was further examined for

- Smooth terrain with constant 1% slope
- Undulated terrain with constant 1% slope

In smooth terrains

First, a fictitious contour map with 200 contours lines with 1m spacing and elevation varying from 0 – 2m was created. In this case slope of the terrain is 1% and it is smooth and constant through out the terrain. The resulting contour map and longitudinal section across the terrain is shown in the Figure 8-14

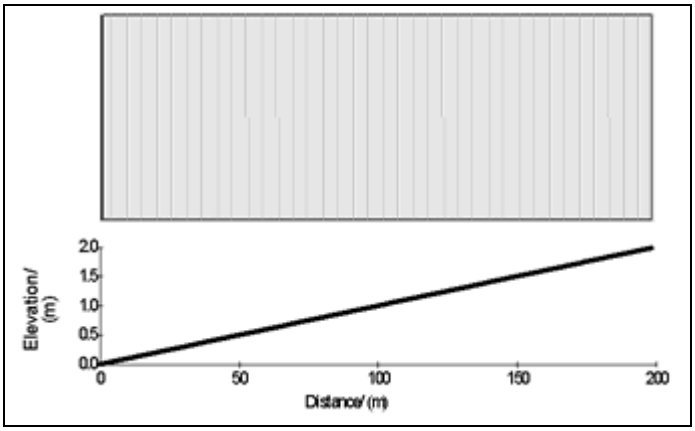

Figure 8-14: Fictitious contour map with 1% smooth slope

Then using this contour map, DEMs of 1m, 5m, 7.5m and 10m were created and slope of the each map was calculated. No slope reduction was observed in this case with the increase of pixel size. When calculated the slope of each DTM is found to be 0.99%. Therefore, with this observation it can be concluded that no slope reduction will occur with the increase of pixel size if the terrain is smooth and constant.

In undulated terrains

The same analysis was conducted by changing the above contour elevation, so that it represents an undulated terrain while maintaining the total terrain slope at 1%. Updated DTM with longitudinal section over the terrain is shown in Figure 8-15.

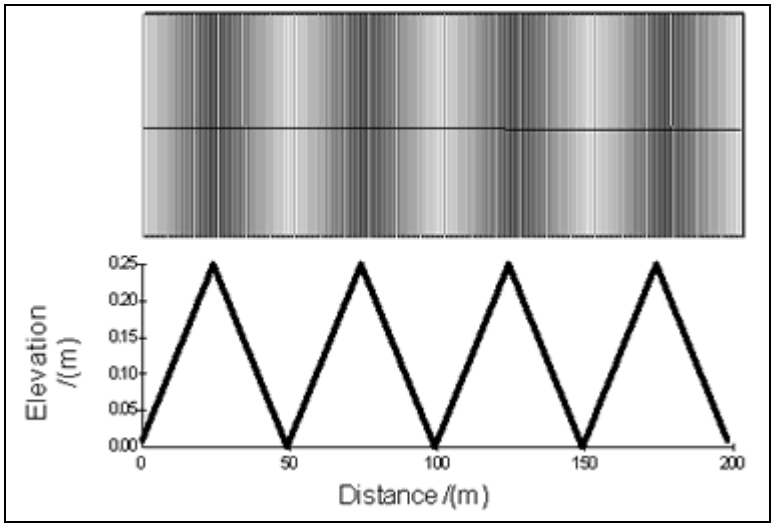

Figure 8-15: Undulated terrain with 1% slope

Then this contour map representing the undulated terrain was used to create DTMs with pixel resolution of 1m, 5m, 7,5m and 10m. Then a slope map corresponding to each DTM was generated and average slope of the each map was calculated. Though original contour represents 1% slope, it has considerably dropped with the increase of pixel size. Resulting average slopes are shown in Table 8-1

Pixel size/ (m)	Original contours	1m	5m	7.5m	10m
Slope (%)	1	0.96	0.82	0.73	0.65

Table 8-1: Slope reduction with the increase of pixel size in an undulated terrain

Therefore this analysis further clarifies that terrain slope does not change with the increase of pixel size in uniformly varying terrains (with constant gradient). However, considerable slope deduction results in undulated terrains with the increase of pixel size.

In general natural terrains are not even and constant slope cannot expect. Especially urban terrains are more undulated due to the various manmade activities.

However this slope reduction is subjected to local areas of the terrain and slope of the entire terrain (along X or Y direction) do not change as the figures given in Table 8-1 above. However local terrain changes more sensitive for any 2D model based on finite element or finite difference approach since it calculates flow velocities from once cell to its neighbouring lowest elevation cell.

8.6.2. Blockage of flow path due to rasterisation

The second reason for the observations, summarised in the section 8.6 above could be conveniently explained once zoomed into a measurement point shown in the Figure 8-5 above.

Point C was located at centre of a road on the flood plain. Figure 8-16a shows the position of the point C with surrounding building footprints, which were rasterised into 10m pixels. The same location again represented in the Figure 8-16b with neighbouring building footprints, that were rasterised using 7.5m pixels. In the 10m-raster representation most of the spacing between buildings has blocked during the rasterisation. In addition road width has tapered at point C compared to 7.5m raster representa-

tion. Therefore if same discharge passes along the road through the point C, the resulting velocity in 10m DTM should be higher since it has small cross section compared to 7.5m elevation model. It clarifies higher velocity distribution at point C in the 10m DTM.

Figure 8-16a: Narrow and blocked flow paths in 10m DTM

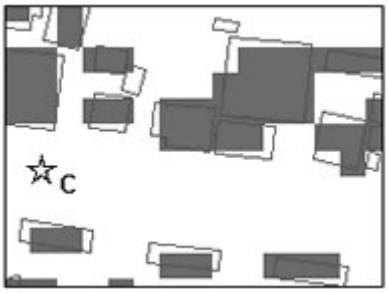

Figure 8-16b: Relatively wider flow path in 7.5m DTM

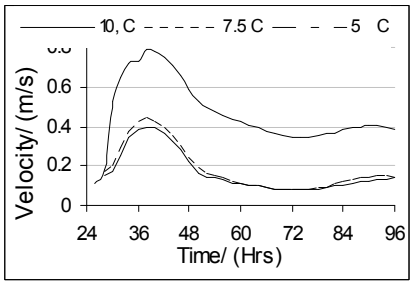

Figure 8.16c: Velocity distribution at point C with pixel size

Figure 8-3 above shows changes in total number of building blocks with spatial resolution. With the increase of spatial resolution adjoining individual building blocks merge each other and number of blocks reduces. It has reduced up to 40% in 10m DTM. Therefore in general whole built up area over land flow paths may have blocked in the 10m DTM with compared to 7.5m DTM and 5m DTM. As a result in the built up area velocity distribution should be higher in the 10m DTM compared to the 7.5m DTM. With this explanation third observation made in the section 8.6 above clarifies.

Before coming to the conclusion that within the built up areas velocity distribution increases with the increase of the pixel size another two more control analyses were conducted by selecting built up and none built up areas for average velocity variations with spatial resolution.

Therefore it can conclude that with the increase of pixel resolution velocity distribution increases in the built up area. Reason for velocity increase in none built up area cannot be explained based on the previous argument of flow path blocks due to dense urban structures. Therefore average slope of the study area was calculated with different pixel resolution to explore variation of the slope with pixel resolution.

Also as a result of this increase in flow path blockages with the increase of pixel size the other out-come would be the increase of water depth. Therefore due to the same reason within the built up area, water depth increases with the increase of pixel size in the input DTM.

8.7. Building as solid blocks or with a higher roughness at footprints?

During a flood event none of the buildings can seal against the floodwater. Therefore buildings act as pools of water and do not flow across the buildings. If buildings were represented as solid blocks in the model storage capacity of buildings has ignored. In order to model storage capacity as well as to avoid any flow across the buildings, it is a good suggestion to remove the buildings from the DTM and instead assign a higher roughness at the building footprints. With the increase of roughness it is possible to reduce the conveyance at building footprints without affecting the storage.

Therefore model behaviour was explored further by removing solid building blocks from the DTM. Instead higher roughness value (i.e. Manning's n=1) was assigned to building footprints in the friction input file of the model. In this case a new simulation was run by input of a DTM without solid building blocks and results were compared with previous simulation, which was conducted with a DTM having solid building blocks.

8.7.1. Flow pattern

Resulting maximum velocity distribution and inundation depth variation were evaluated in both DTMs and shown in the Figure 8-17 and Figure 8-18 respectively below.

Serious flow path deviation was not observed in the input DTM without buildings as solid blocks. Though actual buildings were not represented in the DTM still the main flow paths remained same in the both simulations. Once buildings were input as solid blocks conveyance across the buildings has reduce to very low level. Only a small flow velocity ranging from 0.02 to 0.05m/s was observed across the buildings Therefore, removal of buildings from the DTM does not make large variation in flow pattern within the built up area.

Inundation depth variation also analysed in the above two cases. Once buildings were incorporated, as solid blocks in the DTM pixels representing buildings do not inundated until water level reaches up to the roof level of the buildings. However once they were removed from the DTM, pixels representing buildings blocks inundated up to the same level of their neighbouring pixels. In reality too all the building in the vicinity inundate and cannot seal against the floodwater. However quantity of water enters into a building obviously not equal to volume of the building. As a result once the solid building blocks removed from the DTM obvious under estimation of water depth will result.

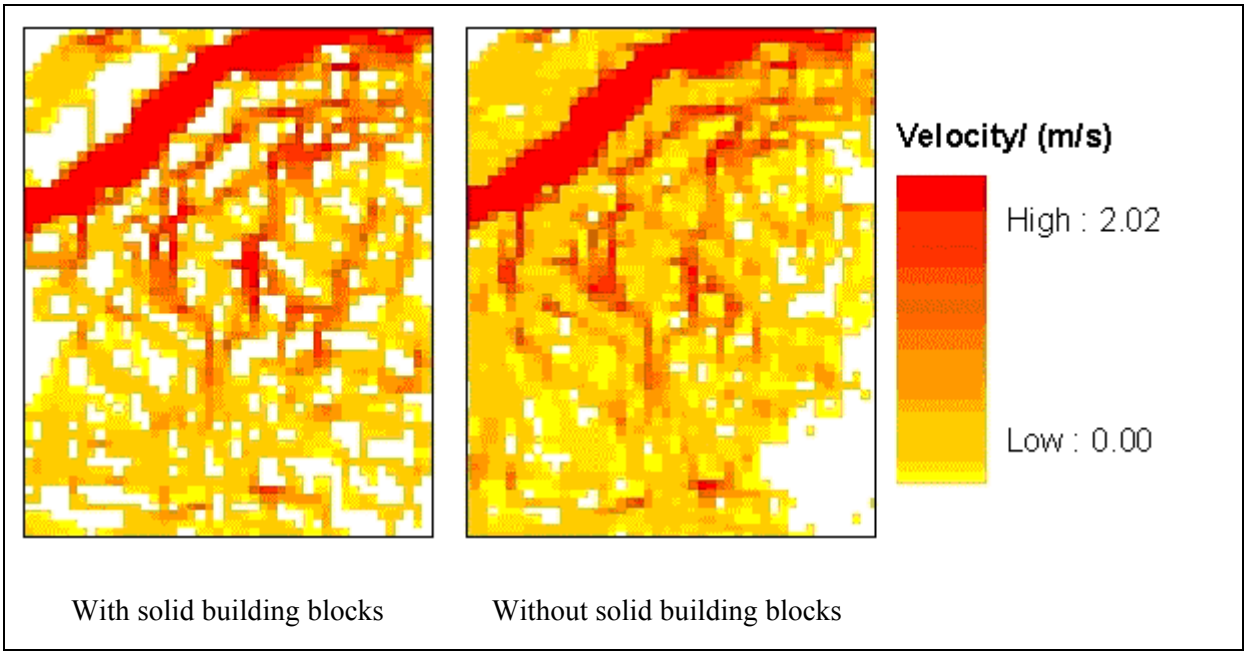

Figure 8-17: Flow pattern with and without buildings as solid blocks in the input DTM

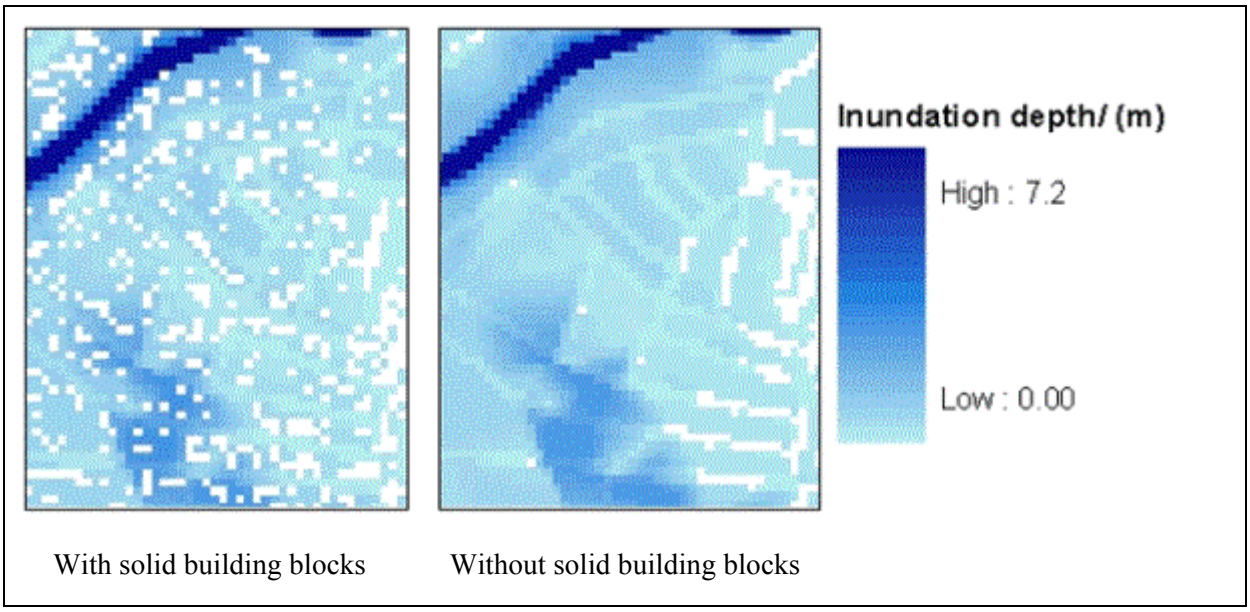

Figure 8-18: Inundation depth pattern with and without buildings as solid blocks

8.7.2. Water level variation

Further observation was made to identify the water level variation as a result of removing solid building blocks from the input DTM. Maximum water depth files for two simulations indicated average inundation depth of 51cm in the DTM without solid building blocks and 57cm in the DTM with solid building blocks. Therefore with respect to the maximum water depth average variation was about 12%

In addition the similar variation was observed throughout the simulation and it is shown in the Figure 8-19. The resulting average deviation of inundation depth for entire period was about 7cm. That is equivalent to 6% increase with compared to the DTM without solid building blocks.

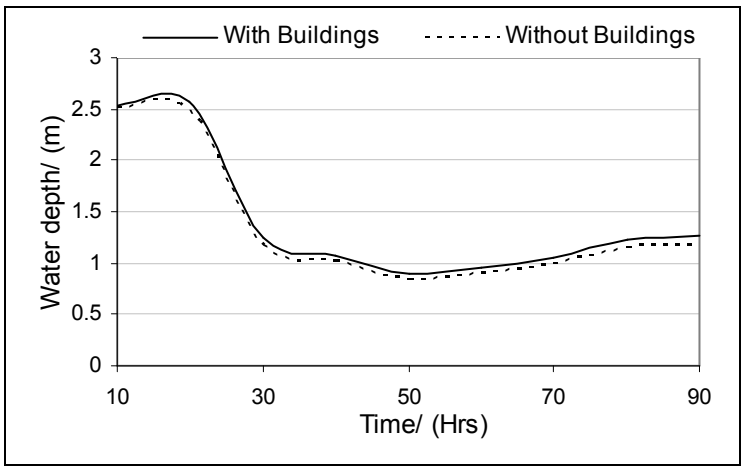

Figure 8-19: Inundation depth variation with and without buildings in the input DTM

Removing the solid buildings blocks from the DTM and assigning higher roughness coefficient at the building footprints in the friction file of the model can avoid this over estimation. However, flow pattern of the flood pain does not vary considerably due to the removal of buildings from the DTM.

However while correcting the overestimation of inundation depth by removing buildings from the DTM on the other hand it results underestimation of inundation depth. Since volume of the buildings is grater than the quantity of water fill inside the buildings during a flood event.

Therefore better modelling approach would be an in-between solution. That is *X* % (X can be selected by field observations i.e. ranging from 60 - 90%) of buildings can be removed from the DTM as solid block while the rest keeping as it is and buildings which are removed from the DTM can assign higher roughness at their footprints in the friction file.

The important remark of this analysis is same flow pattern can be achieved even without solid building blocks in the DTM by assigning higher roughness coefficient

8.8. Flood hazard mapping

Hazardous level of a flood event depend on several factors such as depth of inundation, velocity of flood water, duration of inundation and warning time of the event. Therefore proper representation of hazard cannot be made using single parameter alone. However the information required for deriving velocity of overland flow, duration and warning time of the flood cannot be obtained from conventional 1D modelling approach in urban areas where flow is diverted from the main line. 2D modelling outputs can be manipulated to derive above four hazard parameters by combining with other hydrological data sets.

Therefore depth of inundation, energy of floodwater and duration of inundation for ten year return period four-day flood event was combined in this study to generate the multiple-parameter hazard map. Instead of velocity, the kinetic energy term was used for better representation of hazard level for erosion as well as damage to light structures. Warning time of the flood event was skipped in this study since duration and intensity of the rainfall event was unknown for the input hydrographs used for the study.

Finally combined hazard map was compared with the conventional inundation depth based hazard map. An increase of 16% was observed in high hazard zone in the combined map. The reason for this increase is explained with an example. In a pixel, if water level is less than 0.8m, it has classified as "Low hazard" in the inundation depth based hazard map. However if the same pixel has inundated longer than 64hrs or if the maximum flow velocity exceeds 2m/s, it will be classified as "High hazard" in the multiple-parameter hazard map. Therefore in the multiple-parameter hazard approach the level of hazard represents more meaningfully, compared to the inundation depth based hazard map. The best representation for the decision maker is to hand all four-hazard analysis, since remedial action might require a competent decision that could be erroneous by just having only partial information.

Hazard parameters introduced in this study would be more useful for other applications than the flood hazard mapping. For example energy map would be ideal tool for erosion and sedimentation studies. Warning time is a useful tool for developing evacuation plans for dam break scenarios.

Cut off level of each parameter for hazard zone definition can be changed according to end requirements of each study as well as individual perspective. However the methodology remains the same even if it is needed to combine additional hazard parameters other than mentioned above.

8.8.1. Advantages of the new approach

During the process of generating the combined hazard map, first hazard maps representing individual parameters (i.e. water depths, kinetic energy and duration of flood) were created. These individual hazard maps were shown very useful for specific urban planning activities

Maximum kinetic energy map shown in Figure 7-4a clearly shows the area where high-energy flow paths are resulting during a flood event. Kinetic energy maps can be used to delineate potential eroding areas. This information is useful when prioritising road rehabilitation programs. Particularly, for Naga municipality, roads within the high-energy zones can be converted from asphalt to concrete surfacing to reduce the damage during flood events.

Also the kinetic energy map in the Figure 7-4a indicates the major over land flow path through the lowland between the Naga and Bicol River. This overland flow path is essential information for city planning authorities to avoid any permanent constructions on these low land areas and to study potential remedial actions.

Reliable flood risk map could be derived from the final combined hazard map by incorporating land use, elements at risk and investment of the inundated area.

9. Recommendations and conclusions

9.1. Low cost elevation data for DTM generation

This study revealed that the latest high resolution remotely sensed elevation data sets are not essential for hydrodynamic modelling applications in hazard assessments. Instead detailed urban 2D flood model can be constructed with scattered elevation data sets among different service organisations. Therefore, if detailed single elevation data set is not available it is always advisable to look for scattered data sets in infrastructure development and maintenance organizations in the area. These elevation data sources are usually with large scale and adequate for this kind of 2D modelling requirements. However these data sets alone may not be able to cover entire study area and additional field survey may require filling the data gaps and combining the data into a common reference.

Reliable and detailed flood hazard maps and model simulation for future development scenarios can be generated using those data sets without financing on high cost new elevation data. However a plan for upgrading the available data sets in non-surveyed areas must be contemplated.

9.2. Input DTM for 2D flood models

If different elevation data sets are available it is convenient to generate a TIN DTM and convert it to raster later. Development of separate elevation models for natural terrain and road surfaces is adequate in detailed urban modelling to conduct various scenario analyses (i.e. identify changes in inundation due to increase of road elevation) and remove badly positioned buildings from the road surface.

This study revealed that although the buildings were removed from the DTM, same flow pattern was able to achieve by assigning very high roughness at the buildings footprints. Though, this removes the overestimation of inundation depth by not allowing the floodwater to fill inside the buildings at the same time it make underestimation of water level by removing the complete structure. Therefore it is useful to represent percentage of buildings (i.e. 10% - 40%) as solid blocks removing the rest from the DTM and assign very high roughness (i.e. Manning's=1) for building footprints in the friction file of the model. By replacing buildings blocks by high Manning roughness (flood water fills up the entire building), the water level decreased 7 cm. These are two extreme situations. The evaluation of elements at risk done by urban professionals should identify a proper value of storage as a percentage of the imprint area of the building.

9.3. Optimum pixel resolution for urban flood modelling

This study further reveals that with the increase of pixel size over 10m, urban features cannot be represented with desired accuracy in the input DTM of the raster based 2D models. Specially, if the terrain elevation is significantly differs from the road surface elevation, continuous overland flow along roads cannot be modelled with pixel resolution lass than 10m. If width of the roads is less than

$\sqrt{2}(Pixel\ resolution)$, it is necessary to increase its width up to that level to assure continuous over-land flow along roads.

With the increase of the pixel size individual building blocks get merged with the neighbouring buildings. As a result effective flow paths between buildings blocks disappears. Also the shape and position of building footprints deviates considerably from the original shape and position with the reduction of spatial resolution. However these effects are not significant for small-scale modelling applications as well as flood hazard mapping. In contrast, pixel size less than 10m (i.e. 7.5m) is preferred for detailed flood modelling in built up areas.

More importantly, considerable velocity increase was observed within the flood plain during the propagation of the flood event with the reduction of the spatial resolution. However it contradicts in river reaches. With the reduction of pixel resolution velocity reduces within the rivers. The primary reason for these variations is local slope reductions with the decrease of pixel resolution as explained in section 8.6.1. This slope reduction is very significant at undulated terrains at local levels. However slope reduction is not significant globally within the entire terrain along a section in any direction.

With this observation it was able to clarify the reason for higher velocity distribution in the flood plain while lower velocity within rivers with the increase of pixel size. 2D raster based finite element or finite difference models are sensitive for local terrain undulations. Therefore selection of pixel size should be done carefully before proceeding with the hydrodynamic modelling in rough terrains for sensitive modelling applications where velocity fields are important.

Also velocity distribution is relatively higher in built up areas as compared to none built up areas. This increase results due to the loss of effective flow path in built up areas with the increase of pixel size.

Significant inundation depth variation does not result with the variation of pixel size in none built up areas. However it is significant in built up areas with the increase of pixel size. The following table summarizes the findings in this thesis although is has to be taken with caution for other studies where buildings and land feature have different characteristics to those presented in here.

Applications	5m DTM	7.5m DTM	10m DTM
Flood hazard mapping in urban areas			Adequate
Detailed studies related to velocity measurements, sedimentation and erosion.		Adequate	
Studies (EIA) relating to individual structures or reclamation of small lands	Adequate		
Small scale EIA studies in regional level for investigating effects on new roads/ small scale reclamations projects etc.			More than 10m

Table 9-1: Optimum pixel size for various model applications

9.4. Flood hazard mapping

Conventionally flood hazard maps were based on a single parameter; depth of inundation. However level of hazard cannot be measured by depth of inundation alone, since other attributes of a flooding are considered hazardous as well. In this study flood hazard was defined using three parameters: Depth of inundation, Duration of inundation and Kinetic energy of the floodwater. More meaningful flood hazard delineation was reached by combining multiple parameters rather than the conventional approach, although the four maps are equally relevant when considering the spectrum of different potential users. From the combined parameter approach, increase of 16%, in the high hazard zone was resulted with compared to the inundated depth based hazard map. Therefore, combining multiple hazard parameters in the hazard definition can improve the reliability of the risk map.

Hazard maps based on individual parameter alone also useful for various urban planning activities. For example the kinetic energy map provides very useful information for road development and maintenance organizations for identifying areas where high erosion may take place. This information can be used choosing areas where required to convert the road surface from asphalt to concrete. Because it will leads to reduce the maintenance cost. In addition, the energy map can be used for identifying areas where structural damages are more likely to happen while modelling unsteady scenarios with rapid overland flows (i.e. dam break smulation).

The duration of inundation map plays a vital role in calculating flood risk in any land use (i.e. agricultural to commercial). Also higher duration of inundation implies that the area is acting as a retention or detention pond during floods. This information is useful for planning organizations to protect those areas from future developments.

9.5. Applicability of model results

Though this study aimed to fulfil three research objectives, model results can be used for several applications domains. It provides very clear picture to the Naga city planning authorities' the level of hazard and knowledge required to explore flood free lands for future development. Also it can be used to delineate high-energy zones where erosion and damage to light structures are potential.

The model simulation conducted to analyse the proposed Naga city master plan in the chapter six shows that the mode is sensitive for small terrain changes. Therefore the model is particularly useful for environmental impact assessment (EIA) studies related to various infrastructure development projects in the flood plains. Several simulations can be run for different alternatives and possibly reach to the best solution. Moreover necessary mitigation measure can be implemented during the design phase itself by analysing model results.

Reliable flood risk assessment is feasible by integrating the multiple-parameter hazard map introduced in this study with land use and investments of the area.

Most importantly, the model out put (i.e. AVI movies generating for each simulation) is a very useful media to present the model results for decision makers.

However out come of this study should be used with caution. The study suffered much due to the non-availability discharge measurements, some boundary conditions and inputs that were suggested but not modelled due to lack of data. The boundary conditions, use for the model were based on previous studies and they had not calibrated with actual site observations. Also it was found that the model is very sensitive to the discharge vs. height relation at the Bicol downstream. Therefore it is important to simulate the model with proper boundary conditions in the future before use it for real applications. This conclusion is supported by two other researches that concentrated on hydrodynamic modelling in the Bicol River (BCEOM, 1991) and (Nippon_Koei, 2003a)

9.6. Recommendations for Naga municipality

Though this study was not intended to identify flood control measures for the Naga municipality, following basic suggestions can be made based on various simulation results and field observations. These will be helpful only for controlling further aggravation of the flood threat in the area.

9.6.1. New lands for future developments

The model simulation conducted in chapter six for exploring the effects of proposed Naga city master plan in future floods made the following observations. Present lowlands located at southern side of the city act as retention ponds during the floods and help to ease the flood level in the city. Also over bank flow of Naga River conveys through those lowlands to the Bicol River when the Naga watershed experiencing flash floods or vice versa. Therefore it is of utmost importance to keep that flow passage free from future developments. However according to the Naga city development plan (2000 – 2010) it was chosen to develop as commercial and residential zones in the future. It was observed in the model that this development would eventually result in further aggravation of flood threat in the present commercial centre of the Naga city. Therefore this study recommends not to reclaim and develop present low lands located at south of the city for future land demand.

Alternatively, agricultural lands in north-eastern side of the city, which are not going under water even during a flood event of 20-year return period, can develop without further aggravating the flood condition at the Naga city. Therefore it is vice decision to choose those high lands for developments instead of reclaiming the lowlands at southern side of the city for fulfilling future land demand.

9.6.2. What data should the municipality record in the future?

None availability of proper river discharge measurements in Naga and Bicol Rivers was the major limitation encountered during the data collection and input data preparation for the model. Same conclusion comes out from the summary of the two previous major studies in the area. Therefore it is crucial to establish river discharge measuring stations at both rivers within the Naga city limits. Existing Camaligan water level recording station was not equipped with calibrated rating curve to convert the water levels in to corresponding discharge. Therefore conducting a survey in the river cross section at Camaligan measuring station and recording velocities to establish calibrated rating curve for this station is utmost important. The calibration at this progressive is heavily affected by tidal development so an approach where a third variable is included (tide level downstream) is the only option to build such a relationship. In this cases when the tail water does not follow a normal depth behaviour due to backwater effects or other tidal influences. Some potential equations can reproduce the rating curve,

although a collection of data is required in the field for different functioning of the measuring structure.(Clemmens, 2001)

Continuous records of discharge both in Naga and Bicol Rivers are required for proper calibration of the model. Without such calibration, the model cannot be applied for various development scenarios or any sensitive applications. Therefore establishing a hydrological data recording and monitoring scheme under the municipality will facilitate the future modelling efforts. Also during typhoon events, recording time series water level and inundation extent within selected points of the flood plain will helpful for fine calibration and validation of the model in the future. Many of these efforts cannot be handled at municipality level exclusively due to established jurisdiction policies. However the municipality can request the service of the national agencies in charge of the national river basin planning to coordinate the efforts in view of these findings.

Within the city centre, any detailed elevation data was unavailable and limited spot heights measurement collected during the fieldwork were used for generating the DTM of that area. Therefore, conducting a levelling survey in the data gap region shown in the Figure 3-2 and incorporating them in the DTM will eventually improve the accuracy of model results.

Since this study was aiming to model riverine flood hazards due to higher return periods, drainage and sewerage networks were not incorporated in the model. Also at present the municipality is lacking of proper records on those service networks. However with the availability of those service networks layouts as well as dimensions, those can be incorporated in the model. Then, the model will be capable to assess the drainage network of the city for rainfall events with low return periods once it is combined with SOBEK rainfall runoff module. The resulting model would be very useful for identifying inadequate drainage areas where inundate even during low intercity rainfall events.

9.7. Suggestions for further research

- Combine the model with SOBEK rainfall runoff module. Then, incorporate the sewerage and drainage network in the model and evaluate the model results for low return period flood events (i.e. 1 to 5 year). Also evaluate the drainage network of the Naga city using the combined overland flow and rainfall runoff model.
- Explore the terrain slope reduction with the increase of pixel size using different algorithms available for rasterisation in various GIS software.
- To incorporate the effect of overland flow towards Naga coming from uplands areas away from the riverine floodplains. This effect was not considered in this model and probably lead to some inconsistencies in the evaluation of hazards, mainly in the relatively high areas of the actual Naga (North west)
- In terms of research, to carry out the same study with dense elevation data set (i.e. using air borne laser) and compare the results with the findings of this study (i.e. variation of velocity and inundation depth with the change of pixel resolution).
- Conduct two flood risk assessment studies using conventional inundation depth based hazard map and multiple-parameter hazard map to compare the difference in risk assessment.

- Identify the sensitivity of the model for small-scale terrain changes resulting due to infrastructure development in the flood plain. In view of the pretended planning in the area this study is crucial to avoid developments in hazardous areas.

9.8. Meta data for further studies

Except building footprints and roads all other GIS layers used for this study was prepared by digitising from paper maps. As a matter of fact, this was the most time consuming task of the thesis. The work done to digitize this information is irrelevant at research based so was not presented here, but this built GIS is key for the Naga municipality as well as any future flood modelling efforts. Therefore, Meta data were fed to all digitised shapefiles, resulting analysis layers and raster files generated from the model results. Following information was included in the Meta data file.

- Brief description of data layer including original source of information, method of creation, accuracy of the layer, limitations and temporal information.
- Purpose or the end use of the layer
- Spatial reference information
- Attribute data information

Since all GIS data analysis was conducted in ArcGIS 8.2 and 8.3 versions, Meta data editing facility of ArcCatalog was used for feeding above information. In future, this Meta data information can be viewed in Meta data description section of ArcCatalog for each GIS layer.

In addition all the GIS layers used for the study were organised in a geodatabase with a separate feature data set (i.e. all the elevation data layers were kept inside a feature data set called “Elevation”) The model output raster layers were stored in a separate folder structure for each pixel size (i.e. sub folders of water depth, velocity, energy and duration of inundation corresponding to 7.5m pixel resolution kept under “7.5m output info” main folder. The entire folder structure of the data base is shown in the annexure A8.

References

Adolfo, J. D., Calara P.M. (2003). *Erosion and Development at the Bicol River Basin*. KAIBA news and features. Retrieved 12 February, 2004, from the World Wide Web: http://www.geocities.com/kaibanews/permanent/previousissues/080702erosion.htm

Alkema, D. (2001,b). Flood risk assessment for EIA; an example of a motorway near Trento, Italy. *Studi Trentini di Scienze Naturali – Acta Geologica, 78*, 147 – 153,.

Alkema, D., Cavallin, A., Amicis, M.D. (2001,a). *Strategic application of flood modelling for infrastructure planning and impact assessment.* Paper presented at the Integated Water Resources Management, Davis, California.

Alkema, D., Roo, A. d. (2003). Reconstruction of the inundation of the Ziltendorfer Niederung (Germany) during the 1997 Oder flood using a 2-D flood propagation model.

Alkema, D., Roo, A. d., Schmuck, G. (2002). Reconstruction of the 1997 flood inundation of the Ziltendorfer Niederung (Brandenburg, Germany), Evaluation of alternative scenarios. *IS-PRA, September 2002*, 70.

BCEOM, F. E. C. (1991). *Bicol River basin flood control and irrigation development project, Feasibility report, Volume 2, Annex A - Hydrology*. Naga: BCEOM, French Engineering Consultants and Sir, William Halcrow & Partners.

Beven, K. J. (2000). *Rainfall - Runoff Modelling*. West Sussex: John Wiley & Sons Ltd.

Borsányi, P. (1998). *PHYSICAL HABITAT MODELING IN NIDELVA, NORWAY.* The Norwegian University of science and Technology.

Clemmens, A. J., Wahl, T.L., Bos, M.G., and Replogle, J.A. (2001). Water Measurement with Flumes and Weirs. *ILRI Publications*(58).

Delft_Hydraulics. (2000). Manual DELFT Flooding System (Delft - FLS) (Version 2.47). Delft: Delfts Hydraulics.

Delft_Hydraulics. (2003). *SOBEC web site*. Delft_Hydraulics. Retrieved 10/7, 2003, from the World Wide Web: http://www.sobek.nl/

DHI. (2003). *MIKE 21, 2D Modelling System for Floodplains*. DHI Water and Environment Pty Ltd. Retrieved 11 June, 2003, from the World Wide Web: D:\2D Modelling\MIKE 21 Flood 2d modelling.htm

Drayton, R. S., B. M. Wilde and J. K. Harris. (1992). Geographical information system approach to distributed modelling. *Hydrological Processes, 6*(3), 361-368.

Eltahir, E. A. B., Wang, G.,. (1999). Nilometer Climate and Climate Variability. *Geographical Research Letters, 26*(4), 489 - 492.

ESRI. (2003). Raster encoding; ArcGIS desktop Help (Version 8.3). Redlands: ESRI.

FEMA. (2000). *Guidelines for determining flood hazard on alluvial fans*. Federal Emergency Management Agency. Retrieved 12 12, 2003, from the World Wide Web: http://www.fema.gov/mit/tsd/ft_alfan.htm

Fowler, R. A. (2002). *LIDAR for Flood Mapping*. Earth Observation Magazine. Retrieved 27 June, 2003, from the World Wide Web:

Gourbesville, P. (2002, 10/24). *Key position of GIS in hydro-technologies and hydrological risks assessments.* Paper presented at the ESRI User Conference, San Diego.

Granger, K. (1999). *AN INFORMATION INFRASTRUCTURE FOR DISASTER MANAGEMENT IN PACIFIC ISLAND COUNTRIES*. Canberra: Australian Geological Survey Organisation.

Horritt, M. S., Bates, P.D. (2002). Evaluation of 1D and 2D numerical models for predicting river flood inundation. *Journal of Hydrology, 268*, 87-89.

Horritt, M. S., Bates, P.D.,. (2001). Predicting floodplain inundation: raster-based modelling versus the finite element approach. *Hydrological Processes, 15*, 825-842.

Hutchinson, M. F., Gallant,J.C. (1999). *Representation of terrain*. M.F.: Longley.

Laud, J. M. S., Dizon, D.R. (2001). *Quadrangle Mapping Report; Iriga, Naga and Sibono quadrangles*. Legaspi: Mines and Geosciences Bureau, Region V, Department of Environment and Natural Resources, Philippines.

Maidment, D. R. (1993). *Developing a spatially distributed unit hydrograph by using GIS. In : Application of Geographic Information Systems.* Paper presented at the Hydrology and Water Resources, Proceedings of the Vienna Conference, Vienna.

McAlister, E., Domburg, N., Aspinall, R.,. (1997). *Environmental Mapping and Modelling of a Catchment using GIS.* Paper presented at the ESRI User Conference, Redlands.

McCowan, A., Collins, N. (2003). *THE USE OF MIKE 21 FOR FULL TWO-DIMENSIONAL FLOOD IMPACT ASSESSMENT*. Retrieved 11 July, 2003, from the World Wide Web:

McDonnell, R. A. (1996). Including the spatial dimension: Using geographical information systems in hydrology. *Physical Geography, 20*(2), 159 - 177.

Meulen, G. G. v. d., Leenders, P.H.J.A. (2003). *PoldEvac: Polder Inundation & Evacuation, a step towards the development of an integrated and cross-bordering disaster management approach*. Retrieved 10/14, 2003, from the World Wide Web: http://www.compuplan.nl/documentene/pe-englishdoc01+.htm

Nagacity. (2003, 19 11 2003). *OFFICIAL WEBSITE OF NAGA CITY*. City Government of Naga. Retrieved 19 11 2003, 2003, from the World Wide Web: http://www.naga.gov.ph/cityprofile/eco.html

Nippon_Koei. (2003a). *River basin and watershed management program, Final report for the feasibility study on phase I package*: Nippon Koei Co. Ltd.

Nippon_Koei. (2003b). *River Basin and watershed management programme, Volume III, supporting report - Hydrodynamic modelling: HY*: Nippon Koei Co. Ltd.

OIDC, O. I. D. C., INC. (1999). *DISASTER MITIGATION PLAN (MAIN REPORT), PHILIPPINE CITIES DISASTER MITIGATION PROGRAM, Naga City Disaster Mitigation Project*. Naga: NAGA CITY GOVERNMENT.

Olivera, F. (1997). *Hydrologic Modeling using GIS*. Center for Research in Water Resources, University of Texas at Austin. Retrieved 10 12, 2003, from the World Wide Web: http://www.ce.utexas.edu/prof/maidment/gishydro/txdot/litrev.html

Otieno, J. (2004). *Scenario study for flood hazard assessment in the lower Bicol flood plain Philippines using 2D model.* International Institute for Geo-Information Science and Earth Observation, Enschade.

Rath, S. (2003). *Automatic Description of Fluvial Topography and Relief for Hydrodynamic Flood Wave Simulations*. Department of River and costal engineering, Technical university Hamburg-Hargurg. Retrieved Dec. 12, 2003, from the World Wide Web: http://elbe.wb.tu-harburg.de/forschung/projekte/automatic_description.pdf

Shamsi, S. U. (2002). *GIS Applications in Floodplain Management.* Paper presented at the ESRI User Conference, San Diego.

Stelling, G. S., Kernkamp, H.W.J., Laguzzi, M.M. (1998). *Delft Flooding System, a powerful tool for inundation assessment based upon a positive flow simulation.* Paper presented at the Hydroinformatics '98, Balkema Rotterdam.

Suia., D. Z., Maggiob., R.C.,. (1999). Integrating GIS with hydrological modeling: practices, problems, and prospects. *Computers, Environment and Urban Systems, Volume 23*(Issue 1), Pages 33-51.

USDL&WC. (2001). *Floodplain Management Manual*: Department of Land & Water Conservation.

West_Sacramento. (2002). *Standard specifications, storm drainage*. West Sacramento city hall. Retrieved Nov. 05, 2003, from the World Wide Web: http://www.ci.west-sacramento.ca.us/cityhall/departments/comdev/Documents/ss2002/division1/section4.pdf

Wijetatne., V. G. (2004). *Modelling of flood events in Naga city.* International Institute for Geo-Information Science and Earth Observation, Enschede.

Wise, S. M. (2000). Assessing the quality for hyrdological applications of digital elevation models derived from contours. *Hydrological Processes*(14), 909-1929.

WMS. (2003). Watershed Modeling System (Version 6.1). Sandy, USA: GMS/WMS/SMS Group.

Appendix

A1 Water level records collected during the fieldwork

Mabulo river gauging station, Bicol River	Camaligan station, Bicol River
Location: 13 37 00 N, 123 10 56E	Location: 13 37 17N, 123 09 54E

Stream flow data: Typhoon RUPING, September 1982, Bicol river at Naga

Date	Water level/(m)
9/4/1982	0.93
9/5/1982	0.76
9/6/1982	0.87
9/7/1982	1.25
9/8/1982	2.49
9/9/1982	3.36
9/10/1982	2.42
9/11/1982	2.06
9/12/1982	1.94
9/13/1982	1.75
9/14/1982	1.66
9/15/1982	1.6
9/16/1982	1.5
9/17/1982	1.23
9/18/1982	1.13

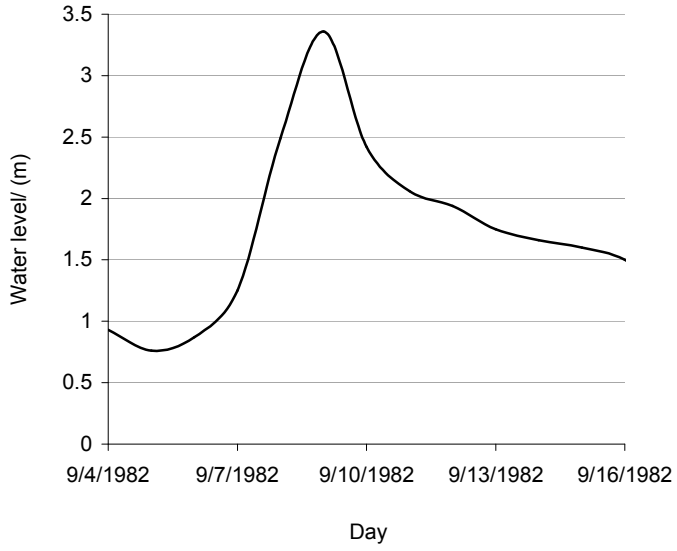

Stream flow data: Typhoon PEPANG, September 1979, Bicol River at Naga

Date	Water level/(m)
9/15/1979	0.32
9/16/1979	0.44
9/17/1979	0.82
9/18/1979	2.01
9/19/1979	2.01
9/20/1979	2
9/21/1979	1.89
9/22/1979	1.98
9/23/1979	1.78
9/24/1979	1.63
9/25/1979	0.47
9/26/1979	0.51
9/27/1979	0.28
9/28/1979	0.59
9/29/1979	0.36

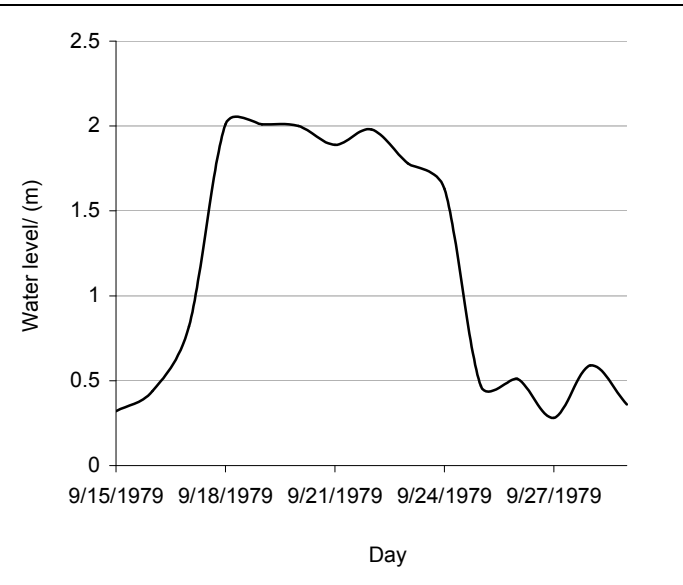

Stream flow data: Typhoon WELLING, September 1978, Bicol River at Naga

Date	Water level/(m)
9/23/1978	0.48
9/24/1978	0.56
9/25/1978	0.36
9/26/1978	0.95
9/27/1978	1.9
9/28/1978	1.96
9/29/1978	1.54
9/30/1978	1.05
10/1/1978	1.2
10/2/1978	0.95
10/3/1978	0.81
10/4/1978	0.86
10/5/1978	0.59
10/6/1978	0.77
10/7/1978	0.89

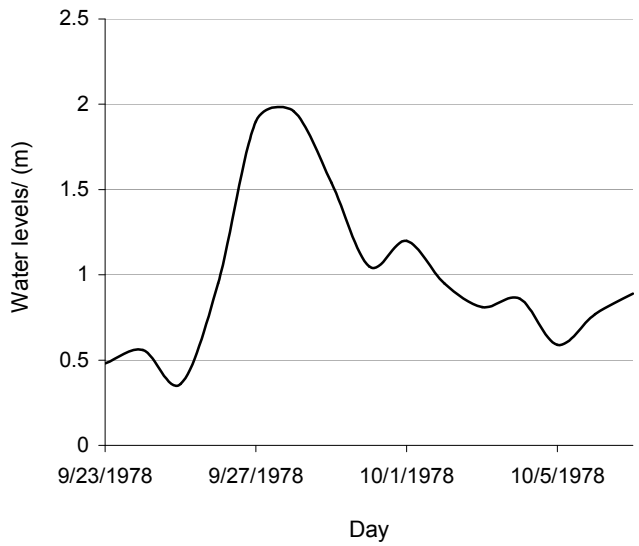

A2 Delft FLS master definition file

```
********************************* DELFT-FLS Master Definition File (*.mdf)
*****************
* Trial 02 with 7.5m DTM for ten year terurn period hydrogapgh in NAga River
********************************* GEOMETRY PARAMETERS
*************************************
MAIN DIMENSIONS                 MMAX  NMAX
                                488   489
GRID                            DX    X0        Y0
                                7.5   518927.75  1505195.75
COMPUTATIONAL GRID ENCLOSURE

HEIGHT                          ARC-INFO dtm7_5m.asc

********************************* INITIAL CONDITIONS
*************************************
INITIAL WATERLEVEL              M    N    ZETA0
                                421  373    0     Naga
                                140   2     0     Bicol_up
                                  4  89     0     Bicol_down

RESTARTFILE

********************************* BOUNDARY CONDITIONS
*************************************
OPEN BOUNDARIES                 M1   N1   M2    N2    TYPE  FILE TIME-SERIES
                                422  373  422   373    5     naga8.flx

                                137  1    145    1     2     bicol8.lev
                                  3  82    3    95     8     10    82    10   95
  -1   Qh_bicol8.qh


BREAKING DAMS                   M    N    T0    FILENAME

PUMPS


********************************* COMPUTATION PARAMETERS
*************************************
TIMEFRAME                       DT (s)  TSTART (h)   TSTOP (h)
                                -10       0          96

BOTTOM FRICTION FORMULATION     MANNING


BOTTOM FRICTION COEFFFICIENT    ARC-INFO    man7_5m.asc

********************************* OUTPUT PARAMETERS
*************************************
TIMES OF HIS,MAP,RST            TIHIS   TIMAP   TFMAP   (h)
                                 1       1      1

QUANTITIES IN MAPFILES           H      C
MAXIMUM QUANTITIES IN MAPFILES   H      C      Z

STATIONS FOR HISTORY             M      N
                                 31     91      Bicol_down
                                163     214     Naga_river
                                104     75      Bicol_up



EXCEL HISTORY                    H      C      Z

CROSS SECTIONS                   M1     N1     M2    N2
                                31      86     31     96    Bicol_down
                                161     214    167   214    Naga_river
                                104     64     104    85    Bicol_up
```

```
RESTART INTERVAL                1

CLASSES OF INCREMENTAL FILE     H       C       Z       U       V
                                0.01    0.01    0.01    0.01    0.01
                                0.2     0.1     0.25    0.50    0.50
                                0.5     0.2     0.50    1.00    1.00
                                1       0.4     0.75    2.00    2.00
                                1.5     0.6     1.00    3.00    3.00
                                2       1       1.50    5.00    5.00
                                4       2       999     999     999
                                999     999     999     999     999
********************************* end of DELFT-FLS definition file
*************************
```

A3 Ten year return period hydrograph of Naga River

Time/ (Hrs)	Water level/(m)
0	0
3	2
6	2
9	2
12	2
15	2
18	3
21	5
24	8
27	12
30	13
33	12
36	14
39	30
42	95
45	216
48	318
51	337
54	285
57	204
60	140
63	99
66	74
69	60
72	52
75	47
78	40
81	31
84	24
87	20
90	20
93	22
96	22
99	18
102	14
105	9
108	6
111	5
114	4
117	3
120	3

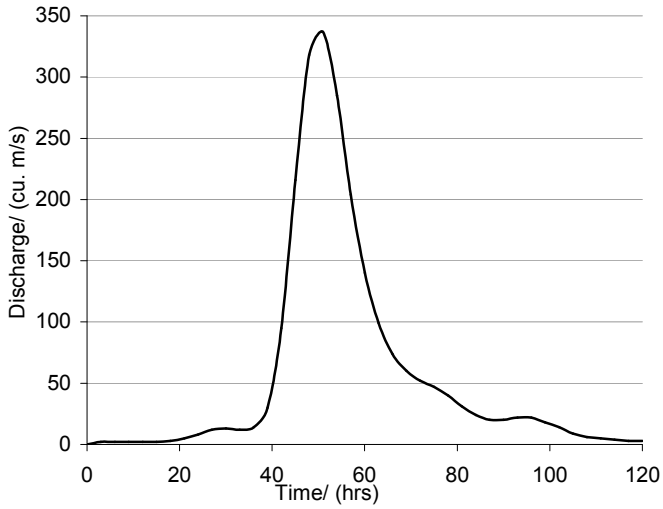

Source: (Nippon_Koei, 2003b)

A4 SOBEK Node structure of the model

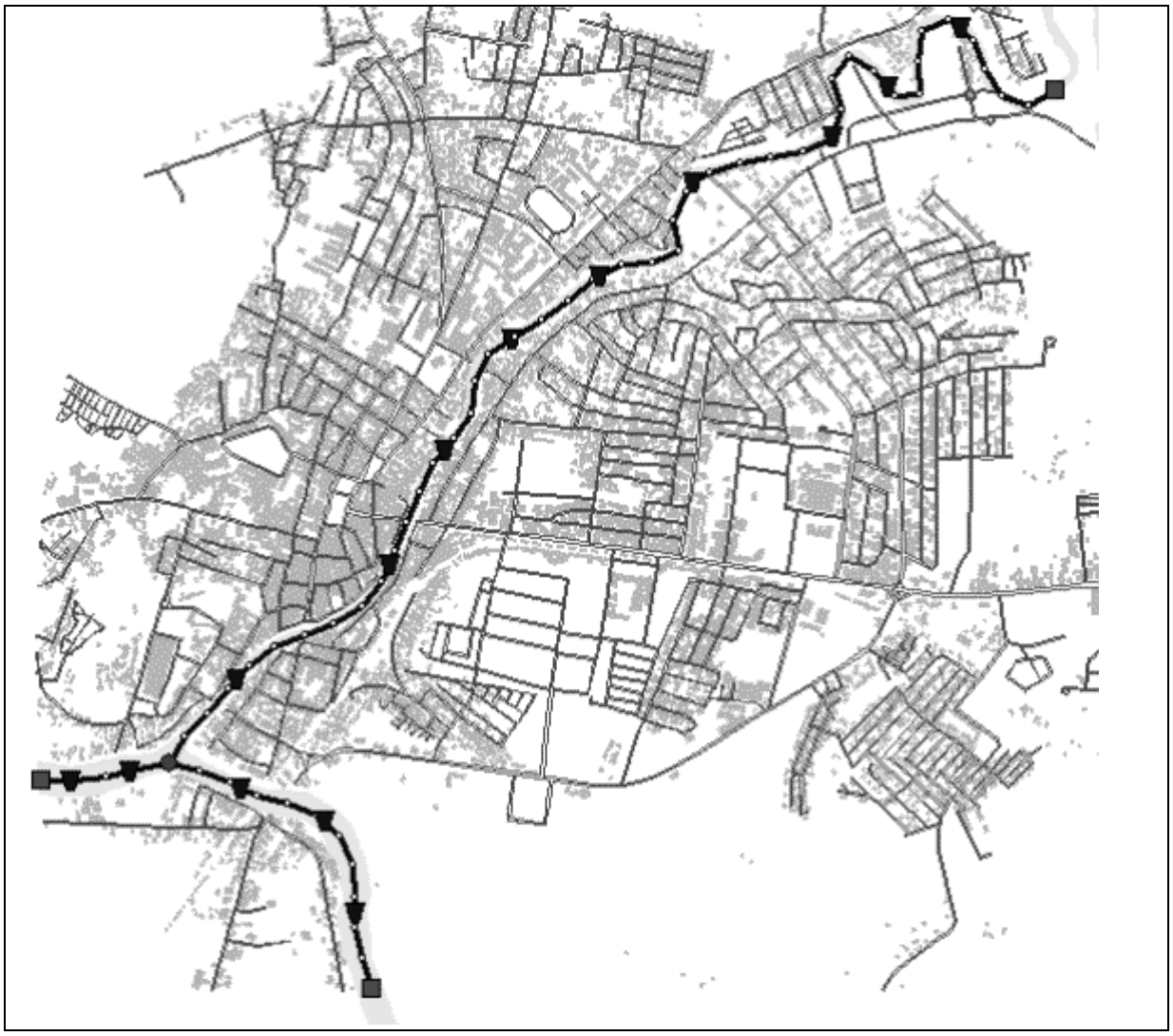

A5 Hazard classification, US Department of Land & Water Conservation

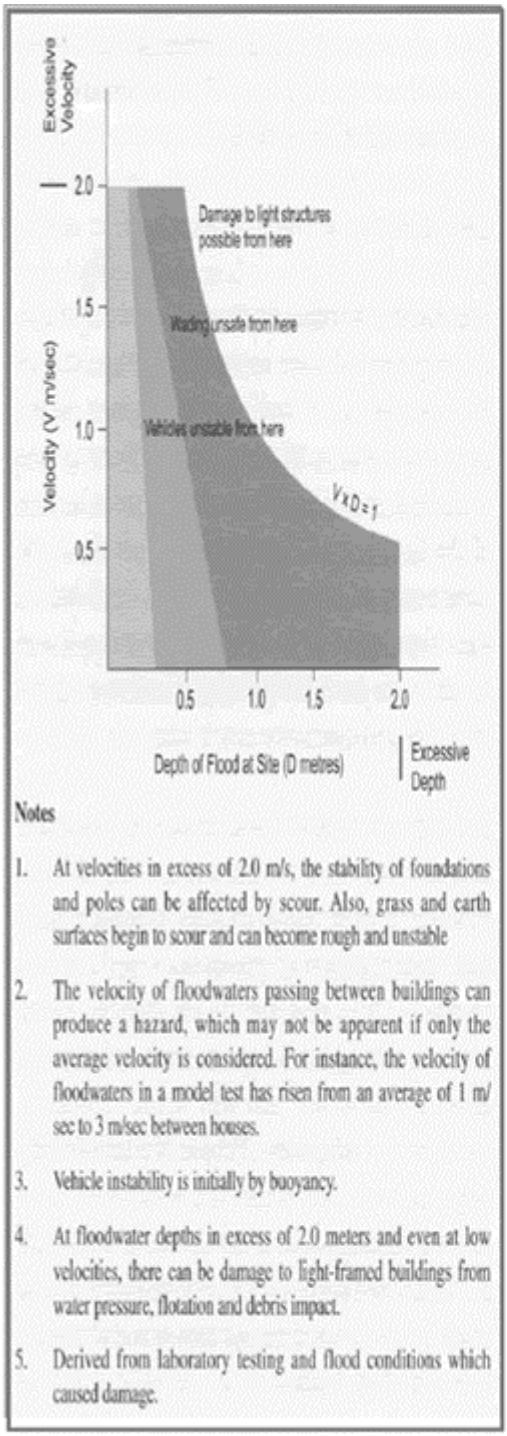

Notes

1. At velocities in excess of 2.0 m/s, the stability of foundations and poles can be affected by scour. Also, grass and earth surfaces begin to scour and can become rough and unstable
2. The velocity of floodwaters passing between buildings can produce a hazard, which may not be apparent if only the average velocity is considered. For instance, the velocity of floodwaters in a model test has risen from an average of 1 m/sec to 3 m/sec between houses.
3. Vehicle instability is initially by buoyancy.
4. At floodwater depths in excess of 2.0 meters and even at low velocities, there can be damage to light-framed buildings from water pressure, flotation and debris impact.
5. Derived from laboratory testing and flood conditions which caused damage.

Figure 1: Depth & Velocity relationships

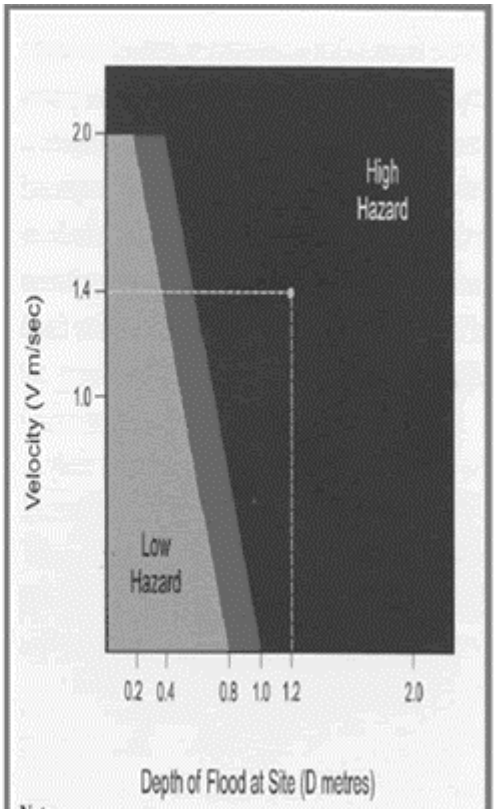

Note

The degree of hazard may be either -

- reduced by establishment of an effective flood evacuation procedure.
- increased if evacuation difficulties exists.

In the transition zone highlight by the median colour, the degree of hazard is dependant on site conditions and the nature of the proposed development.

EXAMPLE

If the depth of flood water is **1.2 m**

and the velocity of floodwater is **1.4 m/sec**

then the provisional hazard is **high**

Figure 2: Hazard Classification derived for able-bodied people

(Source: Floodplain Management Manual 2001 Department of Land & Water Conservation)

A6: Input boundaries and node structure used in exploration of model results with pixel size

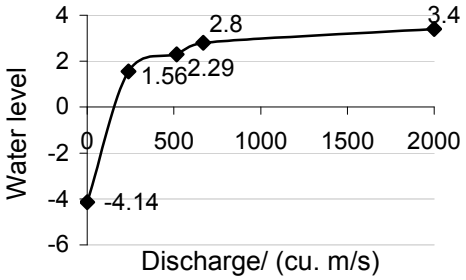

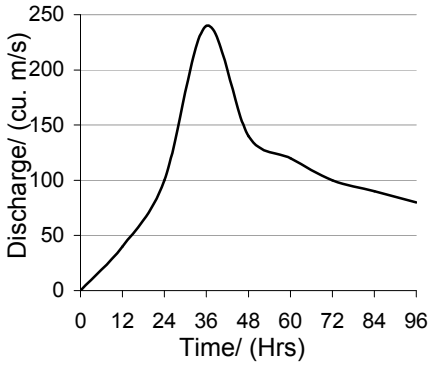

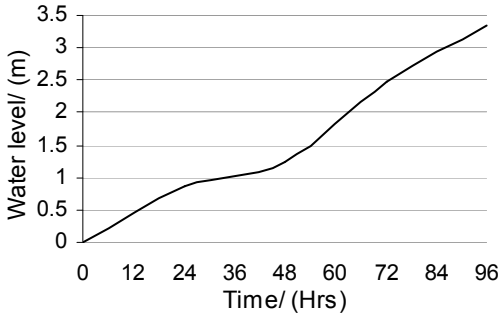

A7 Raster equations used for generating multiple-parameter hazard map

Following equations were used to delineate hazard level from each hazard parameter. These equations were used in the raster calculator of the ArcMap. Where

Ke(i,j) Kinetic energy of flood water at (i,j) pixel
T(i,j) Duration of inundation at (i,j) pixel
D(i,j) Depth of inundation at (i,j) pixel

Water depth vs. energy [d_vs_e]
con(([Ke(i,j)] > 45 | [Ke(i,j)] > (- 56.25 * [D(i,j)] + 67.5)),3,([Ke(i,j)] > 22.5 | [Ke(i,j)] > (- 37.5 * [D(i,j)] + 30)),2,(([Ke(i,j)] < 22.5 & [Ke(i,j)] > 0) | ([Ke(i,j)] < (- 37.5 * [D(i,j)] + 30) & [Ke(i,j)] > 0)),1,0)

Duration vs. depth [dura_vs_depth]
con(([T(i,j)] > 64 | [T(i,j)] > (- 80 * [D(i,j)] + 96)),3,([T(i,j)] > 32 | [T(i,j)] > (- 52.2 * [D(i,j)] + 42.7)),2,(([T(i,j)] < 32 & [T(i,j)] > 0) | ([T(i,j)] < (- 52.2 * [D(i,j)] + 42.7) & [T(i,j)] > 0)),1,0)

Energy vs. Duration [en_vs_dura]
con([Ke(i,j)] > (- 0.703 * [T(i,j)] + 45),3,[Ke(i,j)] > (-0.703 * [T(i,j)] + 22.5),2,([Ke(i,j)] > 0 & [Ke(i,j)] < (-0.703 * [T(i,j)] + 22.5)),1,0)

Combined hazard map
Finally following equation was used in the raster calculator to delineate combined hazard categories from the above three maps.
con([d_vs_e] == 3 | [dura_vs_depth] == 3 | [en_vs_dura] == 3,3,([d_vs_e] == 2 | [dura_vs_depth] == 2 | [en_vs_dura] == 2) & ([d_vs_e] <> 3 | [dura_vs_depth] <> 3 | [en_vs_dura] <> 3),2,([d_vs_e] == 1 | [dura_vs_depth] == 1 | [en_vs_dura] == 1) & ([d_vs_e] < 2 | [dura_vs_depth] < 2 | [en_vs_dura] < 2),1,0)

A8 Database structure prepared for future studies

All the data sets used for this study organized in a database so that it is convenient to trace in the future. Following main folders were created in the root of the main directory.

- Collected and digitised GIS layers
- Hydrological data
- Delft FLS input files and results
- SOBEK input files and results
- Documents

In the GIS layers folder contains three folders for original shadflies collected from the Naga municipality, shape files created and processed during the study and Scanned hard copy maps used for the digitising. All the shape files created and processed during the study are in Philippines zone 1V projected coordinates system. However Naga municipality original files were kept with out converting to the Philippines zone 1V projected coordinates.

"Hydrological data" folder contains data collected during the field work as well as some useful data that were extracted from previous studies of Nippon Koei 2003 and ADB 1991.

Two separate folders were prepared for two models used for the study. In the Delft FLS folder contains sub folders for "input files" and "output files" of the model. "Input files" folder contains master definition files of each simulation and all the input files used for each simulation. "Output file" folder contains Arcinfo grid files of inundation depth, flow velocities, energy files for each step of simulation. Similarly the same information is available in the "SOBEK input files and results" folder.

Documents folder contains this thesis, all the presentations created during the study and literature collected during the study relating to this topic.

Folder structure of the database is shown in the nest page.

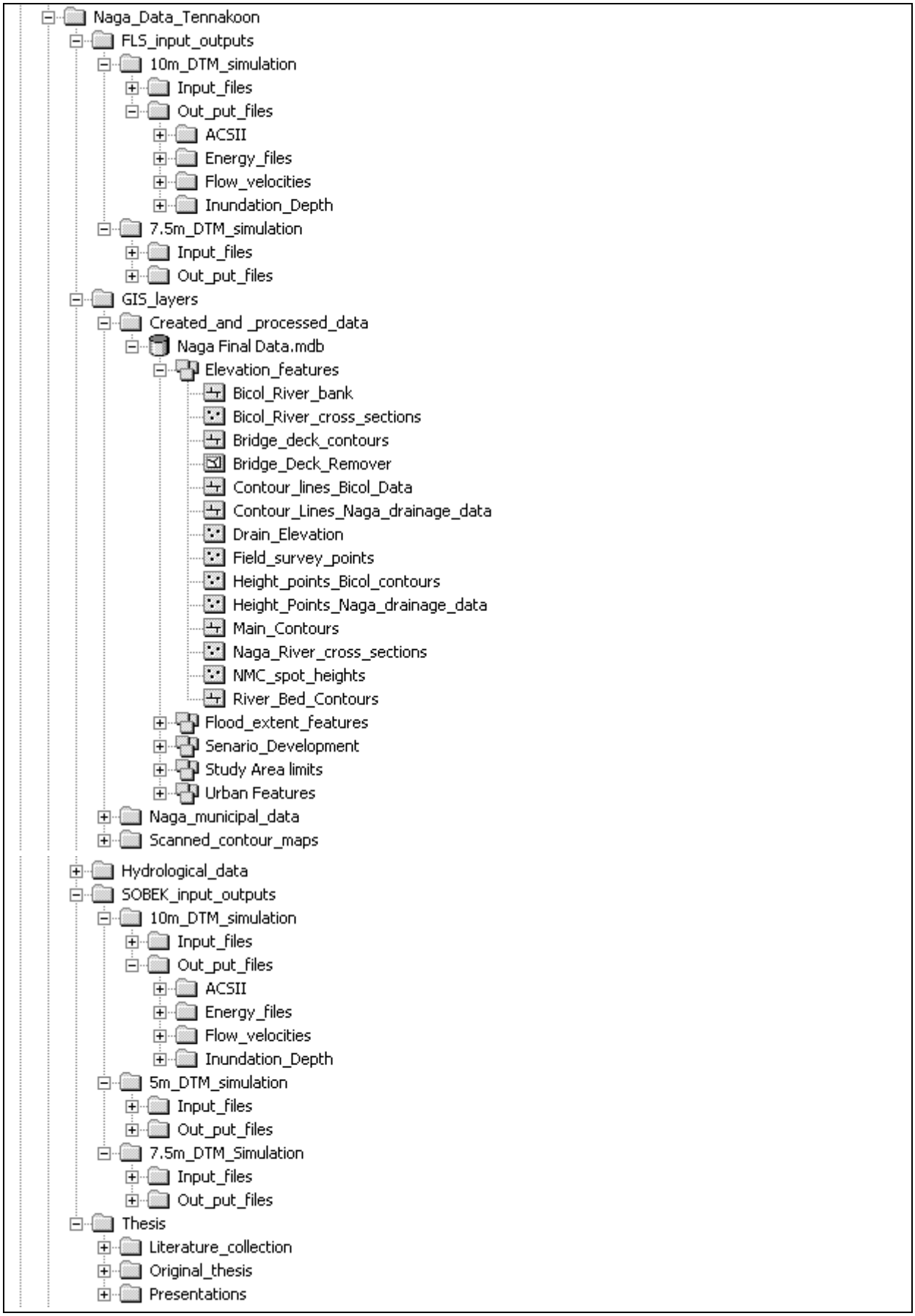

Complete folder structure of the database of this study

A9 Reasons for aggravation of floods in Naga city - Photograpghs

Encroachments of natural flow paths

Unauthorized structure constructed at a main stream

Bicol River with full of water hyacinth

Non maintained natural stream within the Naga city limits